Regulation of the Activity of Mammalian Serine Palmitoyltransferase

---

Dissertation

zur

Erlangung der naturwissenschaftlichen Doktorwürde

(Dr. sc. nat.)

vorgelegt der

Mathematisch-naturwissenschaftlichen Fakultät

der

Universität Zürich

von

Assem Zhakupova

aus

Kasachstan

Promotionskomitee

Prof. Dr. Arnold von Eckardstein (Vorsitz)

Prof. Dr. Thorsten Hornemann

Prof. Dr. Stephan Neuhauss

PD Dr. Sabrina Sonda

Dr. Ludovic Gillet

Zürich, 2016

Table of contents

Abstract

Sphingolipids are a highly diverse class of lipids that play an important role in cell physiology. Sphingolipid *de novo* synthesis starts with the condensation of palmitoyl-CoA and L-serine catalyzed by the enzyme serine palmitoyltransferase (SPT) producing C_{18}-based sphingolipids. SPT can also incorporate other acyl-CoAs (C_{12}-C_{20}) and other amino acids such as L-alanine and L-glycine, generating a wide-range of atypical sphingolipids (SLs). SPT consists of three subunits – SPTLC1, 2 and 3. Several mutations in SPT are associated with Hereditary Sensory and Autonomic Neuropathy Type 1 – HSAN1 and lead to a shift in the substrate preference from L-serine to L-alanine resulting in increased production of atypical 1-deoxy-sphingolipids (1-deoxySLs). Studies in yeast demonstrated that SPT activity is tightly regulated by a metabolic feedback mechanism mediated by Orm1 and Orm2 proteins. Upon adequate sphingolipid levels in the cell Orm proteins bind and inhibit SPT. Once the sphingolipid levels are reduced, Orm proteins are phosphorylated by Ypk1 kinase via TORC2-dependent pathway and release the inhibition of SPT. In contrast to yeast, mammalian cells express three ORM orthologues (ORMDL1-3); however, their role in regulating SPT activity is not clear yet.

This thesis consists of three parts. In chapter 1 we studied the regulation of SPT by ORMDL proteins in mammalian cells. We investigated the association of ORMDL proteins with total sphingolipid levels and SPT activity using several *in vitro* and *in vivo* models. We compared the SL profile in Ormdl3 KO and Ormdl3 TG mice to their WT controls and we observed a small but significant increase in C_{18}-sphinganine levels in Ormdl3 KO mice. Additionally, we found that SPT activity did not change in MEFs from ORMDL3KO mice compared to the WT nor in HEK293 cells overexpressing individual ORMDL1, 2 and 3 proteins. However, the knockdown of all three ORMDLs in HEK293 cells resulted in increased SPT activity.

In chapter 2 we showed that increasing intracellular sphingolipids by exogenously added free sphingoid bases – sphinganine (SA) and sphingosine (SO) or cell-membrane permeable synthetic C_6-Ceramide (C6Cer) results in decreased SPT activity. This proves that SPT regulation is based on the feedback mechanism similar to the one in yeast. HSAN1 mutations SPTL1 p.S331F and SPTLC2 p.I504F result in several-folds increased SPT activity. However, upon supplementation with C6Cer p.331F and p.I504F were also

inhibited by C6Cer. Moreover, we showed that increasing C_{18}-based SLs with the addition of C6Cer resulted in decreased not only canonical (C18SLs), but also atypical C_{16}, C_{17}, C_{19}-sphingoid bases and 1-deoxySLs.

We further investigated C6Cer metabolism in chapter 3. We showed that inhibition of SPT by C6Cer occurs rapidly (30min post-treatment). Moreover, the addition of C6Cer resulted in enrichment of monohexosylceramides (MHCer) levels, but not sphingomyelin (SM). We used chemical inhibitors of the enzymes of SL metabolic pathway and found that fumonisin B1 (FB1) could significantly reverse the C6Cer mediated inhibition of SPT.

In summary, we showed that increasing intracellular SLs inhibits SPT activity. This proves that the regulation of SPT is based on availability of intracellular SLs and that a feedback mechanism exists in the mammalian cells similarly to yeast. However, we could not confirm the role of ORMDL3 in regulation of SPT in mammals. Additionally, we showed that C6Cer-meditated inhibition on SPT decreases *de novo* synthesis of both typical and atypical SLs.

Zusammenfassung

Sphingolipide sind eine sehr vielseitige Klasse von Lipiden, die eine wichtige Rolle in der Zellphysiologie spielen. Die Sphingolipid *de novo* Synthese beginnt mit der Kondensation von Palmitoyl-CoA und L-Serin, katalysiert durch das Enzym Serin-Palmitoyltransferase (SPT), wodurch C_{18}-basierte Sphingolipide gebildet werden. Weiter ist SPT auch in der Lage andere Acyl-CoAs (C_{12}-C_{20}) und Aminosäuren wie L-Alanin oder L-Glycin zu verwenden, was zu einer breiten Palette von atypischen Sphingolipiden (SLs) führt. SPT besteht aus drei Untereinheiten - SPTLC1, 2 und 3. Mehrere Mutationen in SPT sind mit der Hereditären Sensorischen und Autonomen Neuropathie Typ 1 (HSAN1) assoziiert; HSAN1 führt zu einer Verschiebung der Substratpräferenz von L-Serin zu L-Alanin, was zu der erhöhten Produktion von atypischen 1-Deoxy-Sphingolipiden (1-deoxySLs) führt. Studien in Hefe haben gezeigt, dass die SPT Aktivität von Orm1/2 Proteinen durch einen metabolischen Rückkopplungsmechanismus reguliert wird. Bei ausreichender Sphingolipid Konzentration in der Zelle binden ORM-Proteine und hemmen die Aktivität von SPT. Bei sinkender Sphingolipid Konzentration werden die ORM-Proteine über den TORC2-abhängigen Signalweg durch die Ypk1 Kinase phosphoryliert und die Hemmung der SPT wird aufgelöst. Im Gegensatz zu Hefe exprimieren Säugetierzellen drei ORM Orthologe (ORMDL1-3); ihre Rolle in der Regulierung der SPT Aktivität ist jedoch noch nicht geklärt.

Diese Arbeit besteht aus drei Teilen. In Kapitel 1 untersuchten wir die Regulierung von SPT durch ORMDL Proteine in Säugetierzellen. Wir erforschten den Zusammenhang von ORMDL Proteinen mit der totalen Sphingolipid Konzentration und der SPT Aktivität mit mehreren *in vitro* und *in vivo* Modellen. Wir verglichen die SL Profile in Ormdl3 KO und Ormdl3 TG Mäusen mit den zugehörigen WT-Kontrollen und wir beobachteten einen kleinen, aber signifikanten Anstieg der C_{18}-Sphinganin Konzentration in ORMDL3-KO-Mäusen. Ausserdem haben wir festgestellt, dass die SPT Aktivität in MEF Zellen von ORMDL3KO-Mäusen, verglichen zu den WT Zellen, unverändert bliebt, sowie auch die in HEK293-Zellen, welche ORMDL1, 2 und 3 einzeln über exprimieren. Allerdings führte die Inaktivierung der Expression aller drei ORMDLs in HEK293-Zellen zu einer gesteigerten SPT-Aktivität.

In Kapitel 2 konnten wir zeigen, dass die Erhöhung der intrazellulären Sphingolipide durch exogen hinzugefügte, freie Sphingolipidbasen, Sphinganin (SA) und Sphingosin

(SO), und Zellmembran durchlässigem synthetisches C_6-Zeramid (C6Cer), in einer gehemmten SPT-Aktivität resultiert. Dies beweist, dass die Regulierung von SPT in Säugtierzellen auf einem ähnlichen Rückkopplungsmechanismus basiert wie dem der Hefe. Die HSAN1 Mutationen SPTLC1 p.S331F und SPTLC2 p.I504F resultierten in einer mehrfachen Erhöhung der SPT Aktivität. Jedoch wurden auch S.331F und I504F durch die Supplementierung von C6Cer gehemmt. Darüber hinaus konnten wir zeigen, dass die Erhöhung der C_{18}-basierten SLs durch Zugabe von C6Cer, nicht nur die Konzentration der kanonischen (C_{18}SLs), sondern auch die der atypischen C_{16}, C_{17}, C_{19} Sphingolipidbasen und 1-deoxySLs gesenkt wurde.

Den C6Cer Stoffwechsel haben wir in Kapitel 3 weiter untersucht. Wir haben gezeigt, dass die Hemmung von SPT durch C6Cer schnell eintritt (30min nach der Behandlung). Darüber hinaus führte die Zugabe von C6Cer zu der Anreicherung von Monohexosylzeramiden (MHCer), jedoch nicht von Sphingomyelinen (SM). Wir haben chemischen Inhibitoren für die Enzyme des SL Stoffwechselweges verwendet und haben gezeigt, dass Fumonisin B1 (FB1) die hemmende Wirkung von C6Cer auf die SPT Aktivität aufhebt.

Abschliessend konnten wir zeigen, dass eine Erhöhung der intrazellulären SLs die SPT Aktivität hemmt. Dies beweist, dass die Regulierung von SPT auf der Verfügbarkeit von intrazellulären SLs basiert und dass ein Rückkopplungsmechanismus in Säugetierzellen existiert, ähnlich dem der Hefe. Jedoch konnten wir die Rolle von ORMDL3 in der Regulierung von SPT in Säugetierzellen nicht bestätigen. Zusätzlich haben wir gezeigt, dass durch C6Cer vermittelte Hemmung von SPT, die *de novo* Synthese von beiden, typischen und atypischen, SLs verringert wurde.

General Introduction

I. The sphingolipid metabolic pathway

Sphingolipids are a diverse class of lipids that play an important role in cell physiology [1]. Several sphingolipids such as sphingosine, sphingosine-1-phosphate (S1P), ceramide, ceramide-1-phosphate (C1P) and lyso-sphingomyelin were termed 'bioactive', as they mediate key functions in cell survival, endocytosis, cell signaling and migration, senescence and apoptosis [1-5].

Sphingolipid *de novo* synthesis starts with the condensation of L-serine and palmitoyl-CoA in the endoplasmic reticulum (ER) by the enzyme serine palmitoyltransferase (SPT), producing predominantly C_{18}-based sphingolipids [6-11] (Fig. 1). The direct product of this reaction, 3-keto-sphingosine, is quickly reduced to sphinganine (SA) by 3-ketodihydrosphingosine reductase (KDSR) [12, 13] followed by ceramide synthase (CerS) that N-acylates SA to form dihydroceramide [14, 15]. There are six CerS isoforms (CerS1-6) known [16], which are differently expressed in various tissues. Individual CerS isoforms have substrate preferences for certain fatty acyl-CoAs: CerS1 utilizes primarily C18-CoAs, CerS2 – C22-24-CoAs, whereas CerS3 uses C26-CoAs, CerS4 – C18-C22-CoAs, and Cer5 and CerS6 largely utilize C16-CoAs [17-21]. A *trans*-double bond at the C_4-C_5 position is introduced by Δ4-dihydroceramide desaturase (DES1) to form ceramides [22]. Alternatively, dihydroceramides can be hydroxylated by DES2 to form phytoceramide [23, 24]. Notably, with the exception of CerS all of the above mentioned enzymes (SPT, KDSR, DES1-2) are localized at the cytosolic side of the ER [22, 25-30].

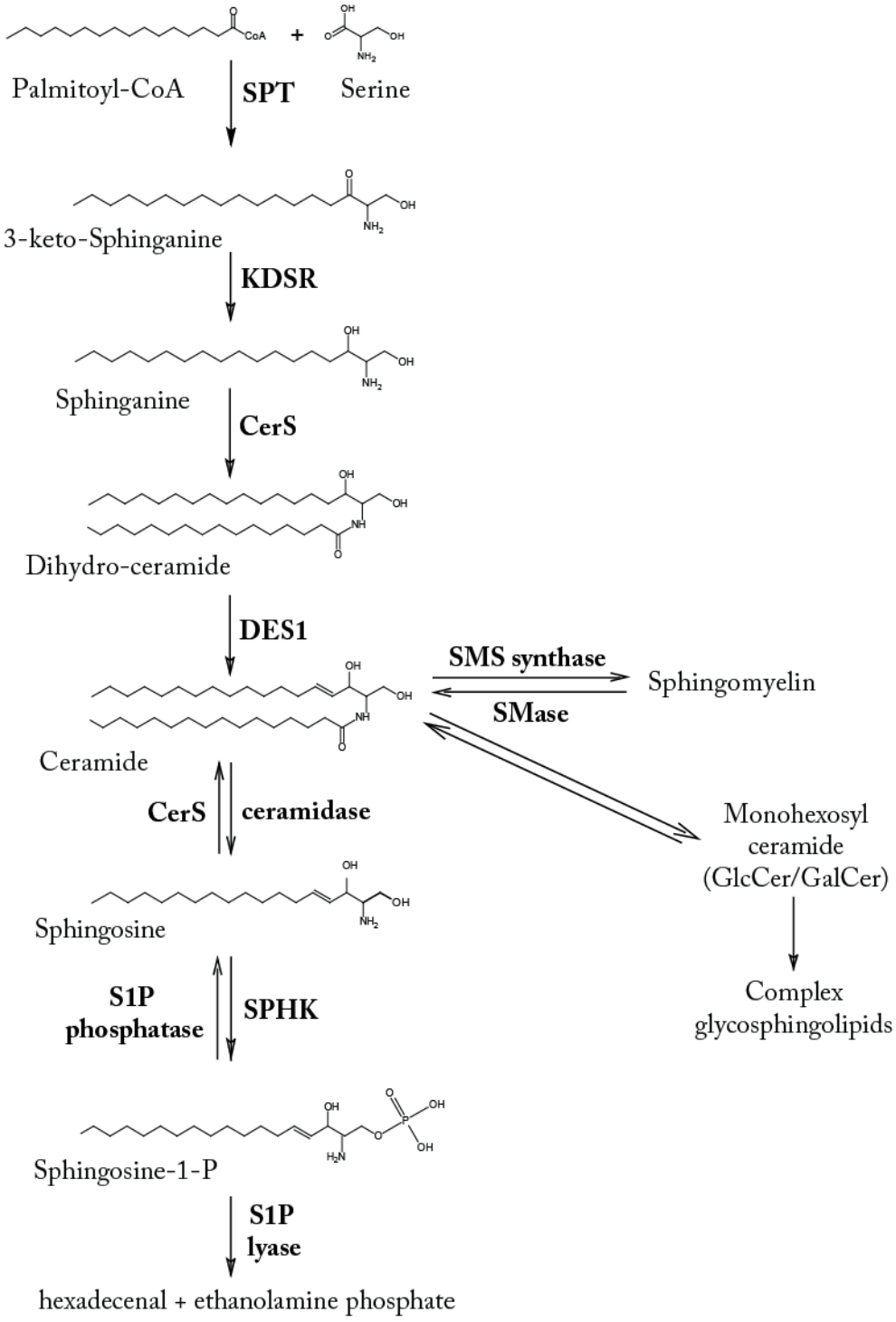

Figure 1. Sphingolipid *de novo* synthesis pathway.

Complex sphingolipids such as sphingomyelin (SM), ceramide-1-phosphate (C1P) and glucosylceramide are produced by the enzymes that are residing in the Golgi. Therefore, ceramides are transported from the ER to the Golgi via vesicular and non-vesicular

transport. The ceramide transfer protein (CERT) mediates the non-vesicular transport of ceramides from the ER to the Golgi [31] (see Fig. 2).

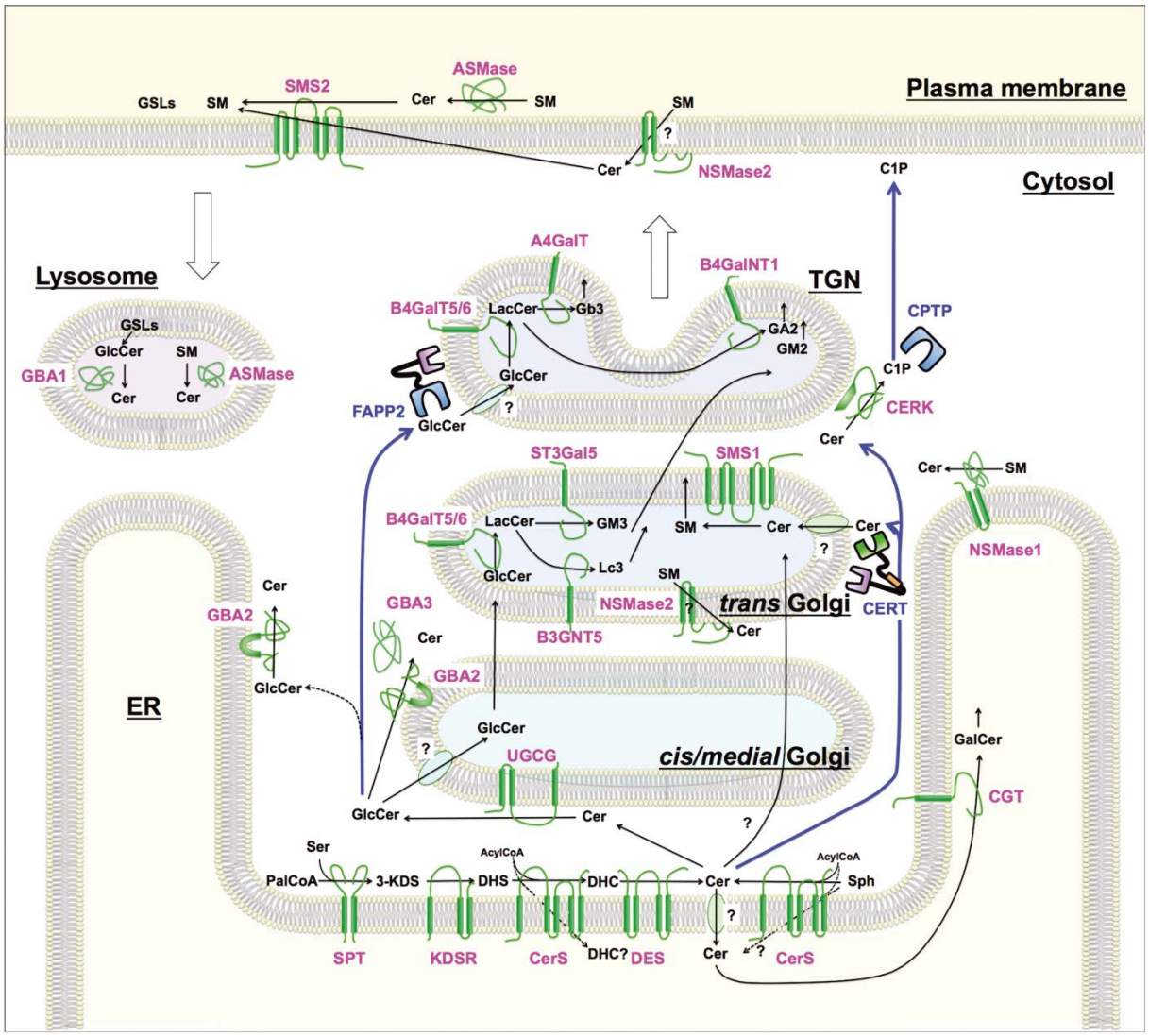

Figure 2. Sphingolipid trafficking showing the enzymes and lipid transfer proteins involved [32].

Ceramides transported via CERT are primarily used for the synthesis of SM. A phosphocholine group from phosphatidylcholine (PC) gets attached to ceramide, thereby forming SM and diacylglycerol (DAG). This reaction is catalyzed by sphingomyelin synthases 1 and 2 (SMS1 and SMS2). SMS1 localizes at the *trans* Golgi and is mainly responsible for the *de novo* synthesis of SM [33, 34]. SMS2 localizes

primarily at the PM and Golgi and it is thought to convert primarily recycled ceramides into SM [34]. Besides SMS1 and 2, mammalian cells express sphingomyelin synthase-related protein (SMSr), which was shown to be localized in the ER. SMSr synthesizes ceramide phosphoethanolamine (CPE) instead of SM [35] and was suggested to be a ceramide sensor in the ER, as blocking SMSr activity resulted in increased ceramide accumulation in the ER [35, 36].

Ceramides can undergo glycosylation by UDP-glucose:ceramide glucosyltransferase (UGCG). UGCG mediates the transfer of glucose from UDP-glucose to ceramide, forming glucosylceramide (GlcCer) [37]. GlcCer is synthesized on the cytosolic surface of *cis* Golgi. Four-phosphate adaptor protein (FAPP2) has a vital role in mediating the transfer of GlcCer to the *trans* Golgi network (TGN) for further metabolism into complex glycosphingolipids (glycoSLs) [38-40]. Complex glycoSLs are made by the addition of different sugar groups and sialic acid (GM3 ganglio series) on the luminal side of the Golgi.

Galactosylceramide (GalCer) is synthesized by UDP-galactose:ceramide galactosyltransferase (CGT), which attaches a galactose moiety from UDP-galactose to ceramide [41-43]. The active site of CGT is localized on the luminal side of the ER. GalCer is the precursor of sulfatides, which are mainly produced in Schwann cells and oligodendrocytes.

Additionally, ceramides are phosphorylated by the action of ceramide kinase (CERK), which forms ceramide-1-phosphate (C1P) [44, 45]. C1P plays a crucial role in inflammation [46].

Ceramides can also be generated by the breakdown of SM, mediated by sphingomyelinases (SMases) [1, 47]. Several SMase isoenzymes were identified – acid SMase, neutral SMase and alkaline SMase, which are located in distinct compartments in the cell [1, 47, 48]. It has been reported that these enzymes are induced in response to TNF-α [49], Fas ligand [50] and oxidative stress [51]. Further breakdown of ceramides by ceramidases results in the formation of sphingosine [52, 53]. Sphingosine can either be reacylated by CerS to form ceramides again or phosphorylated by the sphingosine kinases – SK1 and SK2 [54]. The product of this reaction – S1P is irreversibly degraded by the actions of sphingosine-1-phosphate lyase (S1P lyase), forming ethanolamine

phosphate and hexadecenal (which can be converted back to palmitate and recycled again in the sphingolipid *de novo* synthesis pathway) [55]. Alternatively, S1P can be dephosphorylated to sphingosine by S1P phosphatases [56]. Also SA can be phosphorylated by sphingosine kinase to form sphinganine-1-phosphate.

II. The sphingolipid salvage pathway

The degradation of complex sphingolipids to ceramides and later to sphingosine is part of the salvage pathway [57-59]. This involves the action of SMase, ceramidase and CerS enzymes. Approximately 50-90% of sphingolipids come from the salvage pathway [58, 60]. Mutations in the enzymes responsible for sphingolipid catabolism result in sphingolipid accumulation causing sphingolipidoses such as Niemann-Pick disease, Farber's disease, Tay-Sachs disease, Fabry disease and Gaucher disease [61-63]. The above mentioned diseases are linked to the dysfunction of acid ceramidase [64], glucocerebrosidase [65, 66] and acid SMase [67] respectively.

Salvage pathway of short-chain synthetic ceramides

C_6-ceramide (C6Cer) is a synthetic short-chain ceramide analog (containing C_6 fatty acid attached to sphingosine), which is not naturally occurring (predominant ones are C14:0-C24:0 ceramides). Short-chain ceramides are water-soluble and membrane-permeable. Therefore, unlike long-chain ceramides, they are readily taken up and metabolized by cells [68]. C6Cer treatment is experimentally used in cancer research. Exogenous supplementation with C_6-ceramide (C6Cer), but not with C_2-ceramide, results in deacylation/reacylation of ceramides [57, 69] (Fig. 3). C6Cer metabolism in cancer cells was studied using synthetic metabolites containing a radio label on the sphingosine backbone in combination with the CerS inhibitor Fumonisin B1 (FB1). C6Cer was found to be largely converted to C_{16}-ceramides via the salvage pathway [57]. Moreover, generation of endogenous ceramides from C6Cer seems to be specific for D-*erythro*-C6Cer, but not to L-*erythro*-C6Cer or its biologically inactive form dihydroceramide [57]. Additionally, exogenously added C6Cer can be converted to C6-SM and C6-glucosylceramides [57, 70, 71]. Cabot and colleagues showed that with increasing concentration of C6Cer added to the cells, C6-glucosylceramide levels, and not C6-SM levels, increased [70].

Exogenously added lipids typically enter the cell via the endocytotic pathway. Passaging from early to late endosomes the lipids finally end up in lysosomes, where acid sphingomyelinase (SMase) degrades them to ceramides and ceramidase then further degrades them to sphingosine. Sphingosine (SO) can leave the lysosome and can either be reacylated to ceramides by CerS or phosphorylated by sphingosine kinase (SK) to produce sphingosine-1-phosphate (S1P). S1P is transported to the plasma membrane (PM) or irreversibly degraded in the ER by the action of S1P lyase.

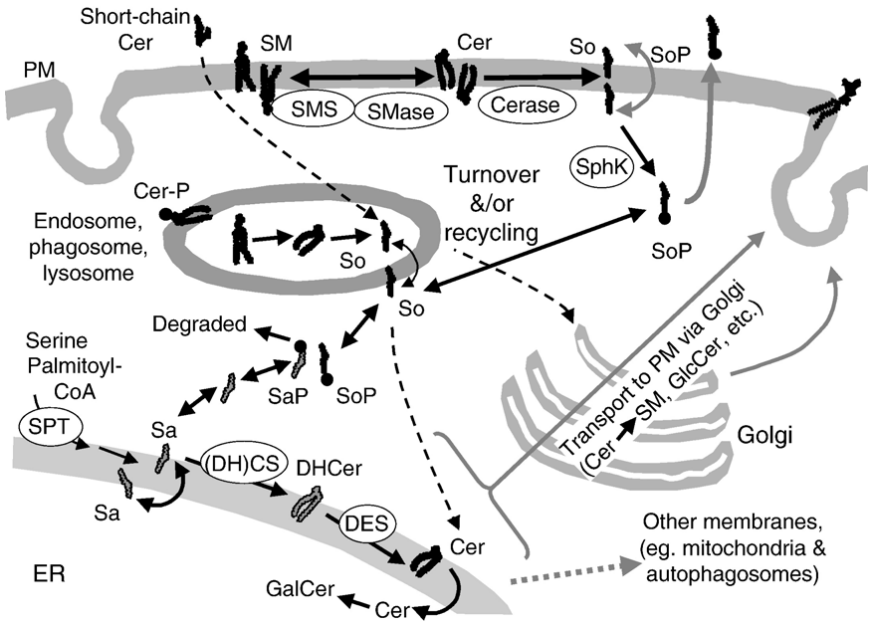

Figure 3. Schematic view of short-chain ceramide (C6Cer) metabolism in the cell via salvage pathway [73].

III. Intracellular sphingolipid trafficking and transport

Ceramide Transport by CERT

As mentioned previously, CERT is responsible for the non-vesicular transport of ceramides that are used for SM synthesis. CERT exclusively binds to ceramides and not to any other sphingolipids. It carries C14:0-20:0 ceramides most efficiently [74]. Additionally, D-*erythro*-ceramides are preferentially transported due to the formation of a hydrogen bonds in the CERT pocket [32].

CERT has N-terminal Pleckstrin homology (PH) domain that recognizes and binds phosphoinositol-4-phosphate (PI4P) in the Golgi [31]. Binding of the PH domain to PI4P seems to be crucial for CERT activity, as the LY-A cells, which bear a mutation in this domain showed a disruption of ceramide transfer from ER to the Golgi [31]. Additionally, CERT contains a C-terminal steroidogenic acute regulatory proteins (StAR)-related lipid transfer (START) domain for ceramide transport [31]. A FFAT motif (located on the N-terminal of the START domain) binds to Vesicle-associated membrane protein-associated protein (VAP) in the ER.

CERT is phosphorylated at two sites – the serine repeat (SR) motif and serine 315 at the FFAT domain [75, 76]. DAG released from SM synthesis accumulates in the Golgi and activates protein kinase D (PKD). CERT is inactivated upon phosphorylation by PKD and casein kinase I (CKIγ2) at the SR motif, resulting in inhibition of ceramide transport. Hence, PKD and CKI act as negative regulators of CERT. Low levels of SM induce dephosphorylation of the serine motif of CERT by protein phosphatase (PP2Cε) and protein phosphatase 1-like protein (PPM1L) and activate CERT [75]. CERT dephosphorylation by PP2Cε is dependent on VAP-A levels, thereby increasing the association of CERT with VAP-A.

Similar to CERT, the oxysterol binding protein (OSBP) contains a PH domain to bind PI4Ps at the Golgi and a FFAT motif binding to VAPs in the ER. Several phosphatidylinositol 4-kinases (PI4-kinases) such as PI4KII α and PI4KIII β phosphorylate phosphoinositol (PI) to PI4P. OSBP stimulates CERT-mediated ceramide transport by activating PI4KII α, which raises PI4P levels in Golgi. This further enhances CERT binding to the Golgi and results in increased SM production. Another PI4-kinase (PI4KIII β) was shown to be activated upon phosphorylation by PKD. PI4KIII β and PKD

are further stimulated by ADP-ribosylation factor 1 (Arf1). The phosphoinositide 4 phosphatase Sac1 has the opposite function than PI4Ks; it dephosphorylates PI4P to PI at the ER and Golgi.

Vesicular ceramide transport

Vesicular transport of ceramides is a minor pathway for SM synthesis and the major one for GlcCer production. FAPP2 also contains a PH domain and glycolipid transfer protein (GLTP) domain, which allows it to transport glucosylceramides (GluCer) from the *cis* Golgi to the TGN for further synthesis of glycosphingolipids (glycoSLs) [38]. FAPP2 is specific to GluCer and it cannot transport other sphingolipids [38].

Ceramide-1-phosphate transport

Transport of C1P is mediated by ceramide-1-phosphate transfer protein (CPTP), which was identified to transport C1P only and not glycolipids. However, CPTP does not contain any PH or FFAT binding domain [32], hence, it is unclear how this transport is mediated.

IV. The mammalian SPT complex

Serine palmitoyltransferase (SPT) is a member of the PLP-dependent α-oxoamine synthase (POAS) family of enzymes [7, 77], which includes other members such as 2-amino-3-ketobutyrate ligase (KBL), 8-amino-7-oxononaoate synthase (AONS) and 5-aminolevulinic acid synthase (ALAS) [7, 78]. Members of the POAS family are normally soluble homodimers, whereas SPT is an ER bound multi-subunit complex [7] composed of the three subunits: SPTLC1 (53-kDa), SPTLC2 (63-kDa) and SPTLC3 (62-kDa). The POAS family of enzymes catalyzes pyridoxal-5-phosphate (PLP)-dependent reaction and typically have a conserved motif close to the PLP-binding lysine (T[FL][GTS]**K**[SAG][FLV]G), which is present in SPTLC2 and SPTLC3, but absent in SPTLC1 [7, 78]. Moreover, while SPTLC1 and SPTLC2 are ubiquitously expressed, SPTLC3 is restricted to certain tissues primarily placenta, liver, heart, kidney and skin [79].

SPT was described as a multi-subunit complex with a presumed total molecular mass of 480 kDa [78], although the protein structure of the active SPT enzyme was not yet elucidated. However, it is believed to be an octamer with four SPTLC1/SPTLC2 or SPTLC1/SPTLC3 dimers forming a dynamic complex [7, 78].

In vitro mammalian SPT showed the strongest CoA preference for palmitoyl-CoA [7]. However, SPT can also incorporate other acyl-CoAs (C_{12}-C_{20}) [80], resulting in a diverse range of atypical sphingolipids. Moreover, while SPTLC2 has a preference for palmitoyl-CoA, SPTLC3 can use C_{14}-C_{18} acyl-CoAs [80]. Overexpression of SPTLC3 in HEK293 cells resulted in the generation of short-chain (C_{16}) and long chain (C_{19}, C_{20}) sphingoid bases [80]. However, the physiological effect of these sphingolipids is not clear yet. Interestingly, the fruit fly *D. melanogaster* predominantly contains C_{14} and C_{16} sphingoid bases [81].

V. Serine palmitoyltransferase and HSAN1

Several missense mutations in the subunits of SPT were found to be associated with Hereditary Sensory and Autonomic Neuropathy Type 1 – HSAN1 [82-91]. HSAN1 is an autosomal dominant peripheral neuropathy, characterized by a loss of sensation mainly in distal limbs [92-94]. Mutations associated with HSAN1 induce a permanent shift in the substrate preference of SPT from L-serine to L-alanine, resulting in the production of atypical and toxic 1-deoxysphingolipids (1-deoxySLs) [95]. 1-deoxySLs lack the C_1-hydroxyl group of regular sphingolipids and are therefore not converted to more complex sphingolipids neither degraded. Elevated 1-deoxySLs were found in plasma and EBV-transformed lymphoblasts of HSAN1 patients and are a hallmark for this disease [95, 96]. Notably, 1-deoxySLs [95] are also elevated in patients with metabolic syndrome and type 2 diabetes [97-100].

Bode et al showed that in some HSAN1 mutants, canonical SPT activity was higher compared to the WT control [101]. The authors classified the most common mutations in SPT using a principle component analysis (PCA) to cluster mutations according to their clinical manifestations, SPT activity and production of 1-deoxySLs [101]. HSAN1 mutations associated with a severe phenotype – SPTLC1 p.S331F and SPTLC2 p.I504F [84, 86] – clustered together in one group and showed increased canonical SPT activity,

elevated formation of 1-deoxySLs and C_{20}SL. In particular these mutations were also shown to be residing on the surface of the protein complex [101], which implies that binding of the regulatory proteins may be impaired in these mutants.

VI. Regulation of SPT by ORMDL proteins

a) Regulation of SPT by ORM proteins in yeast

Studies in budding yeast *S. cerevisiae* revealed that SPT is negatively regulated by a family of Orm1 and 2 proteins through a metabolic feedback loop [102-110]. Upon high intracellular sphingolipid levels, Orm proteins bind to and inhibit SPT. Once sphingolipid levels are low, Orm proteins are increasingly phosphorylated at their N-terminal residue by Ypk1 kinase and release SPT inhibition [104]. Once the sphingolipid levels in the cell are restored, Orm proteins are dephosphorylated completing the rheostat cycle. Yeast cells with mutations in the phosphorylation sites of Orm1/2 have disrupted sphingolipid synthesis and are unable to survive [102, 111]. Moreover, ORM deletion (*orm1*Δ/*orm2*Δ) results in the overproduction sphingolipids, which becomes harmful to cells [102, 109, 111].

Another study in *S. cerevisiae* by Shimobayashi et al [106] found that Orm proteins regulate both *de novo* synthesized sphingolipids and complex sphingolipids. Orm proteins themselves are regulated by Target of Rapamycin Complex 1 (TORC1) and TORC2 [106]. Inhibition with myriocin or sphingolipid-deprived conditions activate TORC2, which in turn induces Ypk1 to phosphorylate Orm proteins [106], thereby leading to release of SPT inhibition. On the contrary, nutrient deprivation and rapamycin treatment lead to TORC1 inhibition, which causes inhibition of Sit3-PP2A. This activates Npr1, which stimulates Orm proteins and the synthesis of complex sphingolipids. Therefore, the production of complex sphingolipids is increased, while bypassing *de novo* synthesis. This mechanism seems to be a cellular starvation response [106].

In yeast, Orm proteins form a complex with SPT termed SPOTS (Serine Palmitoyltransferase, Orm1/2, Tsc3, and phosphoinositide phosphatase Sac1) [102, 112]. Notably, Breslow et al found that Sac1 and Orm1/2 bind to SPT independently of each other, indicating that Sac1 controls SPT activity directly, but apparently in a

manner different from Orm1/2 [102]. Moreover, it was reported that orm1 binds not only to SPT, but also to lac1 (CerS) [107].

Slm1 and 2 proteins were first shown to be substrates of TORC2 and were known for playing a major role in phosphoinositol phosphate signaling in yeast. Inhibition of sphingolipids or mechanical stretch of the plasma membrane was shown to cause relocation of Slm1/2 proteins from eisosomes to the plasma membrane [113]. This results in a further association of Slm proteins with TORC2 and Ypk1 activation [113, 114]. Relocation of Slm proteins to TORC2-containing membranes was found to be essential for Ypk1 phosphorylation [113]. These findings are particularly intriguing, since TORC2 was shown to be regulating ceramide biosynthesis [115].

b) Regulation of SPT in mammalian cells by ORMDL proteins

However, all of the above findings have been demonstrated in yeast. The role of ORM proteins in regulating SPT activity in mammalian cells is not completely understood. There are three ORM isoforms in mammals – ORMDL1, 2 and 3, which are ubiquitously expressed in almost all human tissues [116]. However, the phosphorylation sites found in yeast are not conserved as the mammalian isoforms are lacking the N-terminal serine residues [116]. Moreover, ORMDL proteins do not contain phosphorylation sites for the mammalian Ypk1 equivalent – SGK kinase.

Overexpression of ORMDL1, 2 and 3 proteins individually as well as in combination did not have any effect on ceramide biosynthesis in mammalian cells [117]. Only when HEK293 cells overexpressing all three ORMDL proteins were further stimulated with palmitate, *de novo* synthesized ceramide levels decreased [117]. Additionally, the simultaneous knockdown of all three ORMDLs, but not of the individual isoforms, was needed to restore ceramide levels in HeLa [118] and HEK293 [102, 117] cells. Moreover, ORMDL1-3 depletion resulted in elevated *de novo* dihydroshingosine-1-phosphate and sphingosine-1-phosphate levels [119].

Siow et al showed that ceramide biosynthesis was increased in serum-starved conditions [118]. However, the mechanism behind the enhancement of ceramide biosynthesis in serum-free conditions is not clear. In A549 cells this effect was gone with ORMDL knockdown, however in HeLa and PC3 cells it seems to be ORMDL independent [118]. Hagen-Euteneuer et al [120] reported that the homeostatic rheostat between *de*

novo synthesis and degradation of sphingolipids is maintained in S1P lyase-deficient model. Moreover, the authors indicated that ORMDL1-3 mRNA levels were increased in neurons of S1P lyase-deficient mice, corresponding to reduced SPT activity [120].

c) Regulation of SL levels by other proteins

Furthermore, the relationship with sterols and sphingolipid regulation was analyzed by studying the cholesterol effect on cells. Free-cholesterol (FC) loading increased SPT activity and SM levels and resulted in ORMDL1 displacement from the ER to the cytoplasm [121]. Notably, serum starvation and ER stress did not result in ORMDL1 degradation.

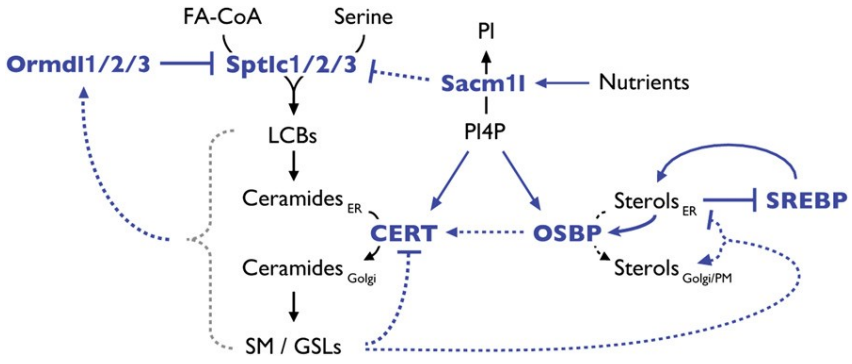

Figure 4. Regulation of sphingolipids through interconnected pathways [111].

Fluctuations in sphingolipid levels may be sensed via changes in sterol, glycerolipid and phospholipid levels, as these are metabolically connected to each other. Therefore, regulation of sphingolipid metabolism involves coordinated actions between these lipids (Fig. 4). Perry et al reported that sterols regulate sphingolipid metabolism, as the addition of 25-hydroxylcholesterol (25-HC) resulted in increased SM biosynthesis, which was shown to be OSBP, CERT and VAP dependent [122]. There seems to be interplay between OSBP, CERT, PI4K and Sac1. It was reported that OSBP transfers cholesterol to the Golgi and brings PI4P to the ER, where it is dephosphorylated by Sac1 to PI [123]. Interestingly, upon nutrient limitation [124] in mammals and glucose starvation in yeast [125, 126] Sac1 was shown to translocate from the ER to the Golgi, thereby depleting PI4P levels. On the other hand, OSBP seems to activate CERT, and OSBP itself is induced by SM reduction.

Phosphoinositide glycerolipids are interconnected to sphingolipids as well, especially because the PI4P phosphatase Sac1 was shown to be part of the SPOTS complex in yeast. Cells devoid of Sac1 were found to be resistant to myriocin (a potent inhibitor of SPT) [102]. As Sac1 relocates to the Golgi upon nutrient deprivation, it affects protein trafficking. Hence, this mechanism might have an effect on SL transport by CERT and FAPP2, as well as *de novo* SL biosynthesis, by changing SPOTS complex components and their localization. PI4P may therefore play a role in connecting SL biosynthesis, SL transport and protein secretion.

d) The role of small subunits ssSPTa/b in SPT activity

The small subunits of SPT (ssSPTa and ssSPTb) have been shown to be associated with SPTLC1/SPTLC2 and SPTLC1/SPTLC3 and to consequently increase SPT activity [127]. This increase was more distinct when ssSPTa was co-expressed together with SPT. Co-expression of ssSPTa and ssSPTb with other SPT subunits was proposed to alter the preference of the enzyme for different carbon chain length acyl-CoAs [127]. The expression of mammalian SPTLC1/SPTLC2/ssSPTa in a yeast strain devoid of endogenous SPT increased the preference for C16-CoA, which resulted in a preferential formation of C_{18}-based LCBs. On the other hand, yeast expressing the combination of SPTLC1/SPTLC3/ssSPTa had a preference for C_{14}-CoA, producing C_{16}-based LCBs. Interestingly co-expression with ssSPTb seems to induce the use of C_{18}-CoA thereby generating C_{20}-based SLs. Notably, the single residues Met in ssSPTa and Val in ssSPTb were reported to be responsible for this acyl-CoA preference [128]. Moreover, in a recently published report a somatic mutation in ssSPTb was found to be associated with elevated levels of C_{20}-long chain bases and linked to neurodegenerative effects in mice [129].

VII. ORMDL and asthma

Genome-wide association studies (GWAS) revealed a strong association of the single nucleotide polymorphism (SNP) *rs*7216389 with the risk of non-allergic childhood asthma [130, 131]. The SNP is located in an intronic region on chromosome 17q21 close to ORMDL3/gasdermin B (GSDMB) genes. This association was later confirmed by different studies in patients of various ethnicities [132-140]. However, it is not known

how the asthma predisposition 17q21 locus contributes to the disease itself. Asthma is a disease that is caused by a combination of genetic and environmental factors [141]. Moffatt et al reported that Epstein-Barr transformed lymphoblastoid cells had higher ORMDL3 expression levels associated with *rs*7216389 [130]. Hence, it was proposed that SNPs in this locus could influence the expression of ORMDL3. Additionally, expression of both GSDMB and ORMDL3 was found to be influenced by rhinovirus infection [142]. Transcript levels of GSDMB/ORMDL3 are associated with each other, which suggest that these two genes are co-regulated [143]. A transgenic hORMDL3zp3-Cre mouse model overexpressing the human ORMDL3 gene showed increased airway remodeling and elevated IgE response after an allergen challenge [144].

There are currently two mechanisms hypothesized to explain how ORMDL3 could be linked to asthma: 1) the upregulation of sarco/endoplasmic reticulum Ca^{2+}-ATPase (SERCA) pump activity, as ORMDL3 was shown to have a role in calcium signaling in the ER [145, 146] and thereby stimulating the unfolded protein response (UPR), leading to increased inflammation and airway remodeling. 2) A decrease in *de novo* SL production leading to bronchial hyperreactivity [147].

However, the exact role of sphingolipids and SPT activity in the pathomechanism of asthma is not clear. Worgall et al showed that decreasing *de novo* sphingolipid biosynthesis due to an intranasal treatment with the SPT inhibitor myriocin or using $Sptlc2^{+/-}$ mice (SPT heterozygous knockout mice with 60% less activity compared to the WT) led to elevated bronchial reactivity without inflammation [147]. However, a direct functional connection demonstrating that ORMDL3 expression levels influence SPT activity and thereby contributing to the asthma pathogenesis *in vivo* has not been demonstrated.

Aim of the study:

The aim of this thesis was to investigate the regulation of SPT activity in mammalian cells.

1. The first approach to study the mechanism of SPT inhibition was by investigating the role of ORMDL proteins in mammals. Since the yeast orthologues of ORM proteins were found to be negative regulators of SPT, we investigated whether these proteins play the same role in the mammalian system.
2. Moreover, the effect of exogenously added sphingolipids, namely C6Cer, was examined to confirm the feedback mechanism in mammalian cells. Studies in yeast have demonstrated the existence of feedback regulation based on sphingolipid availability in the cell. We further tested whether such feedback mechanism exists also in mammals.
3. Additionally, C6Cer metabolism in the cell was investigated to study which of the sphingolipid metabolites is being detected by the regulator of SPT. If increasing intracellular sphingolipids inhibit SPT, we pondered how this mechanism is mediated.

References

1. Hannun, Y.A. and L.M. Obeid, *Principles of bioactive lipid signalling: lessons from sphingolipids.* Nature Reviews Molecular Cell Biology, 2008. **9**(2): p. 139-150.
2. Smith, E.R., et al., *Effects of sphingosine and other sphingolipids on protein kinase C.* Methods Enzymol, 2000. **312**: p. 361-73.
3. Hannun, Y.A. and L.M. Obeid, *The Ceramide-centric Universe of Lipid-mediated Cell Regulation: Stress Encounters of the Lipid Kind.* Journal of Biological Chemistry, 2002. **277**(29): p. 25847-25850.
4. Hla, T., *Physiological and pathological actions of sphingosine 1-phosphate.* Semin Cell Dev Biol, 2004. **15**(5): p. 513-20.
5. Chalfant, C.E. and S. Spiegel, *Sphingosine 1-phosphate and ceramide 1-phosphate: expanding roles in cell signaling.* J Cell Sci, 2005. **118**(Pt 20): p. 4605-12.
6. Hanada, K., et al., *A mammalian homolog of the yeast LCB1 encodes a component of serine palmitoyltransferase, the enzyme catalyzing the first step in sphingolipid synthesis.* Journal of Biological Chemistry, 1997. **272**(51): p. 32108-32114.
7. Hanada, K., *Serine palmitoyltransferase, a key enzyme of sphingolipid metabolism.* Biochim Biophys Acta, 2003. **1632**(1-3): p. 16-30.
8. Nagiec, M.M., et al., *The LCB2 gene of Saccharomyces and the related LCB1 gene encode subunits of serine palmitoyltransferase, the initial enzyme in sphingolipid synthesis.* Proc Natl Acad Sci U S A, 1994. **91**(17): p. 7899-902.
9. Nagiec, M.M., R.L. Lester, and R.C. Dickson, *Sphingolipid synthesis: Identification and characterization of mammalian cDNAs encoding the Lcb2 subunit of serine palmitoyltransferase.* Gene, 1996. **177**(1-2): p. 237-241.
10. Weiss, B. and W. Stoffel, *Human and murine serine-palmitoyl-CoA transferase - Cloning, expression and characterization of the key enzyme in sphingolipid synthesis.* European Journal of Biochemistry, 1997. **249**(1): p. 239-247.
11. Merrill, A.H., Jr., *Characterization of serine palmitoyltransferase activity in Chinese hamster ovary cells.* Biochim Biophys Acta, 1983. **754**(3): p. 284-91.
12. Beeler, T., et al., *The Saccharomyces cerevisiae TSC10/YBR265w gene encoding 3-ketosphinganine reductase is identified in a screen for temperature-sensitive suppressors of the Ca2+-sensitive csg2 Delta mutant.* Journal of Biological Chemistry, 1998. **273**(46): p. 30688-30694.
13. Kihara, A. and Y. Igarashi, *FVT-1 is a mammalian 3-ketodihydrosphingosine reductase with an active site that faces the cytosolic side of the endoplasmic reticulum membrane.* J Biol Chem, 2004. **279**(47): p. 49243-50.
14. Levy, M. and A.H. Futerman, *Mammalian Ceramide Synthases.* IUBMB Life, 2010. **62**(5): p. 347-356.
15. Pewzner-Jung, Y., S. Ben-Dor, and A.H. Futerman, *When do Lasses (longevity assurance genes) become CerS (ceramide synthases)?: Insights into the regulation of ceramide synthesis.* J Biol Chem, 2006. **281**(35): p. 25001-5.
16. Pewzner-Jung, Y., et al., *A critical role for ceramide synthase 2 in liver homeostasis: I. alterations in lipid metabolic pathways.* J Biol Chem, 2010. **285**(14): p. 10902-10.
17. Venkataraman, K., et al., *Upstream of growth and differentiation factor 1 (uog1), a mammalian homolog of the yeast longevity assurance gene 1 (LAG1), regulates N-stearoyl-sphinganine (C18-(dihydro)ceramide) synthesis in a fumonisin B1-independent manner in mammalian cells.* J Biol Chem, 2002. **277**(38): p. 35642-9.
18. Riebeling, C., et al., *Two mammalian longevity assurance gene (LAG1) family members, trh1 and trh4, regulate dihydroceramide synthesis using different fatty acyl-CoA donors.* J Biol Chem, 2003. **278**(44): p. 43452-9.
19. Laviad, E.L., et al., *Characterization of ceramide synthase 2: tissue distribution, substrate specificity, and inhibition by sphingosine 1-phosphate.* J Biol Chem, 2008. **283**(9): p. 5677-84.
20. Mizutani, Y., A. Kihara, and Y. Igarashi, *Mammalian Lass6 and its related family members regulate synthesis of specific ceramides.* Biochem J, 2005. **390**(Pt 1): p. 263-71.
21. Mizutani, Y., A. Kihara, and Y. Igarashi, *LASS3 (longevity assurance homologue 3) is a mainly testis-specific (dihydro)ceramide synthase with relatively broad substrate specificity.* Biochem J, 2006. **398**(3): p. 531-8.
22. Michel, C., et al., *Characterization of ceramide synthesis - A dihydroceramide desaturase introduces the 4,5-trans-double bond of sphingosine at the level of dihydroceramide.* Journal of Biological Chemistry, 1997. **272**(36): p. 22432-22437.

23. Ternes, P., et al., *Identification and characterization of a sphingolipid Delta 4-desaturase family.* Journal of Biological Chemistry, 2002. **277**(28): p. 25512-25518.
24. Omae, F., et al., *DES2 protein is responsible for phytoceramide biosynthesis in the mouse small intestine.* Biochemical Journal, 2004. **379**: p. 687-695.
25. Mandon, E.C., et al., *Subcellular-Localization and Membrane Topology of Serine Palmitoyltransferase, 3-Dehydrosphinganine Reductase, and Sphinganine N-Acyltransferase in Mouse-Liver.* Journal of Biological Chemistry, 1992. **267**(16): p. 11144-11148.
26. Yasuda, S., M. Nishijima, and K. Hanada, *Localization, topology, and function of the LCB1 subunit of serine palmitoyltransferase in mammalian cells.* J Biol Chem, 2003. **278**(6): p. 4176-83.
27. Cadena, D.L., R.C. Kurten, and G.N. Gill, *The product of the MLD gene is a member of the membrane fatty acid desaturase family: overexpression of MLD inhibits EGF receptor biosynthesis.* Biochemistry, 1997. **36**(23): p. 6960-7.
28. Michel, C. and G. van Echten-Deckert, *Conversion of dihydroceramide to ceramide occurs at the cytosolic face of the endoplasmic reticulum.* FEBS Lett, 1997. **416**(2): p. 153-5.
29. Beauchamp, E., et al., *Myristic acid increases the activity of dihydroceramide Delta4-desaturase 1 through its N-terminal myristoylation.* Biochimie, 2007. **89**(12): p. 1553-61.
30. Enomoto, A., et al., *Dihydroceramide:sphinganine C-4-hydroxylation requires Des2 hydroxylase and the membrane form of cytochrome b5.* Biochem J, 2006. **397**(2): p. 289-95.
31. Hanada, K., et al., *Molecular machinery for non-vesicular trafficking of ceramide.* Nature, 2003. **426**(6968): p. 803-809.
32. Yamaji, T. and K. Hanada, *Sphingolipid metabolism and interorganellar transport: localization of sphingolipid enzymes and lipid transfer proteins.* Traffic, 2015. **16**(2): p. 101-22.
33. Halter, D., et al., *Pre- and post-Golgi translocation of glucosylceramide in glycosphingolipid synthesis.* J Cell Biol, 2007. **179**(1): p. 101-15.
34. Tafesse, F.G., et al., *Both sphingomyelin synthases SMS1 and SMS2 are required for sphingomyelin homeostasis and growth in human HeLa cells.* J Biol Chem, 2007. **282**(24): p. 17537-47.
35. Vacaru, A.M., et al., *Sphingomyelin synthase-related protein SMSr controls ceramide homeostasis in the ER.* J Cell Biol, 2009. **185**(6): p. 1013-27.
36. Tafesse, F.G., et al., *Sphingomyelin synthase-related protein SMSr is a suppressor of ceramide-induced mitochondrial apoptosis.* J Cell Sci, 2014. **127**(Pt 2): p. 445-54.
37. Ichikawa, S., et al., *Expression cloning of a cDNA for human ceramide glucosyltransferase that catalyzes the first glycosylation step of glycosphingolipid synthesis.* Proc Natl Acad Sci U S A, 1996. **93**(10): p. 4638-43.
38. D'Angelo, G., et al., *Glycosphingolipid synthesis requires FAPP2 transfer of glucosylceramide.* Nature, 2007. **449**(7158): p. 62-7.
39. Marks, D.L., et al., *Identification of active site residues in glucosylceramide synthase. A nucleotide-binding catalytic motif conserved with processive beta-glycosyltransferases.* J Biol Chem, 2001. **276**(28): p. 26492-8.
40. Jeckel, D., et al., *Glucosylceramide is synthesized at the cytosolic surface of various Golgi subfractions.* J Cell Biol, 1992. **117**(2): p. 259-67.
41. Schulte, S. and W. Stoffel, *Ceramide Udpgalactosyltransferase from Myelinating Rat-Brain - Purification, Cloning, and Expression.* Proceedings of the National Academy of Sciences of the United States of America, 1993. **90**(21): p. 10265-10269.
42. Stahl, N., et al., *Isolation, Characterization, and Expression of Cdna Clones That Encode Rat Udp-Galactose - Ceramide Galactosyltransferase.* Journal of Neuroscience Research, 1994. **38**(2): p. 234-242.
43. Kapitonov, D. and R.K. Yu, *Cloning, characterization, and expression of human ceramide galactosyltransferase cDNA.* Biochemical and Biophysical Research Communications, 1997. **232**(2): p. 449-453.
44. Bajjalieh, S.M., T.F.J. Martin, and E. Floor, *Synaptic Vesicle Ceramide Kinase - a Calcium-Stimulated Lipid Kinase That Co-Purifies with Brain Synaptic Vesicles.* Journal of Biological Chemistry, 1989. **264**(24): p. 14354-14360.
45. Kolesnick, R.N. and M.R. Hemer, *Characterization of a Ceramide Kinase-Activity from Human Leukemia (Hl-60) Cells - Separation from Diacylglycerol Kinase-Activity.* Journal of Biological Chemistry, 1990. **265**(31): p. 18803-18808.
46. Gomez-Munoz, A., et al., *New insights on the role of ceramide 1-phosphate in inflammation.* Biochim Biophys Acta, 2013.
47. Marchesini, N. and Y.A. Hannun, *Acid and neutral sphingomyelinases: roles and mechanisms of regulation.* Biochem Cell Biol, 2004. **82**(1): p. 27-44.

48. Marchesini, N., C. Luberto, and Y.A. Hannun, *Biochemical properties of mammalian neutral sphingomyelinase 2 and its role in sphingolipid metabolism.* J Biol Chem, 2003. **278**(16): p. 13775-83.
49. Kim, M.Y., et al., *Identification of sphingomyelin turnover as an effector mechanism for the action of tumor necrosis factor alpha and gamma-interferon. Specific role in cell differentiation.* J Biol Chem, 1991. **266**(1): p. 484-9.
50. Brenner, B., et al., *Fas/CD95/Apo-I activates the acidic sphingomyelinase via caspases.* Cell Death Differ, 1998. **5**(1): p. 29-37.
51. Goldkorn, T., et al., *H2O2 acts on cellular membranes to generate ceramide signaling and initiate apoptosis in tracheobronchial epithelial cells.* J Cell Sci, 1998. **111 (Pt 21)**: p. 3209-20.
52. Xu, R., et al., *Golgi alkaline ceramidase regulates cell proliferation and survival by controlling levels of sphingosine and S1P.* Faseb j, 2006. **20**(11): p. 1813-25.
53. Galadari, S., et al., *Identification of a novel amidase motif in neutral ceramidase.* Biochem J, 2006. **393**(Pt 3): p. 687-95.
54. Hait, N.C., et al., *Sphingosine kinases, sphingosine 1-phosphate, apoptosis and diseases.* Biochim Biophys Acta, 2006. **1758**(12): p. 2016-26.
55. Bandhuvula, P. and J.D. Saba, *Sphingosine-1-phosphate lyase in immunity and cancer: silencing the siren.* Trends Mol Med, 2007. **13**(5): p. 210-7.
56. Johnson, K.R., et al., *Role of human sphingosine-1-phosphate phosphatase 1 in the regulation of intra- and extracellular sphingosine-1-phosphate levels and cell viability.* J Biol Chem, 2003. **278**(36): p. 34541-7.
57. Ogretmen, B., et al., *Biochemical mechanisms of the generation of endogenous long chain ceramide in response to exogenous short chain ceramide in the A549 human lung adenocarcinoma cell line. Role for endogenous ceramide in mediating the action of exogenous ceramide.* J Biol Chem, 2002. **277**(15): p. 12960-9.
58. Gillard, B.K., R.G. Clement, and D.M. Marcus, *Variations among cell lines in the synthesis of sphingolipids in de novo and recycling pathways.* Glycobiology, 1998. **8**(9): p. 885-90.
59. Becker, K.P., et al., *Selective inhibition of juxtanuclear translocation of protein kinase C betaII by a negative feedback mechanism involving ceramide formed from the salvage pathway.* J Biol Chem, 2005. **280**(4): p. 2606-12.
60. Tettamanti, G., et al., *Salvage pathways in glycosphingolipid metabolism.* Biochimie, 2003. **85**(3-4): p. 423-37.
61. Ginzburg, L., Y. Kacher, and A.H. Futerman, *The pathogenesis of glycosphingolipid storage disorders.* Semin Cell Dev Biol, 2004. **15**(4): p. 417-31.
62. Schulze, H. and K. Sandhoff, *Lysosomal lipid storage diseases.* Cold Spring Harb Perspect Biol, 2011. **3**(6).
63. Kolter, T. and K. Sandhoff, *Sphingolipid metabolism diseases.* Biochimica Et Biophysica Acta-Biomembranes, 2006. **1758**(12): p. 2057-2079.
64. Park, J.H. and E.H. Schuchman, *Acid ceramidase and human disease.* Biochim Biophys Acta, 2006. **1758**(12): p. 2133-8.
65. Xu, Y.H., et al., *Viable mouse models of acid beta-glucosidase deficiency: the defect in Gaucher disease.* Am J Pathol, 2003. **163**(5): p. 2093-101.
66. Tybulewicz, V.L., et al., *Animal model of Gaucher's disease from targeted disruption of the mouse glucocerebrosidase gene.* Nature, 1992. **357**(6377): p. 407-10.
67. Horinouchi, K., et al., *Acid sphingomyelinase deficient mice: a model of types A and B Niemann-Pick disease.* Nat Genet, 1995. **10**(3): p. 288-93.
68. Ghidoni, R., G. Sala, and A. Giuliani, *Use of sphingolipid analogs: benefits and risks.* Biochim Biophys Acta, 1999. **1439**(1): p. 17-39.
69. Takeda, S., et al., *Apoptosis occurs via the ceramide recycling pathway in human HaCaT keratinocytes.* J Biochem, 2006. **139**(2): p. 255-62.
70. Chapman, J.V., et al., *Metabolism of short-chain ceramide by human cancer cells--implications for therapeutic approaches.* Biochem Pharmacol, 2010. **80**(3): p. 308-15.
71. Jiang, Y., et al., *Combinatorial therapies improve the therapeutic efficacy of nanoliposomal ceramide for pancreatic cancer.* Cancer Biol Ther, 2011. **12**(7): p. 574-85.
72. Lingwood, D. and K. Simons, *Lipid rafts as a membrane-organizing principle.* Science, 2010. **327**(5961): p. 46-50.
73. Zheng, W., et al., *Ceramides and other bioactive sphingolipid backbones in health and disease: lipidomic analysis, metabolism and roles in membrane structure, dynamics, signaling and autophagy.* Biochim Biophys Acta, 2006. **1758**(12): p. 1864-84.
74. Kumagai, K., et al., *CERT mediates intermembrane transfer of various molecular species of ceramides.* J Biol Chem, 2005. **280**(8): p. 6488-95.

75. Kumagai, K., et al., *Interorganelle trafficking of ceramide is regulated by phosphorylation-dependent cooperativity between the PH and START domains of CERT.* J Biol Chem, 2007. **282**(24): p. 17758-66.
76. Kumagai, K., M. Kawano-Kawada, and K. Hanada, *Phosphoregulation of the ceramide transport protein CERT at serine 315 in the interaction with VAMP-associated protein (VAP) for inter-organelle trafficking of ceramide in mammalian cells.* J Biol Chem, 2014. **289**(15): p. 10748-60.
77. Braun, P.E. and E.E. Snell, *The biosynthesis of dihydrosphingosine in cell-free preparations of Hansenula ciferri.* Proc Natl Acad Sci U S A, 1967. **58**(1): p. 298-303.
78. Hornemann, T., Y. Wei, and A. von Eckardstein, *Is the mammalian serine palmitoyltransferase a high-molecular-mass complex?* Biochem J, 2007. **405**(1): p. 157-64.
79. Hornemann, T., et al., *Cloning and initial characterization of a new subunit for mammalian serine-palmitoyltransferase.* J Biol Chem, 2006. **281**(49): p. 37275-81.
80. Hornemann, T., et al., *The SPTLC3 subunit of serine palmitoyltransferase generates short chain sphingoid bases.* J Biol Chem, 2009. **284**(39): p. 26322-30.
81. Fyrst, H., et al., *Characterization of free endogenous C14 and C16 sphingoid bases from Drosophila melanogaster.* J Lipid Res, 2004. **45**(1): p. 54-62.
82. Bejaoui, K., et al., *SPTLC1 is mutated in hereditary sensory neuropathy, type 1.* Nature genetics, 2001. **27**(3): p. 261-262.
83. Dawkins, J.L., et al., *Mutations in SPTLC1, encoding serine palmitoyltransferase, long chain base subunit-1, cause hereditary sensory neuropathy type I.* Nature genetics, 2001. **27**(3): p. 309-312.
84. Rotthier, A., et al., *Mutations in the SPTLC2 Subunit of Serine Palmitoyltransferase Cause Hereditary Sensory and Autonomic Neuropathy Type I.* American Journal of Human Genetics, 2010. **87**(4): p. 513-522.
85. Rotthier, A., et al., *Genes for hereditary sensory and autonomic neuropathies: a genotype-phenotype correlation.* Brain, 2009. **132**(Pt 10): p. 2699-711.
86. Auer-Grumbach, M., et al., *Mutations at Ser331 in the HSN type I gene SPTLC1 are associated with a distinct syndromic phenotype.* Eur J Med Genet, 2013. **56**(5): p. 266-9.
87. Ernst, D., et al., *Novel HSAN1 Mutation in Serine Palmitoyltransferase Resides at a Putative Phosphorylation Site That Is Involved in Regulating Substrate Specificity.* Neuromolecular Medicine, 2015. **17**(1): p. 47-57.
88. Suriyanarayanan, S., et al., *The Variant p.(Arg183Trp) in SPTLC2 Causes Late-Onset Hereditary Sensory Neuropathy.* NeuroMolecular Medicine, 2015. **18**(1): p. 81-90.
89. Bejaoui, K., et al., *SPTLC1 is mutated in hereditary sensory neuropathy, type 1.* Nat Genet, 2001. **27**(3): p. 261-2.
90. Auer-Grumbach, M., et al., *Molecular genetics of hereditary sensory neuropathies.* Neuromolecular Med, 2006. **8**(1-2): p. 147-58.
91. Murphy, S.M., et al., *Hereditary sensory and autonomic neuropathy type 1 (HSANI) caused by a novel mutation in SPTLC2.* Neurology, 2013. **80**(23): p. 2106-11.
92. Fridman, V., et al., *Natural history and biomarkers in hereditary sensory neuropathy type 1.* Muscle & Nerve, 2015. **51**(4): p. 489-495.
93. Auer-Grumbach, M., *Hereditary sensory neuropathy type I.* Orphanet Journal of Rare Diseases, 2008. **3**.
94. Houlden, H., et al., *Clinical, pathological and genetic characterization of hereditary sensory and autonomic neuropathy type 1 (HSAN I).* Brain, 2006. **129**: p. 411-425.
95. Penno, A., et al., *Hereditary sensory neuropathy type 1 is caused by the accumulation of two neurotoxic sphingolipids.* J Biol Chem, 2010. **285**(15): p. 11178-87.
96. Eichler, F.S., et al., *Overexpression of the wild-type SPT1 subunit lowers Desoxysphingolipid levels and rescues the phenotype of HSAN1.* J Neurosci, 2009. **29**(46): p. 14646-51.
97. Othman, A., et al., *Plasma deoxysphingolipids: a novel class of biomarkers for the metabolic syndrome?* Diabetologia, 2012. **55**(2): p. 421–431.
98. Bertea, M., et al., *Deoxysphingoid bases as plasma markers in diabetes mellitus.* Lipids Health Dis, 2010. **9**: p. 84.
99. Dohrn, M.F., et al., *Elevation of plasma 1-deoxy-sphingolipids in type 2 diabetes mellitus: a susceptibility to neuropathy?* Eur J Neurol, 2015. **22**(5): p. 806-14, e55.
100. Othman, A., et al., *Plasma 1-deoxysphingolipids are predictive biomarkers for type 2 diabetes mellitus.* BMJ Open Diabetes Res Care, 2015. **3**(1): p. e000073.
101. Bode, H., et al., *HSAN1 mutations in serine palmitoyltransferase reveal a close structure-function-phenotype relationship.* Hum Mol Genet, 2015.

102. Breslow, D.K., et al., *Orm family proteins mediate sphingolipid homeostasis.* Nature, 2010. **463**(7284): p. 1048-53.
103. Han, S., et al., *Orm1 and Orm2 are conserved endoplasmic reticulum membrane proteins regulating lipid homeostasis and protein quality control.* Proc Natl Acad Sci U S A, 2010. **107**(13): p. 5851-6.
104. Roelants, F.M., et al., *Protein kinase Ypk1 phosphorylates regulatory proteins Orm1 and Orm2 to control sphingolipid homeostasis in Saccharomyces cerevisiae.* Proc Natl Acad Sci U S A, 2011. **108**(48): p. 19222-7.
105. Sun, Y., et al., *Orm protein phosphoregulation mediates transient sphingolipid biosynthesis response to heat stress via the Pkh-Ypk and Cdc55-PP2A pathways.* Mol Biol Cell, 2012. **23**(12): p. 2388-98.
106. Shimobayashi, M., et al., *TORC1-regulated protein kinase Npr1 phosphorylates Orm to stimulate complex sphingolipid synthesis.* Mol Biol Cell, 2013. **24**(6): p. 870-81.
107. Liu, M., et al., *Regulation of sphingolipid synthesis through Orm1 and Orm2 in yeast.* J Cell Sci, 2012. **125**(Pt 10): p. 2428-35.
108. Gururaj, C., R. Federman, and A. Chang, *Orm Proteins Integrate Multiple Signals to Maintain Sphingolipid Homeostasis.* Journal of Biological Chemistry, 2013. **288**(28): p. 20453-20463.
109. Walther, T.C., *Keeping sphingolipid levels nORMal.* Proc Natl Acad Sci U S A, 2010. **107**(13): p. 5701-2.
110. Tafesse, F.G. and J.C. Holthuis, *Cell biology: A brake on lipid synthesis.* Nature, 2010. **463**(7284): p. 1028-9.
111. Breslow, D.K., Weissman, J.S., *Membranes in Balance: Mechanisms of Sphingolipid Homeostasis.* Molecular Cell, 2010. **40**: p. 267-279.
112. Gupta, S.D., et al., *Tsc10p and FVT1: topologically distinct short-chain reductases required for long-chain base synthesis in yeast and mammals.* J Lipid Res, 2009. **50**(8): p. 1630-40.
113. Berchtold, D., et al., *Plasma membrane stress induces relocalization of Slm proteins and activation of TORC2 to promote sphingolipid synthesis.* Nat Cell Biol, 2012. **14**(5): p. 542-7.
114. Niles, B.J., et al., *Plasma membrane recruitment and activation of the AGC kinase Ypk1 is mediated by target of rapamycin complex 2 (TORC2) and its effector proteins Slm1 and Slm2.* Proc Natl Acad Sci U S A, 2012. **109**(5): p. 1536-41.
115. Aronova, S., et al., *Regulation of ceramide biosynthesis by TOR complex 2.* Cell Metab, 2008. **7**(2): p. 148-58.
116. Hjelmqvist, L., et al., *ORMDL proteins are a conserved new family of endoplasmic reticulum membrane proteins.* Genome Biol, 2002. **3**(6): p. RESEARCH0027.
117. Kiefer, K., et al., *Coordinated regulation of the orosomucoid-like gene family expression controls de novo ceramide synthesis in mammalian cells.* J Biol Chem, 2015. **290**(5): p. 2822-30.
118. Siow, D.L. and B.W. Wattenberg, *Mammalian ORMDL proteins mediate the feedback response in ceramide biosynthesis.* J Biol Chem, 2012. **287**(48): p. 40198-204.
119. Siow, D., et al., *Regulation of de novo sphingolipid biosynthesis by the ORMDL proteins and sphingosine kinase-1.* Adv Biol Regul, 2015. **57**: p. 42-54.
120. Hagen-Euteneuer, N., et al., *Sphingosine 1-phosphate (S1P) lyase deficiency increases sphingolipid formation via recycling at the expense of de novo biosynthesis in neurons.* J Biol Chem, 2012. **287**(12): p. 9128-36.
121. Wang, S., et al., *ORMDL orosomucoid-like proteins are degraded by free-cholesterol-loading-induced autophagy.* Proc Natl Acad Sci U S A, 2015. **112**(12): p. 3728-33.
122. Perry, R.J. and N.D. Ridgway, *Oxysterol-binding protein and vesicle-associated membrane protein-associated protein are required for sterol-dependent activation of the ceramide transport protein.* Mol Biol Cell, 2006. **17**(6): p. 2604-16.
123. Mesmin, B., et al., *A four-step cycle driven by PI(4)P hydrolysis directs sterol/PI(4)P exchange by the ER-Golgi tether OSBP.* Cell, 2013. **155**(4): p. 830-43.
124. Blagoveshchenskaya, A., et al., *Integration of Golgi trafficking and growth factor signaling by the lipid phosphatase SAC1.* J Cell Biol, 2008. **180**(4): p. 803-12.
125. Faulhammer, F., et al., *Cell growth-dependent coordination of lipid signaling and glycosylation is mediated by interactions between Sac1p and Dpm1p.* J Cell Biol, 2005. **168**(2): p. 185-91.
126. Faulhammer, F., et al., *Growth control of Golgi phosphoinositides by reciprocal localization of sac1 lipid phosphatase and pik1 4-kinase.* Traffic, 2007. **8**(11): p. 1554-67.
127. Han, G., et al., *Identification of small subunits of mammalian serine palmitoyltransferase that confer distinct acyl-CoA substrate specificities.* Proc Natl Acad Sci U S A, 2009. **106**(20): p. 8186-91.

128. Harmon, J.M., et al., *Topological and functional characterization of the ssSPTs, small activating subunits of serine palmitoyltransferase.* J Biol Chem, 2013. **288**(14): p. 10144-53.
129. Zhao, L., et al., *Elevation of 20-carbon long chain bases due to a mutation in serine palmitoyltransferase small subunit b results in neurodegeneration.* Proc Natl Acad Sci U S A, 2015. **112**(42): p. 12962-7.
130. Moffatt, M.F., et al., *Genetic variants regulating ORMDL3 expression contribute to the risk of childhood asthma.* Nature, 2007. **448**(7152): p. 470-3.
131. Moffatt, M.F., et al., *A large-scale, consortium-based genomewide association study of asthma.* N Engl J Med, 2010. **363**(13): p. 1211-21.
132. Galanter, J., et al., *ORMDL3 gene is associated with asthma in three ethnically diverse populations.* Am J Respir Crit Care Med, 2008. **177**(11): p. 1194-200.
133. Hirota, T., et al., *Genetic polymorphism regulating ORM1-like 3 (Saccharomyces cerevisiae) expression is associated with childhood atopic asthma in a Japanese population.* Journal of Allergy and Clinical Immunology, 2008. **121**(3): p. 769-770.
134. Yang, F.F., et al., *Single nucleotide polymorphisms in the ORM1-like 3 gene associated with childhood asthma in a Chinese population.* Genet Mol Res, 2012. **11**(4): p. 4646-53.
135. Hrdlickova, B. and L.I. Holla, *Relationship between the 17q21 locus and adult asthma in a Czech population.* Hum Immunol, 2011. **72**(10): p. 921-5.
136. Ferreira, M.A., et al., *Association between ORMDL3, IL1RL1 and a deletion on chromosome 17q21 with asthma risk in Australia.* Eur J Hum Genet, 2011. **19**(4): p. 458-64.
137. Karunas, A.S., et al., *[Genome-wide association study of bronchial asthma in the Volga-Ural region of Russia].* Mol Biol (Mosk), 2011. **45**(6): p. 992-1003.
138. Leung, T.F., et al., *Asthma and atopy are associated with chromosome 17q21 markers in Chinese children.* Allergy, 2009. **64**(4): p. 621-8.
139. Tavendale, R., et al., *A polymorphism controlling ORMDL3 expression is associated with asthma that is poorly controlled by current medications.* Journal of Allergy and Clinical Immunology, 2008. **121**(4): p. 860-863.
140. Sleiman, P.M., et al., *ORMDL3 variants associated with asthma susceptibility in North Americans of European ancestry.* J Allergy Clin Immunol, 2008. **122**(6): p. 1225-7.
141. Drake, K.A., J.M. Galanter, and E.G. Burchard, *Race, ethnicity and social class and the complex etiologies of asthma.* Pharmacogenomics, 2008. **9**(4): p. 453-62.
142. Caliskan, M., et al., *Rhinovirus wheezing illness and genetic risk of childhood-onset asthma.* N Engl J Med, 2013. **368**(15): p. 1398-407.
143. Verlaan, D.J., et al., *Allele-specific chromatin remodeling in the ZPBP2/GSDMB/ORMDL3 locus associated with the risk of asthma and autoimmune disease.* Am J Hum Genet, 2009. **85**(3): p. 377-93.
144. Miller, M., et al., *ORMDL3 transgenic mice have increased airway remodeling and airway responsiveness characteristic of asthma.* J Immunol, 2014. **192**(8): p. 3475-87.
145. Carreras-Sureda, A., et al., *ORMDL3 modulates store-operated calcium entry and lymphocyte activation.* Human Molecular Genetics, 2013. **22**(3): p. 519-530.
146. Cantero-Recasens, G., et al., *The asthma-associated ORMDL3 gene product regulates endoplasmic reticulum-mediated calcium signaling and cellular stress.* Human Molecular Genetics, 2010. **19**(1): p. 111-121.
147. Worgall, T.S., et al., *Impaired sphingolipid synthesis in the respiratory tract induces airway hyperreactivity.* Sci Transl Med, 2013. **5**(186): p. 186ra67.

Chapter 1:

ORMDL3 EXPRESSION LEVELS HAVE NO INFLUENCE ON SPHINGOLIPID DE NOVO SYNTHESIS

Assem Zhakupova[1*], Nincy Debeuf[2, 3*], Michiel Krols[4], Wendy Toussaint[2, 3], Leen Vanhoutte[2, 5], Irina Alecu[1], Zoltán Kutalik[6,7], Peter Vollenweider[8], Daniela Ernst[1], Arnold von Eckardstein[1], Bart N. Lambrecht[2, 3, 9], Sophie Janssens[2, 3], Thorsten Hornemann[1#]

(submitted to FASEB journal)

1- Institute of Clinical Chemistry, University of Zurich and University Hospital Zurich, Switzerland;
2- Laboratory of Immunoregulation and Mucosal Immunology, Inflammation Research Center, VIB, Ghent, Belgium;
3- Department of Internal Medicine, Ghent University, Ghent, Belgium;
4- Department of Molecular Genetics, VIB-Antwerp University, Antwerp, Belgium;
5- Department of Biomedical Molecular Biology, Ghent University, Ghent, Belgium
6- Institute of Social and Preventive Medicine (IUMSP), Centre Hospitalier Universitaire Vaudois (CHUV), University of Lausanne, Lausanne, Switzerland;
7- Swiss Institute of Bioinformatics, Lausanne, Switzerland;
8- Department of Medicine, Internal Medicine, Centre Hospitalier Universitaire Vaudois (CHUV), Lausanne, Switzerland;
9- Department of Pulmonary Medicine, Erasmus Medical Center, Rotterdam, Netherlands.

* contributed equally to this work

corresponding author:
Thorsten Hornemann
Institute of Clinical Chemistry
University and University Hospital of Zurich,
Raemistrasse 100,
CH-8091 Zurich
Switzerland

Abstract

Objective: ORMDL proteins are believed to be negative regulators of serine palmitoyltransferase (SPT), which catalyzes the rate limiting step in sphingolipid *de novo* synthesis. Several SNPs close to the ORMDL3 locus were reported to be associated with increased ORMDL3 expression and the risk for early childhood asthma. However, the effect of ORMDL3 on SPT activity and sphingolipid formation and its link to asthma remains elusive. In this study we investigated whether ORMDL3 expression is associated with changes in SPT activity and altered total sphingolipid levels.

Methods: Ormdl3 knock-out ($Ormdl3^{-/-}$) and transgenic ($Ormdl3^{Tg/wt}$) mice were generated to study the effect of ORMDL3 on total sphingolipid levels in plasma and tissues. Cellular SPT activity was measured using an isotope labelling assay in mouse embryonic fibroblasts (MEFs) from $Ormdl3^{-/-}$ mice, as well as in ORMDL1, 2 and 3 overexpressing and silenced HEK293 cells under various conditions. In addition, we analyzed the association of the reported ORMDL3 asthma SNPs with total plasma sphingoid base levels in a population based cohort with 971 individuals.

Results: Total C_{18}-sphingoid base levels were not altered in $Ormdl3^{-/-}$ mice, except for a slight but significant elevation of C_{18}-sphinganine levels in some individual tissues. SPT activity was not changed in MEF cells from $Ormdl3^{-/-}$ mice compared to those from $Ormdl3^{+/-}$ and $Ormdl3^{+/+}$ mice. The individual overexpression or knockdown of ORMDL1, 2 or 3 in HEK293 cells did not influence cellular SPT activity, whereas the parallel knockdown of all three ORMDL isoforms increased enzyme activity significantly. Moreover, none of the annotated asthma SNPs in ORMDL3 were associated with altered plasma sphingolipid levels in patients from a clinical cohort.

Conclusion: In conclusion, ORMDL3 expression levels appear not to be directly associated with changes in total sphingolipid levels neither with changes in SPT activity or sphingolipid *de novo* synthesis.

Abbreviations:

C_{18}-sphingosine – C18SO, C_{18}-sphinganine – C18SA, C_6-ceramide – C6Cer, SL – sphingolipid

Introduction

Sphingolipids (SLs) are a highly diverse class of lipids that play important roles in cell physiology [1]. Sphingolipid *de novo* synthesis starts with the formation of a long chain base (LCB) by the condensation of L-serine and palmitoyl-CoA, catalyzed by the enzyme serine palmitoyltransferase (SPT) [2, 3]. SPT consists of three subunits (SPTLC1, SPTLC2 and SPTLC3) [4, 5] and can also metabolize other acyl-CoAs (C_{12}-C_{20}) as well as other amino acids, thereby generating a diverse spectrum of atypical LCBs [5, 6]. The product of the SPT reaction, 3-keto-dihydro-sphingosine (3KDS), is rapidly reduced to sphinganine (C18SA) [7] which is then acylated by ceramide synthases (CerS1-6) to form dihydroceramide [8]. Next, a 4-5 trans double bond is introduced into the C18SA backbone by dihydroceramide desaturase 1 (DES1), which forms ceramide. Ceramide itself is then typically conjugated to a variety of headgroups forming complex sphingolipids like sphingomyelins or glucosylceramide. The variability in head groups can form several hundred sphingolipid subspecies. Among total sphingolipids in human plasma about 60% contain a C18SO and 10% a C18SA backbone [9].

In yeast, SPT activity is regulated by a negative metabolic feedback loop to prevent harmful overproduction of the pro-apoptotic ceramides. This regulation is mediated by Orm1 and Orm2 proteins [10-16] that act as inhibitors of SPT [10, 17, 18]. In yeast, Orm1 and 2 form a complex together with the SPT subunits and the proteins Tsc3 and Sac1 termed SPOTS (Serine Palmitoyltransferase, Orm1/2, Tsc3, and Sac1) [10]. Upon sphingolipid deficiency, Orm proteins get phosphorylated by Ypk1 and Npr1 via TOR complex 1 and 2 (TORC1/2) dependent pathways [12-14]. When phosphorylated, Orm proteins dissociate from SPT and release the inhibition, which then leads to increased *de novo* sphingolipid synthesis [17, 18].

However, in mammalian cells the role of the ORM proteins as regulators of SPT activity seems to be distinct from that in yeast and is not fully understood. In contrast to yeast, mammalian cells have three ORM isoforms (ORMDL1-3) and the phosphorylation sites reported in yeast are not conserved in the mammalian orthologues [19]. The ORMDL proteins are ubiquitously expressed in almost all human tissues [19].

Wide-spread attention was given to the observation that single nucleotide polymorphisms (SNPs) in the ORMDL3/GSDMB locus (chr17q21) were significantly associated with the risk of early childhood asthma [20, 21]. This association was later

confirmed in other genome-wide association studies (GWAS) and in cohorts with different ethnicities [22-30]. Interestingly, the very same ORMDL3 SNPs were also found to be associated with other autoimmune related disorders like Crohn's disease [31], type 1 diabetes [32] and ulcerative colitis [33]. Asthma is typically caused by a combination of genetic and environmental factors [34]. How exactly ORMDL3 contributes to asthma is not known, but the reported function of ORMDL3 as a regulator of SPT suggests that SPT activity and sphingolipid *de novo* synthesis is involved in this process. Moffatt et al [20] reported that the SNP *rs*7216389, which showed the strongest association with childhood asthma, was also functionally associated with increased ORMDL3 expression, indicating a suppression of SPT activity. Decreasing levels of newly synthesized sphingolipids in mice, either by intranasal inhalation of the SPT inhibitor myriocin or in heterozygous Sptlc2$^{+/-}$ KO mice, led to increased bronchial reactivity [35]. The involvement of ORMDL3 in airway inflammation and airway remodeling was tested in a transgenic mouse model overexpressing the human ORMDL3 gene [36]. However, no analysis of the sphingolipid levels or SPT activity was performed. Despite this set of evidences a functional link between ORMDL3 expression and altered sphingolipid *de novo* synthesis has not yet been demonstrated. The aim of this study was to investigate the role of the ORMDLs, in particular of ORMDL3, as putative regulators of mammalian SPT and sphingolipid *de novo* synthesis.

Methods

Mice

Ormdl3 knockout (Ormdl3$^{-/-}$) mice, Ormdl3 transgenic (Ormdl3$^{Tg/wt}$) mice and wildtype littermates were bred under specific-pathogen-free conditions at the animal house of the VIB/UGent Inflammation Research Center. All mice were backcrossed for at least 10 crosses onto a C57BL/6 background. Flp expressing mice (tg(actflpe)9205dym strain) and Sox2-Cre mice (Tg(Sox2-cre)1Amc/J strain) were obtained from Jackson laboratories. Ormdl3$^{-/-}$ mice and wildtype controls were between 6-8 weeks of age. Ormdl3$^{Tg/wt}$ mice and wildtype littermates were 13-14 weeks of age. Male and female mice were used. All performed animal procedures were approved by the ethical committee of Ghent University.

Construction of Ormdl3 knockout mice

To generate Ormdl3 knockout mice, a targeting construct of the EUCOMM consortium (project 72180) was inserted into the first intron of the Ormdl3 gene (see Fig. 1). In this construct, 2 FRT sites were flanking a sequence consisting of an En2 splice acceptor site, an internal ribosome entry site, a lacZ sequence, a polyA-tail, a loxP site and a neomycin coding sequence driven by a human β-actin promoter. Exon 2, 3 and part of exon 4 of the Ormdl3 gene were flanked by 2 other loxP sites. Removal of the lacZ/neo cassette was achieved by crossing the Ormdl3LacZ mice with Flp expressing mice (tg(actflpe)9205dym strain). The obtained Ormdl3Fl mice were further crossed with mice expressing the Cre recombinase behind the Sox2 promoter (Tg(Sox2-cre)1Amc/J strain) to generate full knockout mice.

Generation of Ormdl3 transgenic mice

The transgenic Ormdl3 overexpressing mouse was generated by injection of a 34 kb genomic BAC fragment into the pronuclei of C57BL/6 zygotes. To allow screening of the randomly integrated transgene, the 3´end of the injection fragment was modified by inserting a FRT-Kan/Neo-FRT into BAC RP24-346O10 using RedET recombination in E. coli (Francis Stewarts method [37]). Using Flpe, the selection cassette was removed, leaving one FRT site intact. PCR primers designed around the FRT site allowed discrimination of the transgene over the wildtype locus. The modified BAC was digested

by SnaBI and the 34 kb fragment containing the murine Ormdl3 locus was separated by PFGE, isolated using electro elution and washed and concentrated using an Amicon Ultra filter unit (Millipore).

Isolation of mouse embryonic fibroblasts (MEFs)

Embryonic day 13.5-14.5 embryos were dissected from timed pregnant females. Following removal of the heads and internal organs, embryos were minced and the tissue suspension was incubated with 110 µl of trypsin (0.2% in EDTA) for 20 minutes at 37°C. The cell suspension (passage 1) was transferred to a T75 flask and cultured in DMEM supplemented with 10% (vol/vol) FCS, 0.1% beta-mercaptoethanol, 0.2% penicillin/streptomycin, 1% glutamine and 1% non-essential amino acids (NEAA). Twenty-four hours later, the embryonic fibroblast culture was split and designated as passage 2. Immortalization was done in passage 3 by transfecting the cells with 2 µg large T antigen expression vector using Fugene. Cells were split 1/10 multiple rounds to negatively select against non-transformed cells.

RT-qPCR

Total RNA was isolated from mouse lung tissues using the AurumTM Total RNA Mini Kit (Bio-Rad). One µg of RNA was converted to cDNA by an iScript advanced reverse transcriptase (Bio-Rad), according to the manufacturer's instructions. The target cDNA was amplified by 30 cycles of PCR using the following primers: Ormdl3 forward primer: CCC TCA CCA ACC TTA TCC AC; Ormdl3 reverse primer: GGA CCC CGT AGT CCA TCT G and universal probe #109 (Universal Probe Library, Roche). Expression levels were calculated by qBase+ software (Biogazelle) and normalized to the reference genes hmbs and sdha, which had the highest stability amongst four analyzed reference genes. Hmbs forward primer: GAA ACT CTG CTT CGC TGC ATT; hmbs reverse primer: TGC CCA TCT TTC ATC ACT GTA TG; sdha forward primer: TTT CAG AGA CGG CCA TGA TCT; sdha reverse primer: TGG GAA TCC CAC CCA TGT T.

Generation of stable SPT and ORMDL overexpressing cell lines

HEK293 cells were grown to 70-90% confluence. Four µg of DNA (SPTLC1-2, ORMDL1-3) were added to 400 µL of Opti-MEM; 6µL of TurboFect *in vitro* transfection reagent (Fermentas) was added to the DNA mix and incubated for 20 min at RT. Afterwards 400 µL of the TurboFect/DNA mixture was added drop-wise to HEK293 cells. Twenty-four to

48 hours after transfection, cells were grown in DMEM containing 4 µg/mL Geneticin (Gibco, Thermo Scientific). Overexpression of the plasmids was confirmed by western blotting using V5 and His-antibodies (Serotec).

Stable isotope labelling assay to measure SPT activity

Approximately 200,000 cells were grown for three days in DMEM (Sigma Aldrich) containing 10% fetal bovine serum (Gibco, Life Technologies) and 1% penicillin/streptomycin (100 U/ml, Sigma Aldrich). Afterwards the medium was exchanged to L-serine free DMEM (Genaxxon, Ulm, Germany) containing either 10% serum or 10% delipidated serum (Sigma Aldrich). Four hours later the cells were treated with the isotope labeled deuterated substrate 1mM L-serine (2,3,3-D3, 98%; 15N, 98%) (Cambridge Isotopes). Following 24 h incubation, cells were washed once with PBS, collected in 900 µl of PBS and counted (Z2 Coulter Counter, Beckman Coulter, CA). The cells were pelleted by centrifugation (1200g x 5min, at 4°C) and stored at -20°C.

C_6-ceramide treatment

HEK293 cells stably expressing ORMDL1-3 were treated with C_6-ceramide (Sigma-Aldrich; C6Cer was dissolved in ethanol and stored as 5mg/mL stock solution at -20°C), to a final concentration of 5 µM and 10 µM. The treatment was followed by the aforementioned stable isotope labelling assay to measure SPT activity.

siRNA knockdown of ORMDL genes

About 200,000 HEK293 cells were seeded and grown to 70% confluency. The following transfection strategy was used in 6-well plate: 200nmol siRNA – 10 µM siRNA in 80 µL of Opti-MEM (Solution A) was incubated for 30min together with Solution B containing 20 µL Lipofectamine transfection reagent with 80 µL of Opti-MEM. Afterwards 800 µL of Opti-MEM was added to the mix. One mL of siRNA/transfection mix per well was added. The following siRNA sequences were used (Microsynth, Switzerland): ORMDL1 5'-ACA CAG CUU CUC UCC UGA GTT-3'; ORMDL2 5'-AGG CUC GGC UAC UGA CAC ATT-3'; ORMDL3 5'-AAG UAC GAC CAG AUC CAU UTT-3'; n.t. 5'-AGG UAG UGU AAU CGC CUU GTT-3'.

Animal tissue homogenization

Animal tissues from liver, lung and brain were homogenized in lysis buffer (25 mmol/l HEPES pH 8, 0.2% Triton X-100 [vol./vol.]) using a Precellys 24 tissue homogenizer (Bertin Technologies, Montigny-le-Bretonneux, France). Protein concentration was determined using the Bradford assay. A volume containing 100µg protein was filled up to 100 µL with PBS for the sphingolipid extraction.

Lipid extraction and sphingoid base analysis

Five hundred µL of methanol (Honeywell) containing 200 pmol of internal standards (d7-sphinganine and d7-sphingosine, Avanti Polar Lipids) were added to cell pellets dissolved in 100 µL of PBS or 100 µL of serum or tissue homogenate containing 100 µg of protein, followed by gentle agitation at 37°C and 1400 rpm for 1 hour (Thermomixer comfort, Eppendorf; Hamburg, Germany). Samples were then centrifuged at 16,000g x 5min to pellet precipitated proteins and the supernatant was transferred to a new 2mL Eppendorf tube. HCl (≥32%, Sigma-Aldrich) was added and lipids were hydrolyzed for 16h at 65°C and neutralized with 10M KOH. Afterwards free sphingoid bases were extracted by adding chloroform (99.8%, Sigma-Aldrich) in basic conditions containing 2N ammoniac (Sigma-Aldrich). The sphingoid bases were analyzed using TSQ Quantum Ultra and Q Exactive liquid chromatography-mass spectrometers as previously described [38, 39].

SNP Analysis

For the Cohorte Lausannoise (CoLaus) study, genotyping was performed using the Affymetrix GeneChip Human Mapping 500 K array set. Genotypes were called using BRLMM [40]. Duplicate individuals, and first and second degree relatives, were identified by computing genomic identity-by-descent coefficients using PLINK [41]. The younger individual from each duplicate or relative pair was removed. Individuals with a call rate below 90% were excluded from further analysis. The full set of unmeasured HapMap II SNPs (release 21) was imputed using 390,631 measured SNPs (with Hardy-Weinberg P-value above 10^{-7} and MAF above 1%). Imputation was performed using IMPUTE [42] version 0.2.0. Expected allele dosages were computed for 2,557,249 SNPs.
The sphingoid base profile was analyzed in 971 individuals selected from the CoLaus cohort as described previously [38, 39]. The association of 12 sphingoid bases with the

previously reported and asthma associated ORMDL3 SNPs (rs2290400, rs3894194, rs7216389, rs3859192, rs11650680) was analyzed.

Statistical Analysis

Statistical analysis was done using GraphPad Prism 5.

Results

Generation and validation of Ormdl3 knockout and transgenic mice

To generate Ormdl3 knockout mice, a targeting construct obtained from the EUCOMM Consortium (project 72180) was inserted into the first intron of Ormdl3 (Fig.1A). The LacZ/neo cassette was removed by crossing these mice with Flp expressing mice. Subsequent crossing with Sox2-Cre mice removed loxP-sequences flanking exon 2, 3 and 4 (Fig. 1A). This led to full Ormdl3 knockout mice. Ormdl3 gene expression levels were assessed in lungs from homozygous KO ($Ormdl3^{-/-}$), heterozygous ($Ormdl3^{+/-}$) and wildtype ($Ormdl3^{+/+}$) mice by qPCR (Fig. 1B). We observed a dose dependent reduction in Ormdl3 mRNA expression levels, which confirmed the functional deletion of the Ormdl3 gene in the knockout allele.

Transgenic Ormdl3 overexpressing mice ($Ormdl3^{Tg/wt}$) were designed through a BAC transgenic approach (Fig. 2A). In order to obtain physiological regulation of Ormdl3 expression levels, the Ormdl3 gene was expressed under the control of its own promoter. Although this may cause variations in expression levels for different tissues, we consistently observed higher Ormdl3 transcript levels in $Ormdl3^{Tg/wt}$ mice compared to their wildtype littermates (Fig. 2B). Moreover, we also measured Ormdl1 and Ormdl2 mRNA expression in lung tissue. Only the levels of Ormdl3, but not those of Ormdl1 and Ormdl2, were changed in $Ormdl3^{-/-}$ (Fig. 1C) and $Ormdl3^{Tg/wt}$ mice (Fig. 2C).

C18-sphinganine is elevated in plasma and tissues of Ormdl3 knock-out mice

To investigate whether ORMDL3 has an influence on sphingolipid formation, we compared the total sphingoid base content in plasma and tissue samples from $Ormdl3^{+/+}$, $Ormdl3^{+/-}$, $Ormdl3^{-/-}$, $Ormdl3^{Tg/wt}$ and $Ormdl3^{wt/wt}$ mice. As we were primarily interested in SPT activity as a target of ORMDL3 regulation, we subjected the total extracted sphingolipids to a chemical hydrolysis step to remove the N-acyl chain and headgroups. The released sphingoid bases are a measure of the total cellular sphingolipid levels. In total ten different sphingoid bases were analyzed. C_{18}-sphingosine (C18SO) is the predominant sphingoid base, which makes up more than 61% of the total sphingoid bases in plasma [9].

No differences in C18SO levels in plasma (Fig. 3A left panel), lung (Fig. 3B left panel) and liver (Fig. 4A left panel) were observed between $Ormdl3^{-/-}$ mice, $Ormdl3^{+/+}$

and Ormdl3$^{+/-}$ mice. However, C18SA levels were slightly but significantly elevated in plasma (Fig. 3A right panel) and liver (Fig.4A right panel) of Ormdl3$^{-/-}$ mice. In lung, C18SA levels (Fig. 3B right panel) were higher in Ormdl3$^{-/-}$ mice compared to Ormdl3$^{+/-}$ mice but not compared to Ormdl3$^{+/+}$ mice. No difference in C18SO and C18SA levels was seen in brain tissues (Fig. 4B). Also in transgenic Ormdl3$^{Tg/wt}$ mice in which Ormdl3 levels were elevated, no significant changes in C18SO and C18SA levels were observed in neither plasma nor tissues (Fig. 3-4). Overall, we could not detect a consistent change in C18SO and C18SA levels neither in Ormdl3$^{-/-}$ nor in Ormdl3$^{Tg/wt}$ mice.

Although palmitoyl-CoA is a preferred substrate, SPT can also metabolize other acyl-CoAs in the range of C_{14}-C_{20}, thereby generating sphingoid bases with different carbon chain lengths [5]. Therefore, we also compared the profile of atypical sphingoid bases in Ormdl3$^{-/-}$ compared to Ormdl3$^{+/+}$ and Ormdl3$^{+/-}$, Ormdl3$^{Tg/wt}$ compared to Ormdl3$^{wt/wt}$ mice (Supplemental Fig. 1). We observed slightly increased levels of C_{18}-sphingadiene in plasma (Supplemental Fig. 1A), lung and brain of Ormdl3$^{+/+}$ mice, while C20SO levels were elevated in brain of Ormdl3$^{+/+}$ mice (Supplemental Fig. 1B). However, apart from these minor differences, atypical sphingoid bases were also not consistently changed in Ormdl3$^{-/-}$ and Ormdl3$^{Tg/wt}$ mice.

SPT activity is not altered in mouse embryonic fibroblasts (MEFs) from Ormdl3$^{-/-}$ mice

As we observed increased C18SA levels in some tissues of Ormdl3$^{-/-}$ mice, next we wanted to see if SPT activity was altered in these mice. We therefore compared SPT activity in MEF cells generated from Ormdl3$^{+/+}$, Ormdl3$^{+/-}$ and Ormdl3$^{-/-}$ mice by measuring time dependent incorporation of stable isotope labeled D3-N15-L-serine into *de novo* formed sphingoid bases. As the condensation reaction leads to a loss of one deuterium, resulting sphingoid bases show a shift in mass over charge (*m/z*) of +3 Da. Also, to control for the potential influence of sphingolipids provided in the cell media we cultured cells in the presence of either 10% normal or 10% delipidated serum (for the sphingoid base composition in the media see Supplemental Fig. 2). We did not observe any difference in *de novo* formed C18SO (d3-C18SO) and C18SA (d3-C18SA) when comparing MEFs from Ormdl3$^{+/+}$, Ormdl3$^{+/-}$ and Ormdl3$^{-/-}$ mice (Fig. 5). However, total SPT activity was slightly increased in the cells which were cultured under delipidated conditions, indicating that the presence of sphingolipids in the medium influences SL *de novo* synthesis, although this effect seems to be independent of ORMDL3 (Fig. 5).

Overexpression of ORMDL1-3 in HEK293 cells does not have an effect on SPT activity

As we did not observe any altered SPT activity in Ormdl3 deficient cells, we tested whether overexpression of the individual ORMDL isoforms influences SPT activity. We therefore transfected and expressed human ORMDL1, 2 and 3 in HEK293 cells. Expression was confirmed by western blot (Fig. 6A). Like before, cells were cultured in the presence of 10% normal or delipidated serum. Overall, SPT activity was not altered in ORMDL1, 2 or 3 overexpressing HEK293 cells (Fig. 6B). As with the MEF cells, we observed a slight but significant increase in *de novo* formed C18SL (d3-C18SO and d3-C18SA) levels for the cells, which were grown in delipidated media conditions (Fig. 6B), but this effect was independent of the expressed ORMDL proteins.

One possible explanation for the absence of the effect of ORMDL overexpression on SPT activity could be the lack of a stoichiometric binding partner. To test this we used HEK293 cells that stably overexpressed the SPTLC1 or 2 subunits of SPT and co-transfected these cells individually with ORMDL1, 2 and 3. Overexpressing SPTLC2 increased SPT activity about two-fold, which is in alignment with an earlier report [43]. However, we did not see any significant changes in activity in response to the co-expression of the ORMDL isoforms (Fig. 6C).

Complementary to overexpression, we performed a knockdown of endogenous ORMDLs in HEK293 cells by transfecting siRNA individually against ORMDL1, 2 and 3 or against all ORMDL isoforms in parallel. We obtained between 45% and 57% silencing as shown by RT-PCR (Supplemental Fig. 3A). The individual knockdown of ORMDL1, 2 or 3 showed no effect (Supplemental Fig. 3B), whereas the simultaneous knockdown of all three ORMDL isoforms resulted in a significant increase in SPT activity (Fig. 6D).

As neither the overexpression nor the silencing of the individual ORMDL isoforms had any significant influence on SPT activity, we tested whether ORMDLs have an influence when SPT activity is metabolically suppressed. For that we treated cells with the membrane permeable C_6-ceramide (C6Cer), which increases intracellular sphingolipid levels and significantly inhibit SPT activity. In line with earlier reports [44], we observed a significant suppression of SPT activity after treating cells with 5μM and 10μM C6Cer. However, this suppressive effect was not altered when overexpressing the individual ORMDL isoforms (Fig. 6E).

SNPs in ORMDL3/GSDMA/GSDMB genes did not show significant association with plasma sphingolipids

Several SNPs in chromosome locus 17q21 close to the ORMDL3/GSDMB gene have been shown to be associated with childhood-onset asthma [20, 21]. One of the suggested asthma causing mechanisms is an effect of ORMDL3 on sphingolipid formation by modulating SPT activity. Therefore, we analyzed the sphingoid base profile in plasma samples from 971 individuals selected from the Cohort Lausanne (CoLaus) study [45-47]. SNP data were available for all analyzed individuals. Genome wide significance was considered for $P<0.001$. The SNP rs7216389, which showed the strongest association with childhood asthma and reported to be associated with increased ORMDL3 expression, had no significant effect on plasma C18SO and C18SA levels (Fig. 7A, B). Neither did any of the other asthma associated ORMDL3/GSDMA SNPs showed any significant association with typical or atypical plasma sphingoid base levels (Supplementary Table 1).

Discussion

SPT catalyzes the formation of long chain bases (LCBs), which serve as backbones for all sphingolipids. ORMDL proteins are believed to be negative regulators of SPT, although most of the reported findings are from yeast [10, 11]. Mammals express three ORMDL isoforms (ORMDL 1, 2 and 3), but ORMDL3 drew a special attention due to its association with asthma [20]. In this study we analyzed for the first time the sphingoid base profile in the ORMDL knockout (Ormdl3$^{-/-}$) and transgenic (Ormdl3$^{Tg/wt}$) mouse models. We showed that ORMDL3 expression was not associated with any changes in either total sphingolipid levels or SPT activity.

We also analyzed the total C18SO and C18SA content in plasma, liver, lung and brain tissues of these mice and did not observe any consistent change in total sphingolipid levels in response to abolished (Ormdl3$^{-/-}$) or augmented (Ormdl3$^{Tg/wt}$) Ormdl3 expression. However, in some tissues from Ormdl3$^{-/-}$ mice we observed a small but significant increase in total C18SA levels which is, however, only a minor fraction compared to the dominant downstream product C18SO. As both C18SA and C18SO are formed downstream of SPT, an isolated increase of C18SA levels without a concomitant change of C18SO cannot be explained by altered SPT activity. In our conditions an increase in C18SA could be expected when the activity of the converting enzymes CerS or DES1 is reduced. A functional interaction of ORMDL3 with CerS or DES1 was not yet reported, but a recent report showed significant changes in the ceramide species in response to ORMDL3 overexpression and knockdown [48]. Silencing of ORMDL3 primarily increased C24:0 and C24:1 ceramide species, indicating that ORMDL3 might influence the activity of certain CerS enzymes. However, changes in SPT activity should result in altered total sphingolipid levels rather than individual ceramide species. For example, an increase in SPT activity by overexpressing the catalytically active SPTLC2 subunit results in a general elevation of all sphingoid bases (Fig. 6C).

To directly assess cellular SPT activity we also measured the incorporation of stable isotope labeled L-serine into total *de novo* formed sphingolipids over time. SPT activity was not altered in MEF cells from Ormdl3$^{-/-}$ mice compared to Ormdl3$^{+/-}$ and Ormdl3$^{+/+}$ mice. Furthermore, neither the individual overexpression of ORMDL1, 2 or 3 nor the knockdown of the individual ORMDL isoforms by siRNA had any significant effect on SPT activity. This is also in agreement with earlier findings in HeLa and

HEK293 cells, which indicated that knockdown or overexpression of individual ORMDL isoforms did not alter ceramide biosynthesis [10, 44]. However, the parallel knockdown of all three ORMDL isoforms increased SPT activity in HEK293 cells, which is also in line with the previous findings [10, 44]. The individual ORMDL isoforms have about 80% similarity to each other [19]. The fact that a reduction of all three ORMDL isoforms is required to alter SPT activity suggests that ORMDL proteins are redundant and that individual changes in ORMDL3 expression can be compensated for by other ORMDL isoforms.

The observation that neither the individual overexpression nor the knockdown of ORMDL3 had an effect on sphingolipid levels or SPT activity further indicates that a change in ORMDL3 expression is not associated with altered sphingolipid formation. Overall, the interplay between ORMDLs and SPT in mammalian cells remains elusive. Siow et al [49] showed that increased ORMDL3 levels do not result in inhibition of *de novo* sphingolipid synthesis, as ORMDLs are expressed in excess compared to SPT. It is possible that a correct stoichiometry between ORMDLs and SPT as well as the other members of the SPOTS complex is essential for their function [48, 49]. However, the co-expression of ORMDL1-3 together with the SPT subunits SPTLC1 or SPTLC2 did not alter SPT activity in an ORMDL-dependent manner. Nevertheless, independent of ORMDL3 expression levels, we observed a significant increase in SPT activity when cells were cultured in the absence of an external sphingolipid source. Similar results were reported by Wattenberg and colleagues, who showed increased ceramide biosynthesis in A549, HeLa and PC-3 cells when cultured in serum free conditions [44, 50]. This indicates that mammalian cells do have a regulatory mechanism that responds to and compensates for low sphingolipid levels. In contrast, increasing intracellular sphingolipid levels by treating cells with membrane permeable C_6-ceramide (C6Cer) resulted in a significant suppression of SPT activity and sphingolipid *de novo* biosynthesis [44, 50]. However, both effects appear to be independent of ORMDL expression levels.

To investigate the pathophysiology of ORDML3 expression, we also analyzed the sphingolipid profile in a cohort of 971 patients for which genome wide SNP data were available. SNP rs7216389 showed to the strongest association with childhood asthma [20] and as well as increased ORMDL3 expression in Epstein–Barr virus (EBV)-transformed lymphoblastoid cell lines, although the reported difference was not significant. However, none of the reported SNPs including rs7216389 was significantly associated with altered plasma C18SO and C18SA levels. In transfected HEK293 cells,

ORMDL3 mRNA levels were approximately 3 to 4-fold higher compared to controls without having any effect on SPT activity. This lends further support to the conclusion that changes in expression of individual ORMDL proteins do not have any effect on sphingolipid formation. In conclusion, it does not appear that the association of ORMDL3 with asthma can be explained by changes in sphingolipids.

In summary, our data indicate that ORMDL3 expression is not directly associated with changes in SPT activity or with altered SL *de novo* synthesis. Also, the strong genetic association seen for SNP rs7216389 and childhood asthma is likely independent of SPT activity and sphingolipid *de novo* formation. Therefore, further mechanistic studies are needed to understand the underlying mechanisms that link ORMDL3 with the risk for childhood asthma.

Acknowledgments:

AZ, IA, DE, AVE and TH want to thank the following funding sources for support: The 7th Framework Program of the European Commission ("RESOLVE", Project number 305707), The Gebert Rüf Foundation (GRS-047/09), The Center of Integrated Human Physiology (ZIHP), the Swiss National Foundation SNF (Project 31003A_153390/1); the Hurka Foundation, the Novartis Foundation and the Rare Disease Initiative Zurich ("radiz", Clinical Research Priority Program for Rare Diseases, University of Zurich). S.J., B.N.L and N.D. are holders of several FWO (Fonds Wetenschappelijk Onderzoek Vlaanderenprogram) grants. S.J. and B.N.L are recipients of a UGent MRP grant (Group-ID). The CoLaus study was and is supported by research grants from GlaxoSmithKline, the Faculty of Biology and Medicine of Lausanne, and the Swiss National Science Foundation (grants 33CSCO-122661, 33CS30-139468 and 33CS30-148401).

References

1. Hannun, Y.A. and L.M. Obeid, *Principles of bioactive lipid signalling: lessons from sphingolipids.* Nature Reviews Molecular Cell Biology, 2008. **9**(2): p. 139-150.
2. Hanada, K., et al., *A mammalian homolog of the yeast LCB1 encodes a component of serine palmitoyltransferase, the enzyme catalyzing the first step in sphingolipid synthesis.* Journal of Biological Chemistry, 1997. **272**(51): p. 32108-32114.
3. Hanada, K., *Serine palmitoyltransferase, a key enzyme of sphingolipid metabolism.* Biochim Biophys Acta, 2003. **1632**(1-3): p. 16-30.
4. Hornemann, T., Y. Wei, and A. von Eckardstein, *Is the mammalian serine palmitoyltransferase a high-molecular-mass complex?* Biochem J, 2007. **405**(1): p. 157-64.
5. Hornemann, T., et al., *The SPTLC3 subunit of serine palmitoyltransferase generates short chain sphingoid bases.* The Journal of biological chemistry, 2009. **284**(39): p. 26322–26330.
6. Penno, A., et al., *Hereditary sensory neuropathy type 1 is caused by the accumulation of two neurotoxic sphingolipids.* J Biol Chem, 2010. **285**(15): p. 11178-87.
7. Kihara, A. and Y. Igarashi, *FVT-1 is a mammalian 3-ketodihydrosphingosine reductase with an active site that faces the cytosolic side of the endoplasmic reticulum membrane.* J Biol Chem, 2004. **279**(47): p. 49243-50.
8. Levy, M. and A.H. Futerman, *Mammalian Ceramide Synthases.* IUBMB Life, 2010. **62**(5): p. 347-356.
9. Quehenberger, O., et al., *Lipidomics reveals a remarkable diversity of lipids in human plasma.* Journal of lipid research, 2010. **51**(11): p. 3299-3305.
10. Breslow, D.K., et al., *Orm family proteins mediate sphingolipid homeostasis.* Nature, 2010. **463**(7284): p. 1048-53.
11. Han, S., et al., *Orm1 and Orm2 are conserved endoplasmic reticulum membrane proteins regulating lipid homeostasis and protein quality control.* Proc Natl Acad Sci U S A, 2010. **107**(13): p. 5851-6.
12. Roelants, F.M., et al., *Protein kinase Ypk1 phosphorylates regulatory proteins Orm1 and Orm2 to control sphingolipid homeostasis in Saccharomyces cerevisiae.* Proc Natl Acad Sci U S A, 2011. **108**(48): p. 19222-7.
13. Sun, Y., et al., *Orm protein phosphoregulation mediates transient sphingolipid biosynthesis response to heat stress via the Pkh-Ypk and Cdc55-PP2A pathways.* Mol Biol Cell, 2012. **23**(12): p. 2388-98.
14. Shimobayashi, M., et al., *TORC1-regulated protein kinase Npr1 phosphorylates Orm to stimulate complex sphingolipid synthesis.* Mol Biol Cell, 2013. **24**(6): p. 870-81.
15. Liu, M., et al., *Regulation of sphingolipid synthesis through Orm1 and Orm2 in yeast.* J Cell Sci, 2012. **125**(Pt 10): p. 2428-35.
16. Gururaj, C., R. Federman, and A. Chang, *Orm Proteins Integrate Multiple Signals to Maintain Sphingolipid Homeostasis.* Journal of Biological Chemistry, 2013. **288**(28): p. 20453-20463.
17. Walther, T.C., *Keeping sphingolipid levels nORMal.* Proc Natl Acad Sci U S A, 2010. **107**(13): p. 5701-2.
18. Tafesse, F.G. and J.C. Holthuis, *Cell biology: A brake on lipid synthesis.* Nature, 2010. **463**(7284): p. 1028-9.
19. Hjelmqvist, L., et al., *ORMDL proteins are a conserved new family of endoplasmic reticulum membrane proteins.* Genome Biol, 2002. **3**(6): p. RESEARCH0027.
20. Moffatt, M.F., et al., *Genetic variants regulating ORMDL3 expression contribute to the risk of childhood asthma.* Nature, 2007. **448**(7152): p. 470-3.
21. Moffatt, M.F., et al., *A large-scale, consortium-based genomewide association study of asthma.* N Engl J Med, 2010. **363**(13): p. 1211-21.
22. Galanter, J., et al., *ORMDL3 gene is associated with asthma in three ethnically diverse populations.* Am J Respir Crit Care Med, 2008. **177**(11): p. 1194-200.
23. Hirota, T., et al., *Genetic polymorphism regulating ORM1-like 3 (Saccharomyces cerevisiae) expression is associated with childhood atopic asthma in a Japanese population.* Journal of Allergy and Clinical Immunology, 2008. **121**(3): p. 769-770.
24. Yang, F.F., et al., *Single nucleotide polymorphisms in the ORM1-like 3 gene associated with childhood asthma in a Chinese population.* Genet Mol Res, 2012. **11**(4): p. 4646-53.
25. Hrdlickova, B. and L.I. Holla, *Relationship between the 17q21 locus and adult asthma in a Czech population.* Hum Immunol, 2011. **72**(10): p. 921-5.

26. Ferreira, M.A., et al., *Association between ORMDL3, IL1RL1 and a deletion on chromosome 17q21 with asthma risk in Australia.* Eur J Hum Genet, 2011. **19**(4): p. 458-64.
27. Karunas, A.S., et al., *[Genome-wide association study of bronchial asthma in the Volga-Ural region of Russia].* Mol Biol (Mosk), 2011. **45**(6): p. 992-1003.
28. Leung, T.F., et al., *Asthma and atopy are associated with chromosome 17q21 markers in Chinese children.* Allergy, 2009. **64**(4): p. 621-8.
29. Tavendale, R., et al., *A polymorphism controlling ORMDL3 expression is associated with asthma that is poorly controlled by current medications.* Journal of Allergy and Clinical Immunology, 2008. **121**(4): p. 860-863.
30. Sleiman, P.M., et al., *ORMDL3 variants associated with asthma susceptibility in North Americans of European ancestry.* J Allergy Clin Immunol, 2008. **122**(6): p. 1225-7.
31. Barrett, J.C., et al., *Genome-wide association defines more than 30 distinct susceptibility loci for Crohn's disease.* Nat Genet, 2008. **40**(8): p. 955-62.
32. Barrett, J.C., et al., *Genome-wide association study and meta-analysis find that over 40 loci affect risk of type 1 diabetes.* Nat Genet, 2009. **41**(6): p. 703-7.
33. McGovern, D.P., et al., *Genome-wide association identifies multiple ulcerative colitis susceptibility loci.* Nat Genet, 2010. **42**(4): p. 332-7.
34. Drake, K.A., J.M. Galanter, and E.G. Burchard, *Race, ethnicity and social class and the complex etiologies of asthma.* Pharmacogenomics, 2008. **9**(4): p. 453-62.
35. Worgall, T.S., et al., *Impaired sphingolipid synthesis in the respiratory tract induces airway hyperreactivity.* Sci Transl Med, 2013. **5**(186): p. 186ra67.
36. Miller, M., et al., *ORMDL3 transgenic mice have increased airway remodeling and airway responsiveness characteristic of asthma.* J Immunol, 2014. **192**(8): p. 3475-87.
37. Zhang, Y., et al., *A new logic for DNA engineering using recombination in Escherichia coli.* Nat Genet, 1998. **20**(2): p. 123-8.
38. Othman, A., et al., *Plasma deoxysphingolipids: a novel class of biomarkers for the metabolic syndrome?* Diabetologia, 2012. **55**(2): p. 421-31.
39. Ziv, C., et al., *Viral serine palmitoyltransferase induces metabolic switch in sphingolipid biosynthesis and is required for infection of a marine alga.* Proceedings of the National Academy of Sciences, 2016.
40. Affymetrix, *BRLMM: an improved genotype calling method for the GeneChip© Human Mapping 500 K array set.* 2006: p. pp. 1–18.
41. Purcell, S., et al., *PLINK: a tool set for whole-genome association and population-based linkage analyses.* Am J Hum Genet, 2007. **81**(3): p. 559-75.
42. Marchini, J., et al., *A new multipoint method for genome-wide association studies by imputation of genotypes.* Nat Genet, 2007. **39**(7): p. 906-13.
43. Bode, H., et al., *HSAN1 mutations in serine palmitoyltransferase reveal a close structure-function-phenotype relationship.* Hum Mol Genet, 2015.
44. Siow, D.L. and B.W. Wattenberg, *Mammalian ORMDL proteins mediate the feedback response in ceramide biosynthesis.* J Biol Chem, 2012. **287**(48): p. 40198-204.
45. Marques-Vidal, P., et al., *Dietary intake of subjects with diabetes is inadequate in Switzerland: the CoLaus study.* European Journal of Nutrition, 2016: p. 1-9.
46. Antiochos, P., et al., *Five year trends in dyslipidaemia prevalence and management in Switzerland: The CoLaus study.* Nutrition, Metabolism and Cardiovascular Diseases, 2015. **25**(11): p. 1007-1015.
47. Antiochos, P., et al., *Association between parental history and genetic risk scores for coronary heart disease prediction: The population-based CoLaus study.* Atherosclerosis, 2016. **244**: p. 59-65.
48. Oyeniran, C., et al., *Aberrant ORM (yeast)-like protein isoform 3 (ORMDL3) expression dysregulates ceramide homeostasis in cells and ceramide exacerbates allergic asthma in mice.* J Allergy Clin Immunol, 2015. **136**(4): p. 1035-46 e6.
49. Siow, D., et al., *ORMDL/serine palmitoyltransferase stoichiometry determines effects of ORMDL3 expression on sphingolipid biosynthesis.* J Lipid Res, 2015. **56**(4): p. 898-908.
50. Siow, D., et al., *Regulation of de novo sphingolipid biosynthesis by the ORMDL proteins and sphingosine kinase-1.* Adv Biol Regul, 2015. **57**: p. 42-54.

Figures

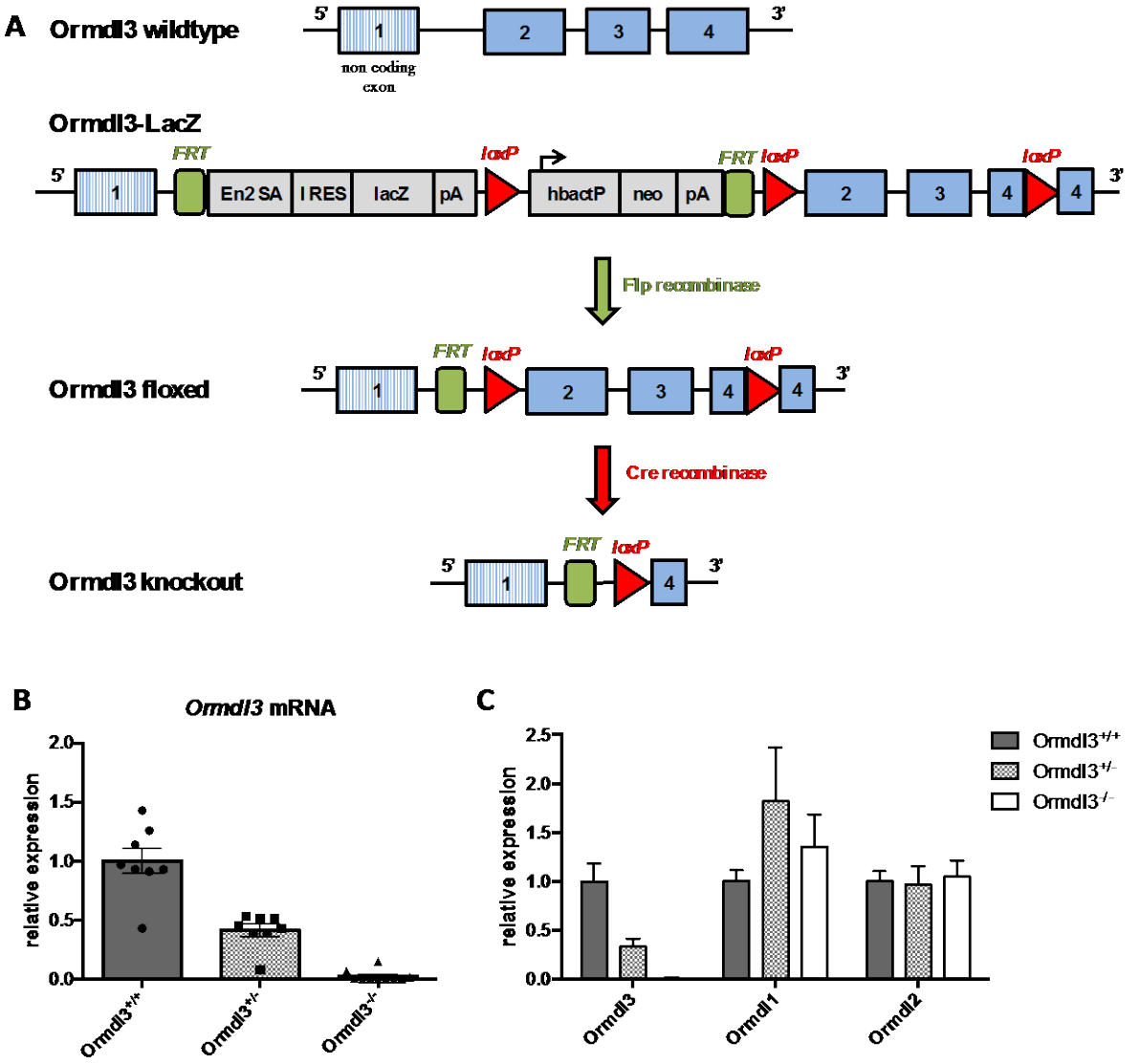

Figure 1. Generation and validation of *Ormdl3* knockout (Ormdl3$^{-/-}$) mice
A) A targeting construct of the EUCOMM consortium (project 72180) was inserted into the first intron of *Ormdl3*. This construct contained 2 FRT sites flanking a sequence consisting of an En2 splice acceptor site, an internal ribosome entry site, a lacZ sequence, a polyA-tail, a loxP site and a neomycin coding sequence driven by a human β-actin promoter (hbactP). Two other loxP sites were flanking exon 2, 3 and part of exon 4 of the *Ormdl3* gene. Removal of the lacZ/neo cassette was achieved by crossing the Ormdl3^{LacZ} mice with Flp expressing mice. The obtained Ormdl3^{floxed} mice were further crossed with mice expressing the Cre recombinase behind the Sox2 promoter to generate full knockout mice. B) *Ormdl3* mRNA expression in lungs from wildtype (Ormdl3$^{+/+}$), heterozygous knockout (Ormdl3$^{+/-}$) and homozygous knockout (Ormdl3$^{-/-}$) mice. Expression values were calculated by qBase+ and normalized to the reference genes *hmbs* and *sdha*. Expression values are shown relative to the mean of the wildtype group. Each dot represents an individual mouse. C) *Ormdl3, Ormdl1* and *Ormdl2* mRNA expression in lungs from wildtype (Ormdl3$^{+/+}$, n=12), heterozygous knockout (Ormdl3$^{+/-}$, n=5) and homozygous knockout (Ormdl3$^{-/-}$, n=9) mice. Expression values were calculated by qBase+ and normalized to the reference genes *hmbs*, *rpl13a* and *sdha*. Expression values are shown relative to the mean of the wildtype group. B/C Data were pooled from 2 experiments and shown as mean ± SEM.

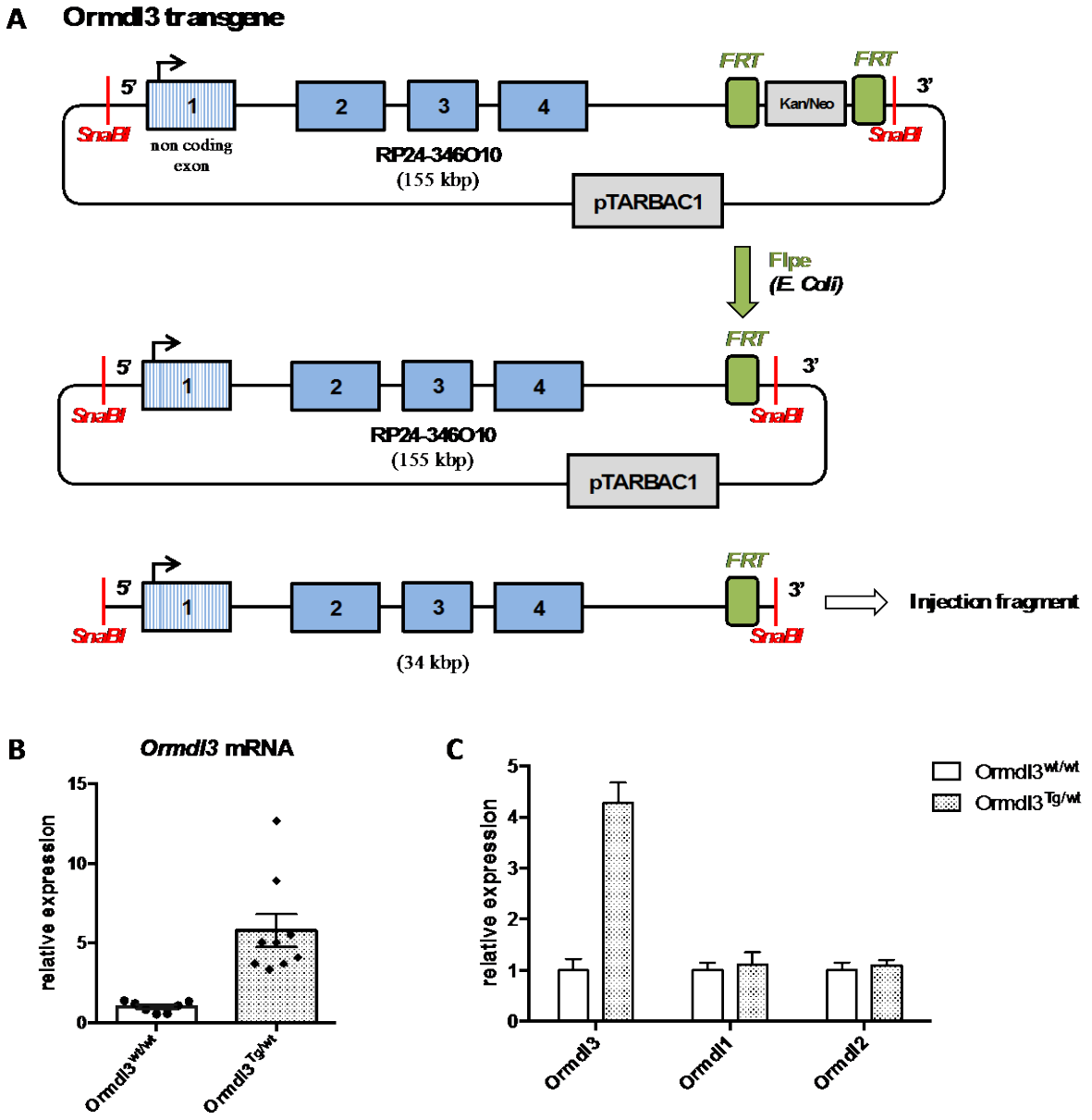

Figure 2. Generation and validation of *Ormdl3* transgenic (Ormdl3$^{Tg/wt}$) mice
A) *Ormdl3* transgenic mice were generated by making use of a bacterial artificial chromosome (BAC) containing murine *Ormdl3* behind its endogenous promoter and an inserted kanamycin/neomycin selection cassette flanked by two FRT sites. Flpe expression in *E. coli* removed the selection cassette, leaving one FRT site intact. PCR primers designed around the FRT site allowed discrimination of the transgene over the wildtype locus. The modified BAC was digested by SnaBI and the 34 kb fragment containing the murine *Ormdl3* locus was used as the injection fragment. B) *Ormdl3* transcript levels in lungs from transgenic mice (Ormdl3$^{Tg/wt}$) and their wildtype littermates (Ormdl3$^{wt/wt}$). Each dot represents an individual mouse. Data were pooled from 2 experiments. C) *Ormdl3, Ormdl1* and *Ormdl2* transcript levels in lungs from *Ormdl3* transgenic mice (Ormdl3$^{Tg/wt}$, n=3) and their wildtype littermates (Ormdl3$^{wt/wt}$, n=3). B/C Expression values were calculated by qBase+ and normalized to the reference genes *hmbs* and *sdha*. Expression values are shown relative to the mean of the wildtype group (mean ± SEM).

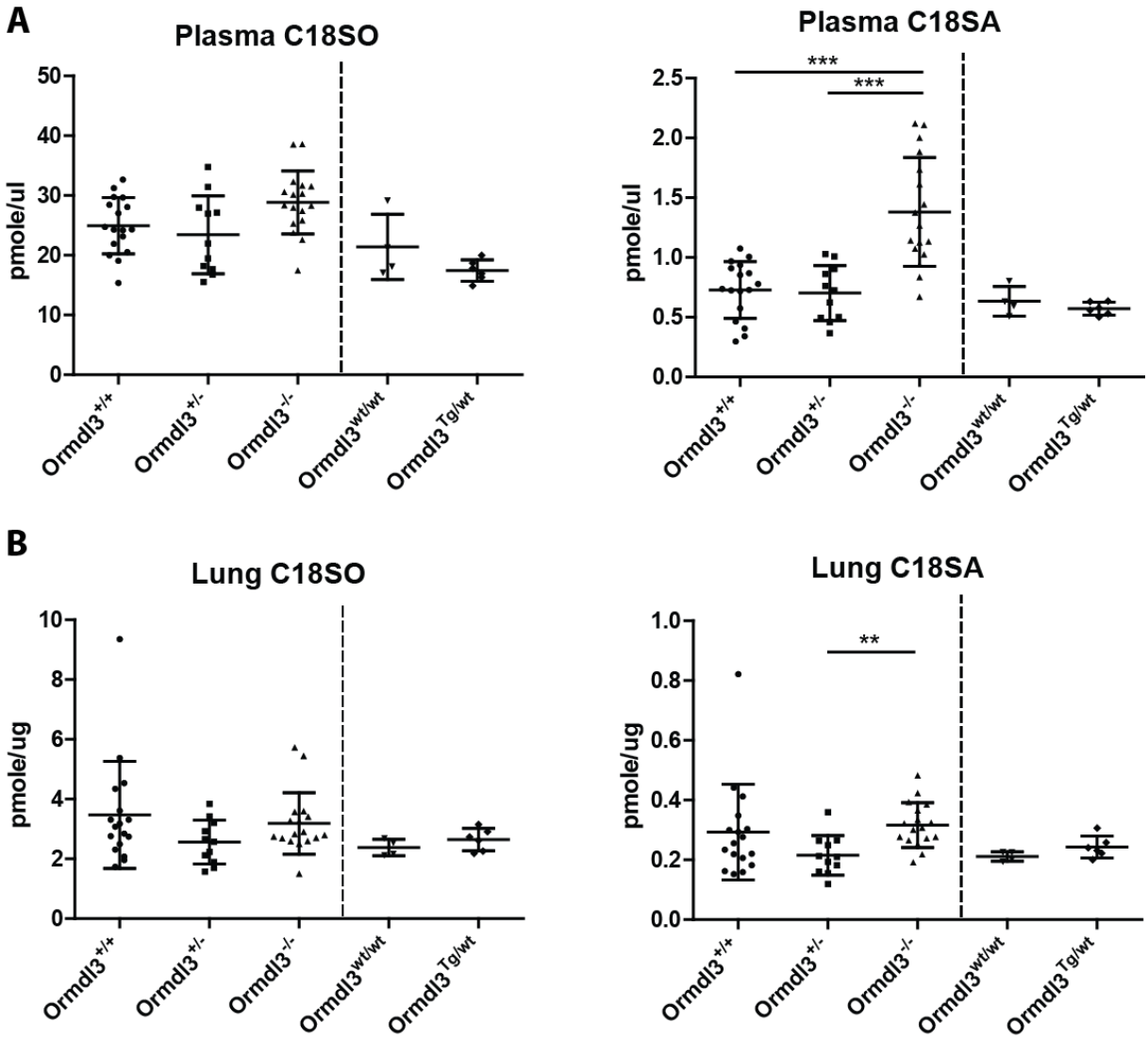

Figure 3. C_{18}-sphingoid base levels in plasma and lung of Ormdl3$^{+/+}$, Ormdl3$^{+/-}$, Ormdl3$^{-/-}$, Ormdl3$^{Tg/wt}$ and Ormdl3$^{wt/wt}$ mice.

Total sphingolipids were extracted and C18SO and C18SA levels analyzed after acid-base hydrolysis by LC/MS. A) Plasma C18SO and C18SA, B) Lung C18SO and C18SA levels. Wildtype Ormdl3$^{+/+}$, n=17; heterozygous knockout Ormdl3$^{+/-}$, n=12; homozygous knockout Ormdl3$^{-/-}$, n=17; transgenic Ormdl3$^{Tg/wt}$, n=6 and their corresponding wildtype littermate Ormdl3$^{wt/wt}$, n=4 (mean ± SD), one-way ANOVA, post-test: Dunn's multiple comparison test, **p<0.01, ***p<0.001.

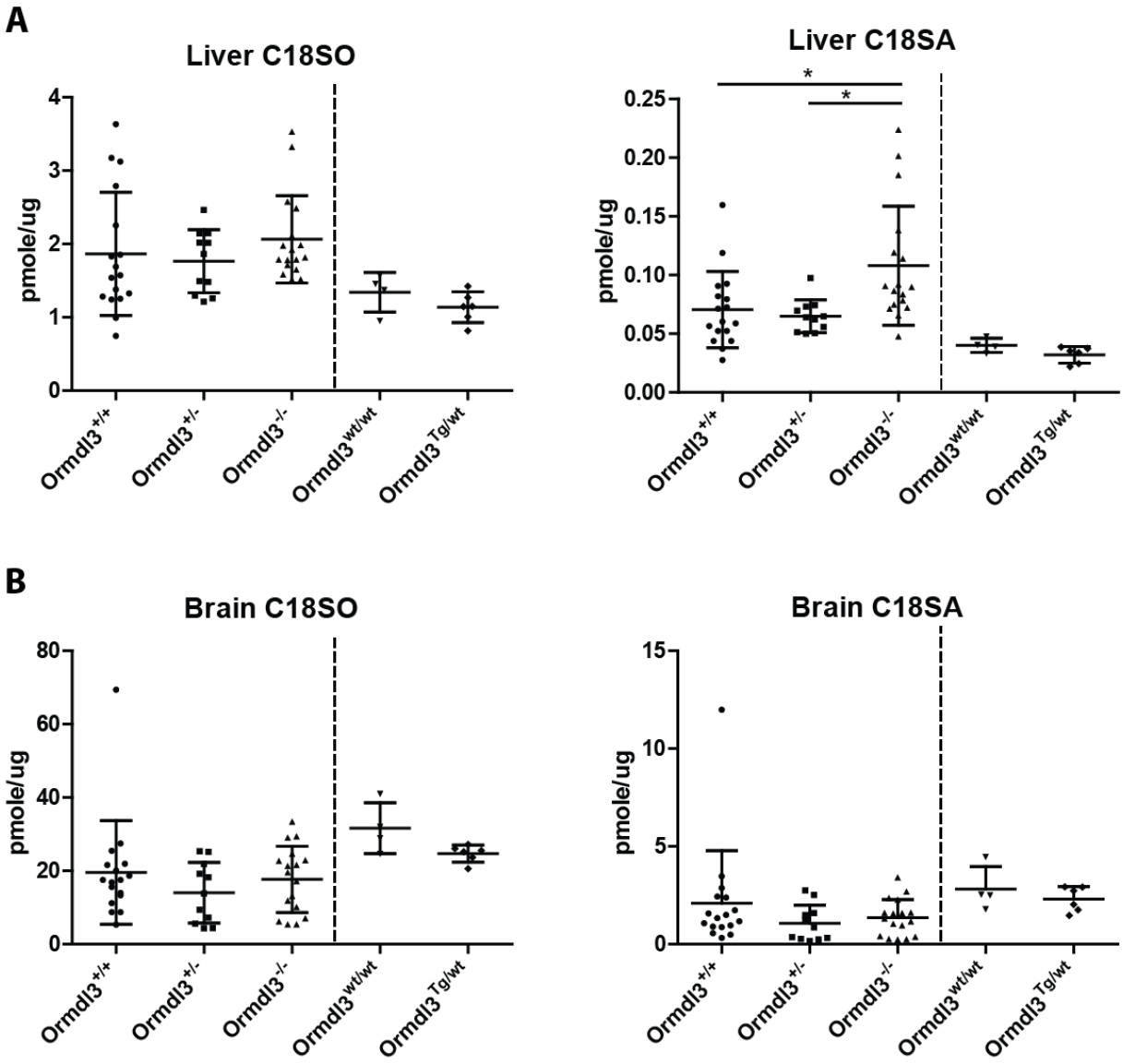

Figure 4. C_{18}-sphingoid base levels in liver and brain of Ormdl3$^{+/+}$, Ormdl3$^{+/-}$, Ormdl3$^{-/-}$, Ormdl3$^{Tg/wt}$ and Ormdl3$^{wt/wt}$ mice.

Total sphingolipids were extracted and C18SO and C18SA levels analyzed after acid-base hydrolysis by LC/MS A) Liver C18SO and C18SA levels B) brain C18SO and C18SA levels. Wildtype Ormdl3$^{+/+}$, n=17; heterozygous knockout Ormdl3$^{+/-}$, n=12; homozygous knockout Ormdl3$^{-/-}$, n=17; transgenic (Ormdl3$^{Tg/wt}$, n=6) and their corresponding wildtype Ormdl3$^{wt/wt}$, n=4. (Mean ± SD), one-way ANOVA, post-test: Dunn's multiple comparison test, *p<0.05.

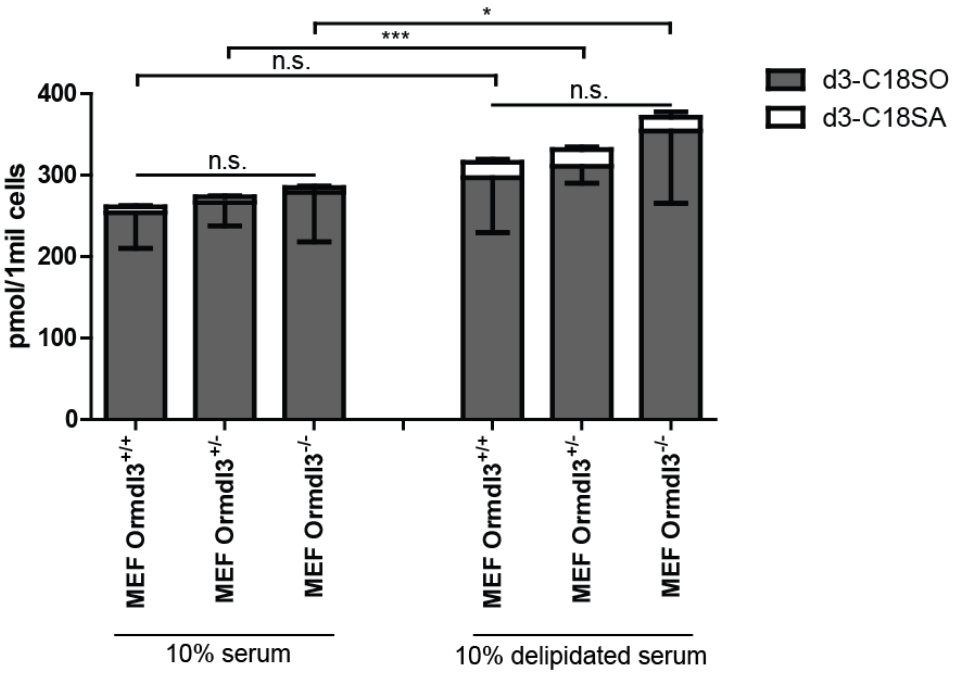

Figure 5. SPT activity in MEF cells from Ormdl3$^{+/+}$, Ormdl3$^{+/-}$ and Ormdl3$^{-/-}$ mice.
MEF cells from Ormdl3+/+, Ormdl3+/- and Ormdl3-/- mice were cultured in presence of 1mM d3-N15-L-serine for 24 hours. SPT activity reflect total of *de novo* formed d3-C18SO and d3-C18SA levels. Bar plots of the sum of d3-C18SO (in grey) and d3-C18SA (in white) levels in MEF cells from Ormdl3$^{+/+}$, Ormdl3$^{+/-}$, Ormdl3$^{-/-}$ mice cultured in DMEM containing either 10% normal serum or 10% delipidated serum. (Mean ± SD, n=10) Significances were calculated by Student t-test; *p<0.05, ***p<0.001.

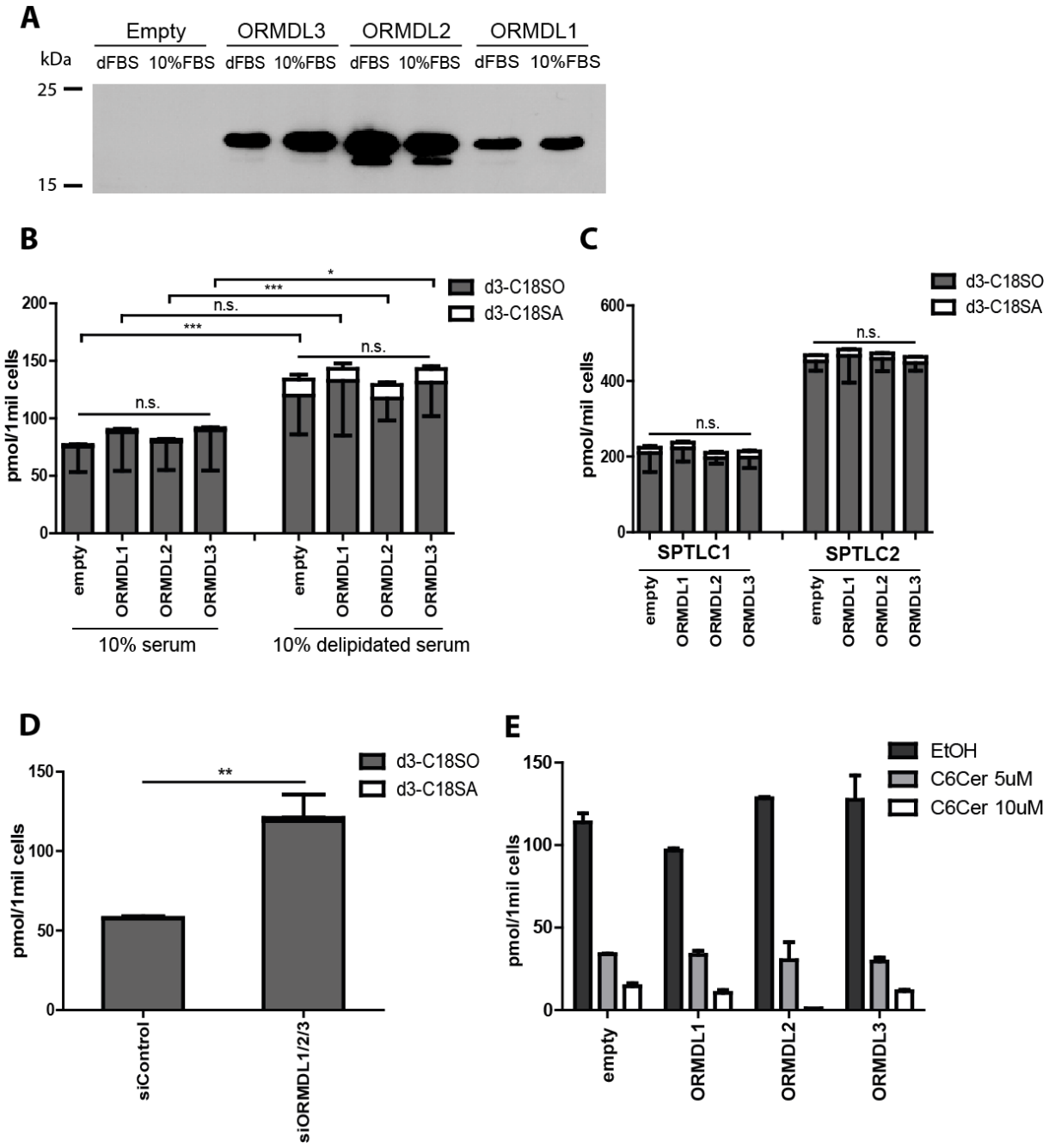

Figure 6. SPT activity in HEK293 cells overexpressing ORMDL1-3 or silenced ORMDL1-3.
A) Western blot of ORMDL1, 2 and 3 expressed in HEK293 cells. ORMDLs were detected by a fused V5-6xHis tag. B) Isotope label assay with d3-N15-L-serine. De-novo formed d3-C18SO (grey) and d3-C18SA (white) in HEK293 cells transfected with the empty vector or ORMDL1-3. Cells were cultured in DMEM with either 10% normal serum or 10% delipidated serum (mean ± SD; n=10). Student t-test, *p<0.05, ***p<0.001. C) SPT activity in HEK293 cells which were first stably transfected with either SPTLC1 or SPTLC2 and then co-transfected with ORMDL1, 2 and 3. De-novo formed d3-C18SO (grey) and d3-C18SA (white) (mean ± SD; n=3). D) Bar plots showing the sum of d3-C18SLs in siRNA mediated knockdown of all three ORMDL proteins in HEK293 cells (mean ± SD; n=3). E) D*e novo* formed d3-C18SLs (sum of d3-C18SO and d3-C18SA) in ORMDL1-3 overexpressing HEK293 cells treated with C6Cer (5uM and 10uM) (mean± SD; n=3).

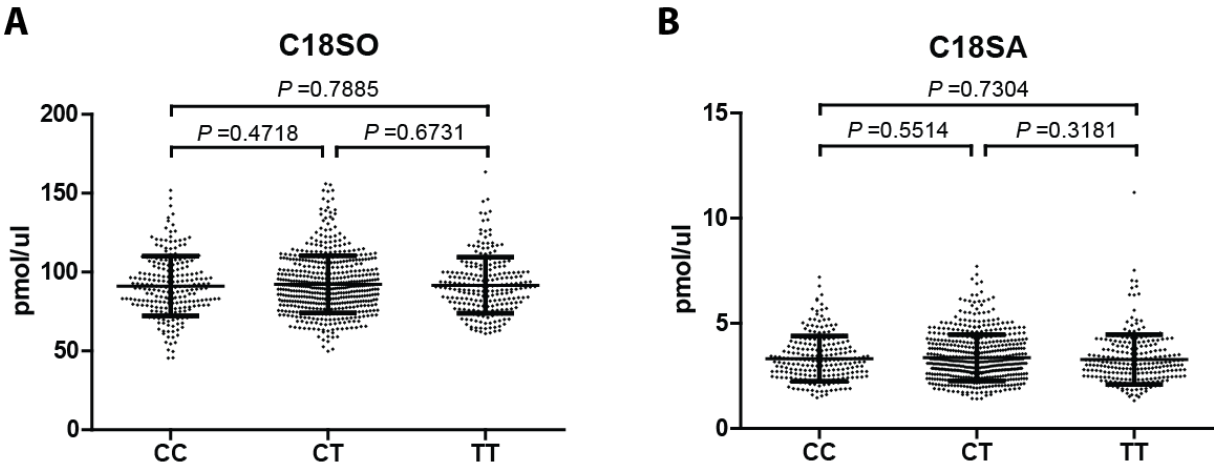

Figure 7. Association of ORMDL3 SNP (rs7216389) with plasma C18SO and C18SA levels. Association of the ORMDL3 SNP rs7216389 with plasma levels of A) C18SO and B) C18SA. The respective SNP genotype is shown. Lines represent mean ± SD. p-values were calculated by student t-test. No significant difference was observed.

Supplementary figures

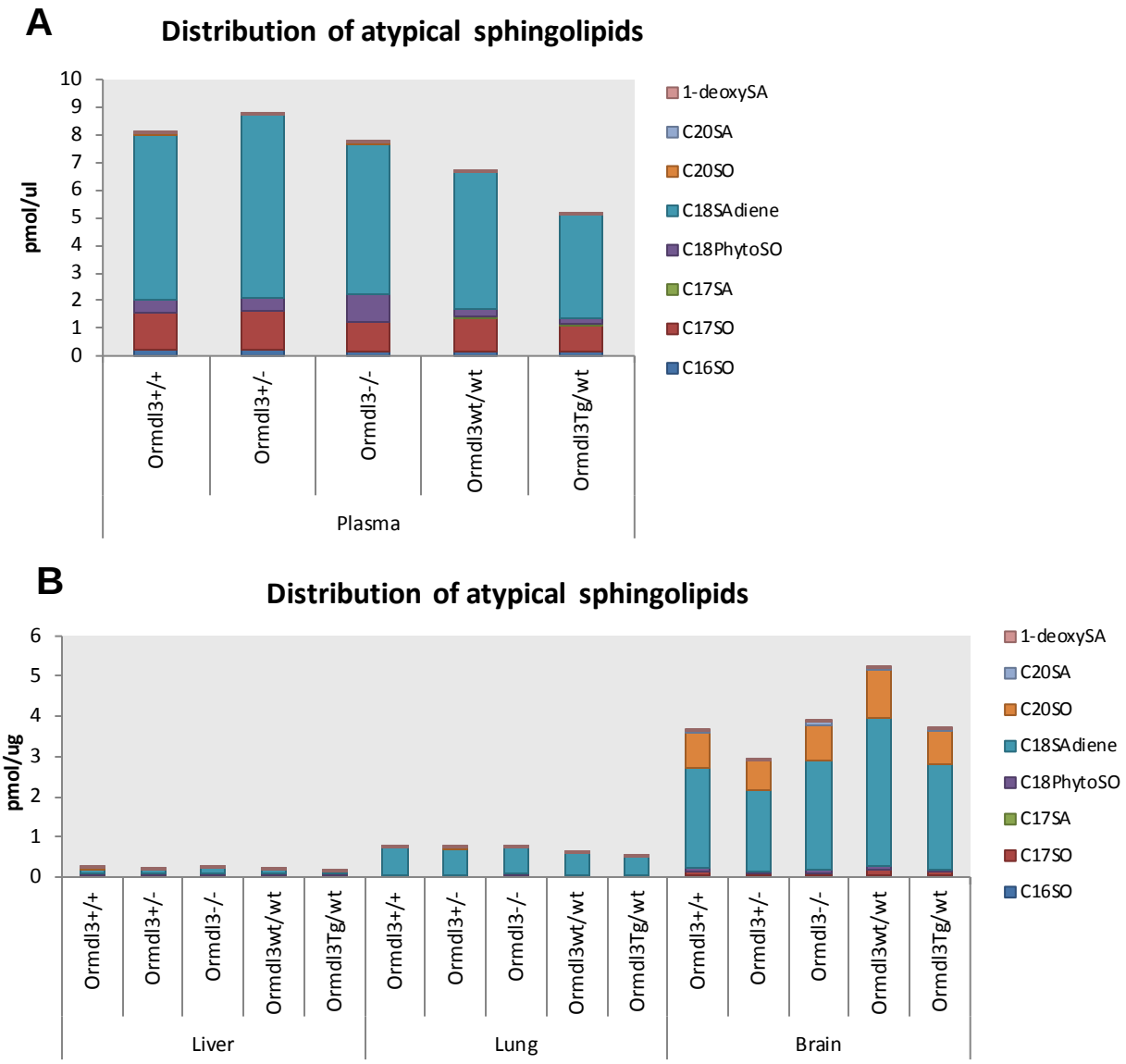

Supplemental Figure 1. Distribution of atypical sphingolipids in wildtype (Ormdl3$^{+/+}$, n=17), heterozygous knockout (Ormdl3$^{+/-}$, n=12), homozygous knockout (Ormdl3$^{-/-}$, n=17), transgenic (Ormdl3$^{Tg/wt}$, n=6) and their corresponding wildtype (Ormdl3$^{wt/wt}$, n=4) mice. Stacked bar plots show atypical sphingolipid levels in plasma, liver, lung and brain tissues.

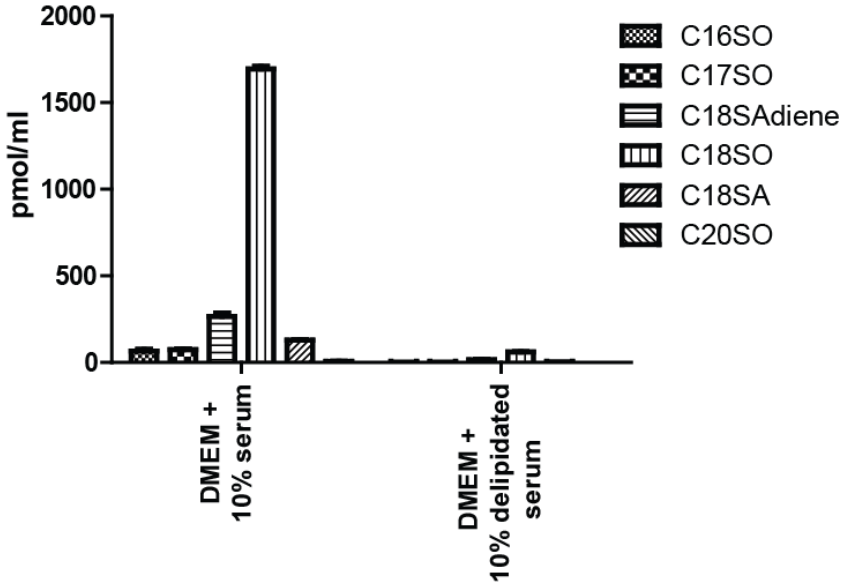

Supplemental Figure 2. Sphingolipid profile in DMEM containing either 10% serum or 10% delipidated serum. Media were lyophilized, lipids were extracted and analyzed using LC-MS.

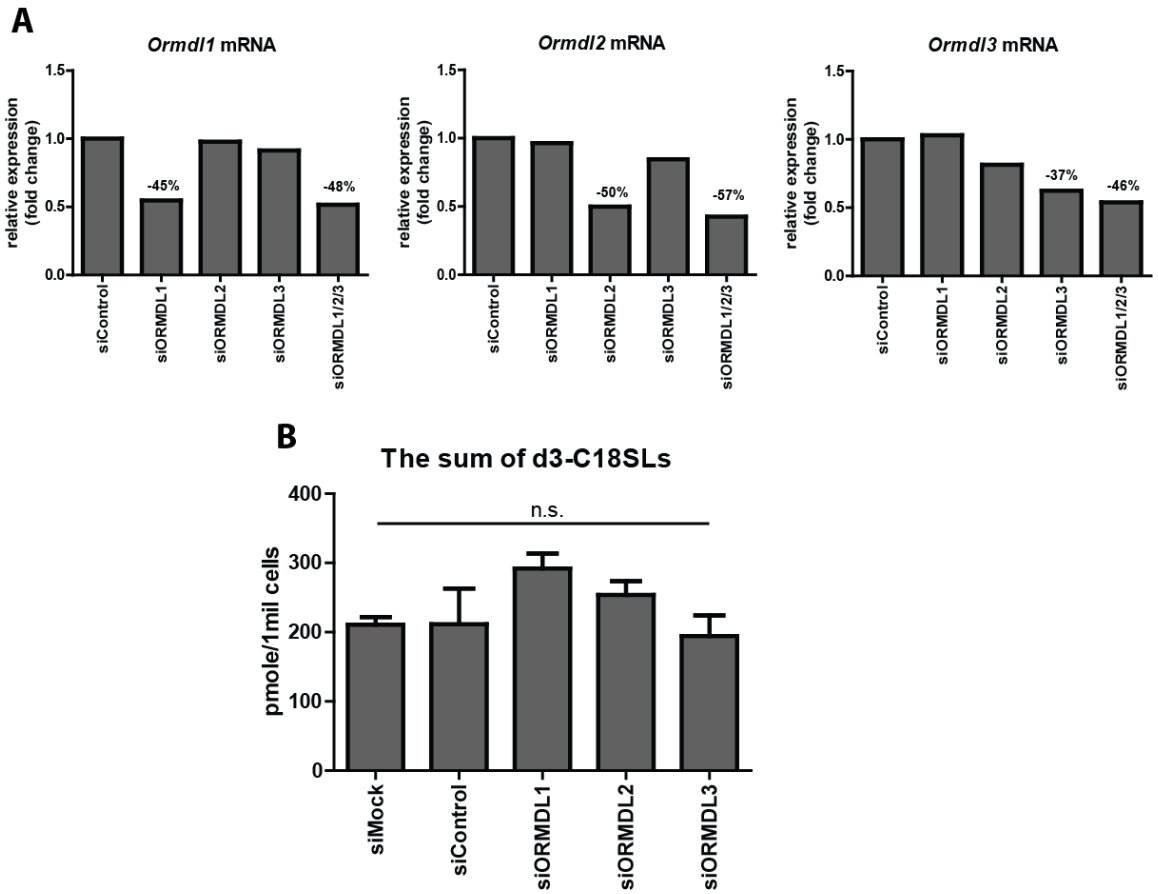

Supplemental Figure 3. siRNA mediated knockdown of ORMDL1-3 in HEK293 cells.
A) mRNA expression levels (fold change) of *Ormdl1*, *Ormdl2* and *Ormdl3* in HEK293 cells transfected with siORMDL1-3. The values were normalized to GAPDH. B) Bar plots showing the sum of d3-C18SLs in siRNA mediated knockdown of individual ORMDL1, 2 and 3 proteins in HEK293 cells. The values are shown as mean ± SD (n=3). One-way ANOVA, post-test: Bonferroni's Multiple Comparison.

Supplementary Table 1. Association of SNPs in ORMDL3/GSDMA/GSDMB genes with plasma sphingoid bases. Associations were calculated as described in methods.

SNP	Gene	C16SO	C16SA	C17SO	C17SA	C18SAdiene	C18SO	C18SA	SL (total)	C19SO	C20SO	C20SA	1-deoxySO	1-deoxySA	1-deoxySL (total)
rs2290400	GSDMB	.470	.683	.880	.452	.779	.965	.527	.956	.765	.535	.234	.103	.109	.093
rs3894194	GSDMA	.826	.986	.747	.781	.381	.985	.840	.981	.020	.199	.521	.129	.122	.114
rs7216389	GSDMB/ORMDL3	.468	.761	.871	.552	.791	.817	.595	.803	.652	.354	.348	.122	.072	.092
rs3859192	GSDMA	.710	.112	.984	.446	.466	.372	.427	.363	.337	.040	.017	.102	.241	.124
rs11650680	GSDMB/ORMDL3	.681	.182	.318	.291	.039	.005	.005	.005	.400	.077	.257	.372	.258	.329
rs12603332	ORMDL3	.530	.904	.989	.536	.461	.888	.455	.871	.543	.198	.173	.046	.019	.029

Chapter 2:

THE ROLE OF C6-CERAMIDE INHIBITION ON SPT SUBUNITS

Assem Zhakupova, Arnold von Eckardstein, Thorsten Hornemann

Author contributions

AZ – acquired, analyzed and interpreted data, wrote the manuscript

AVE – revised the manuscript, supervised the study

TH – revised the manuscript, supervised the study

Abstract

Objective: Sphingolipid *de novo* synthesis is regulated through a metabolic feedback mechanism. In yeast this regulation is mediated by Orm1/2 proteins that act as negative regulators of SPT. However, the underlying mechanism of this regulation in particular for mammalian cells is not yet understood. Increasing intracellular sphingolipid levels by supplementing cells with membrane permeable C_6-ceramide (C6Cer) was shown to decrease ceramide biosynthesis. Several mutations in SPT are associated with increased sphingolipid *de novo* synthesis indicating that the regulatory mechanism is impaired in these mutants. Here, we investigated how C6Cer affects SPT activity and which factors are involved in this regulation.

Methods: HEK293 cells overexpressing SPTLC1 wildtype subunit of SPT were supplemented with C6Cer, sphingomyelin (SM) or the free long chain bases d7-sphingosine (D7SO) and d7-sphinganine (D7SA) to increase intracellular sphingolipid levels. *De novo* formed sphingoid bases were measured by LC-MS after supplementing the cells with stable isotope labeled d3-N^{15}-L-serine and d4-L-alanine for 24h. The results were compared to HEK293 cells expressing SPT mutants (SPTLC1 p.S331F and SPTLC2 p.I504F), which showed increased sphingolipid *de novo* synthesis.

Results: Supplementing SPTLC1 wildtype expressing cells with C6Cer, D7SO and D7SA resulted in a strong decrease of *de novo* formed sphingolipids. This effect was less pronounced when supplementing the cells with SM. Addition of C6Cer similarly decreased sphingolipid formation in HSAN1 mutant expressing cells. Hence, C6Cer addition to the cells triggers regulatory mechanisms, which leads to inhibition of SPT activity. This indicates that the feedback regulation of SPT in mammalian cells is also based on the increase in intracellular sphingolipid levels and therefore similar to yeast.

Conclusion: Raising intracellular sphingolipid levels either by adding C6Cer or free long chain bases (SA or SO) inhibits SPT activity and decreases sphingolipid *de novo* synthesis in mammalian cells.

Abbreviations:

C6Cer – C_6-ceramide; SM – sphingomyelin; D7SO – D-erythro-sphingosine-d7; D7SA – D-erythro-sphinganine-d7; 1-deoxySLs – 1-deoxysphingolipids; 1-deoxySA – 1-deoxysphinganine.

Introduction

Serine palmitoyltransferase (SPT) catalyzes the condensation of palmitoyl-CoA and L-serine, the first step in *de novo* sphingolipid synthesis, which produces C_{18}-based sphingolipids [1, 2]. Besides palmitoyl-CoA, SPT can also metabolize other acyl-CoAs (C_{12}-C_{18}) giving rise to a variety of atypical long chain bases (LCBs) [3]. SPT is composed of three subunits – SPTLC1, 2 and 3 and this alternate activity seems to be primarily mediated by the SPTLC3 subunit as transfecting and overexpressing SPTLC3 in HEK293 cells, which do not express this subunit endogenously, forms increased C_{16}- but also C_{17}- and C_{19}- based sphingolipids [3, 4].

Several missense mutations in SPT cause Hereditary Sensory and Autonomic Neuropathy Type 1 – HSAN1 [5-12]. HSAN1 is an autosomal dominant peripheral neuropathy, characterized by a progressive sensory loss mainly in distal limbs [13-15]. Several mutations in SPT lead to a permanent shift in the substrate preference from L-serine to L-alanine, resulting in a formation of neurotoxic 1-deoxysphingolipids (1-deoxySLs) [16]. Recently Bode et al classified several SPTLC1 and 2 mutations according to their biochemical properties and clinical manifestations [17]. The authors showed that the HSAN1 mutations SPTLC1 p.S331F and SPTLC2 p.I504F, which are associated with an exceptionally severe HSAN1 phenotype [8, 17, 18] have an increased canonical SPT activity on top of increased 1-deoxySLs formation.

In yeast SPT activity is tightly regulated by a negative-feedback loop mediated by Orm1 and 2 proteins [19-21]. The regulation is based on sensing of intracellular sphingolipids, although the mechanism by which cells sense their sphingolipid content is not understood [22, 23]. Upon sufficient cellular sphingolipid levels Orm proteins bind to and inhibit SPT. Once the sphingolipid levels are reduced, Orm proteins get gradually phosphorylated by Ypk1 kinase via TORC2-dependent pathway and release the inhibition of SPT [19, 21-24]. In yeast Orm proteins form a multi-protein complex with SPT named SPOTS (Serine Palmitoyltransferase, Orm1/2, Tsc3 and Sac1) [19]. In contrast to yeast, mammalian cells express three ORM orthologues (ORMDL1-3), although the phosphorylation sites identified in yeast are not conserved [25]. It is therefore not fully clear if and how this feedback regulation by the ORMDLs is organized in mammalian cells. However, adding membrane permeable C6Cer to cells was shown to decrease SPT activity in a time and concentration dependent manner [28, 29] [30, 31]

indicating a metabolic feedback regulation is similar to the one described in yeast [26, 27]. Here, we aimed to elucidate the mechanisms by which exogenously added sphingolipids influence SPT activity in mammalian cells in more detail.

Methods

Cloning and generation of mutants

All mutant constructs were generated as previously described [17].

Generation of stable SPT overexpressing cell lines

HEK293 cells (ATCC) were grown in DMEM (Sigma-Aldrich) containing 10% fetal bovine serum (Gibco, Thermo Scientific) and 1% penicillin/streptomycin (Sigma-Aldrich). DNA mix containing 4 µg of DNA (SPTLC1-3, SPTLC1 p.C133W, SPTLC1 p.S331F, SPTLC2 p.I504F) in 400 µL of Opti-MEM was mixed with 6 µL of TurboFect *in vitro* transfection reagent (Thermo Scientific). After 20 min incubation at RT TurboFect/DNA mixture was added drop-wise to HEK293 cells. Following 24-48 hours after transfection cells were grown in DMEM containing 4µg/mL Geneticin (Gibco, Thermo Scientific). Expression of plasmids was confirmed by WB analysis using V5 and His antibodies (Serotec).

Stable isotope labelling assay to measure SPT activity

Approximately 200,000 HEK293 cells overexpressing either SPTLC1-3wt or SPTLC1 mutants (p.C133W, p.S331F), SPTLC2 mutant (p.I504F) were cultured for three days. After which the medium was exchanged to L-serine and L-alanine free DMEM (Genaxxon, Ulm, Germany) containing 10% delipidated FBS (Sigma Aldrich). Four hours later the cells were treated with the mixture of isotope-labeled deuterated substrates 1mM L-serine (2,3,3-D3, 98%; 15N, 98%) and 2mM L-alanine (2,3,3,3-D4, 98%) (Cambridge Isotopes). Following 24h incubation cells were washed once with PBS, collected with 900ul of PBS and counted (Z2 Coulter Counter, Beckman Coulter, CA). Cell pellets were collected by centrifugation (1200g x 5min, at 4°C) and stored at -20°C.

Lipid extraction and sphingoid base analysis

Cell pellets dissolved in 100µL of PBS were mixed with 500µL of methanol (Honeywell) containing 200pmol of internal standards (d7-sphinganine and d7-sphingosine, Avanti Polar Lipids). The cells were agitated at 37°C for 1 h on a shaker (Thermomixer comfort, Eppendorf; Hamburg, Germany). Followed by centrifugation at 16,000g x 5min protein precipitate was formed and the supernatant was transferred to a new 2mL Eppendorf tube. Lipids were hydrolyzed using HCL (32%, Sigma Aldrich) for 16h at 65°C and

neutralized with 10M KOH. Afterwards free sphingoid bases were extracted by adding chloroform (99.8%, Sigma Aldrich) in basic condition containing 2N ammoniac. The sphingoid bases were analyzed using TSQ Quantum Ultra MS analyzer as previously described [32].

For analysis, total sphingolipids were extracted and subjected to acid and base hydrolyses to cleave off the N-acyl chain and conjugated head groups. Ten sphingoid bases (including C_{18}-sphingosine (C18SO) and C_{18}-sphinganine (C18SA)) were analyzed by LC-MS. During the SPT reaction one deuterium is replaced by hydrogen, as a result *de novo* sphingolipids are detected on the MS by a shift in mass over charge (m/z) of +3Da.

Treatment of cells with C6Cer, SM, D7SA and D7SO

C6Cer was purchased from Sigma Aldrich (5mg/mL in 100% ethanol). D-erythro-sphingosine-d7 (D7SO) and D-erythro-sphinganine-d7 (D7SA) (Avanti Polar Lipids) were dissolved in ethanol to a stock concentration of 1mM. Sphingomyelin (Avanti Polar Lipids) was dissolved in ethanol to a stock concentration of 5mM. All lipids were stored at -20°C.

Statistical analysis

GraphPad Prism 5 software was used to perform statistical analysis, fitting the curve and calculating IC_{50} values. All values are shown as mean and standard deviations.

Results

Increasing intracellular sphingolipids inhibits SPT activity

First, we compared two different medium conditions (DMEM containing 10% serum or 10% delipidated serum) to control for the effect of external sphingolipids present in the culture medium.

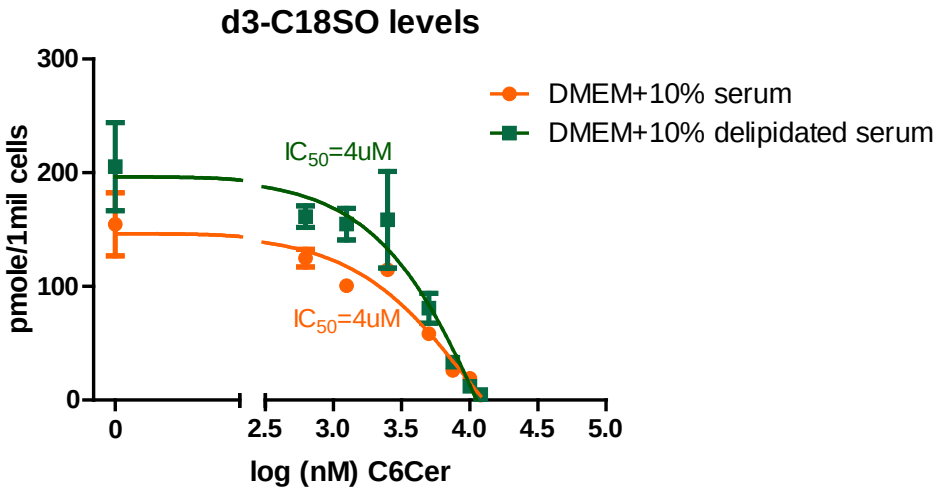

Figure 1. *De novo* formed d3-C18SO levels in HEK293 cells treated with increasing amount of C6Cer (0.625-10µM) in DMEM containing 10% serum and 10% delipidated serum and incubated for 24h. The fitted line was done using log (inhibitor) vs. response function.

SPT activity was measured by quantifying *de novo* sphinganines (d3-C18SA) and sphingosines (d3-C18SO) after acid base hydrolysis of total sphingolipids. Therefore, it reflects the SPT activity. As shown in Fig. 1, the presence of external sphingolipids resulted in a compensatory decrease of *de novo* formed sphingolipids. *De novo* formed d3-C18SO levels were slightly elevated (hence, higher SPT activity) in DMEM+10% delipidated serum. However, the inhibitory effect of C6Cer addition on SPT activity was comparable for both medium conditions.

Next, we compared the effect of increasing intracellular sphingolipid levels by supplementing HEK293 cells overexpressing SPTLC1 with exogenous sphingolipids. SPTLC1 overexpression generally does not alter SPT activity, but was chosen to compare the results to HSAN1 mutant expressing cells (shown in Fig. 5). Cells were supplemented with C6Cer (0.625µM-10µM), d7-sphinganine (D7SA), d7-sphingosine (D7SO) (0.625µM-10µM) and sphingomyelin (SM) (1.25µM-40µM). The highest concentration of SM tested was comparable to the SM concentration found in the cell medium containing

10% FBS. To exclude an additional influence of sphingolipids present in the cell medium, these assays were carried out in the medium containing 10% delipidated serum.

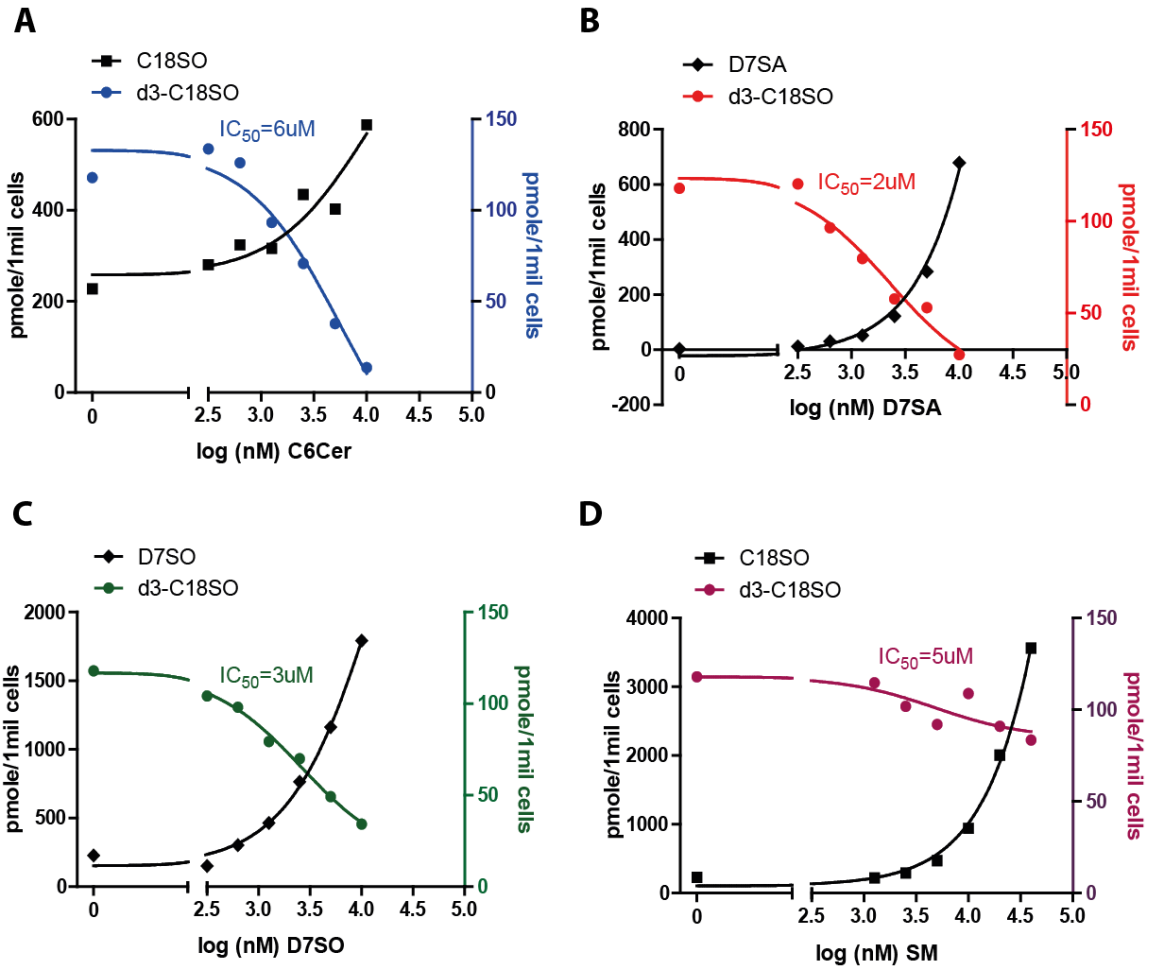

Figure 2. A-D) HEK293 cells overexpressing SPTLC1 were treated with increasing amount of C6Cer (0.625µM-10µM), D7SA and D7SO (0.625µM-10µM), SM (1.25µM-40µM) for 24h. After the acid-base hydrolysis total sphingoid bases were quantified using LC-MS. Intracellular C18SO, D7SO/D7SA levels are shown in black (left y-axis) and *de novo* synthesized d3-C18SO levels are shown in colors corresponding to the right y-axis. The fitted line was done using log (inhibitor) vs. response function. Increasing amounts of exogenously added sphingolipids resulted in decreased *de novo* d3-C18SO levels.

The uptake of the exogenously added C6Cer/SM as well as D7SO/D7SA was followed by an increase in non-labeled C18SO or D7SO/D7SA, respectively (Fig. 2A-D). Upon addition of the exogenous sphingolipids we observed a significant and dose dependent decrease in *de novo* formed d3-C18SO, reflecting a significant decrease in SPT activity. The inhibition of SPT was more pronounced for C6Cer, D7SO and D7SA (Fig. 2A-C) than for SM supplemented cells (Fig. 2D). Although total intracellular sphingolipid

levels (reflected by C18SO levels) were significantly higher in SM treated cells (up to 3500 pmol/1^6 cells), the inhibitory effect on SPT activity was much lower in comparison to C6Cer, D7SO or D7SA supplementation (Fig. 2D).

Atypical sphingolipids are regulated by C6Cer similar to typical sphingolipids

We then were interested to see if SPTLC3 based activity would also be suppressed by C6Cer supplementation. As HEK293 cells do not endogenously express SPTLC3 we used stable SPTLC3 transfected HEK293 to test the influence of C6Cer on SPTLC3 activity. C16SO was the predominant atypical LCB formed in SPTLC3 expressing cells followed by C17SO and C19SO [3], although also the formation of canonical C18SO was slightly increased in these cells.

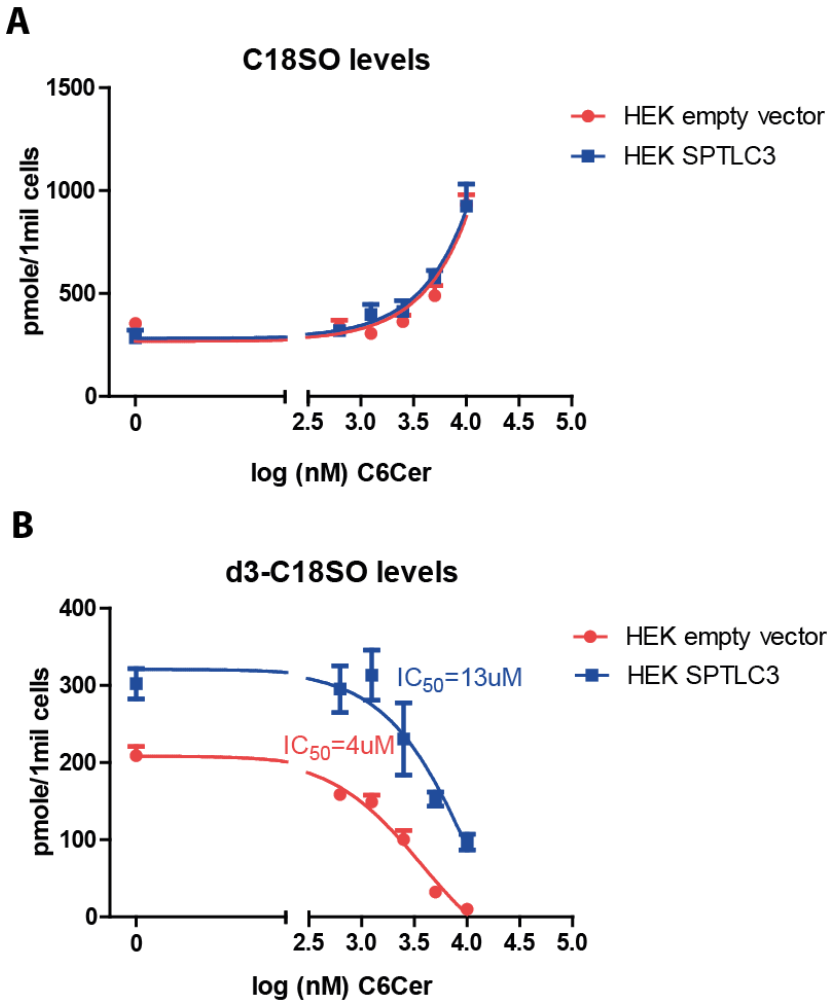

Figure 3. The effect of increasing concentration of C6Cer (0.625µM-10µM) on SPT activity in HEK293 cells overexpressing SPTLC3 and empty vector control. Scatter plots show A) C18SO and B) *de novo* C18SO levels in HEK293 cells overexpressing SPTLC3 and empty vector treated with C6Cer. The fitted line was done using log (inhibitor) vs. response function. The values are shown as mean of triplicates ± SD.

Addition of C6Cer increased intracellular C18SO levels (Fig. 3A) and decreased *de novo* formed d3-C18SO (Fig. 3B). In parallel, also the formation of the SPTLC3 products, d3-C16SO, d3-C17SO and d3-C19SO were decreased (Fig. 4). The IC_{50} was comparable for all atypical LCBs.

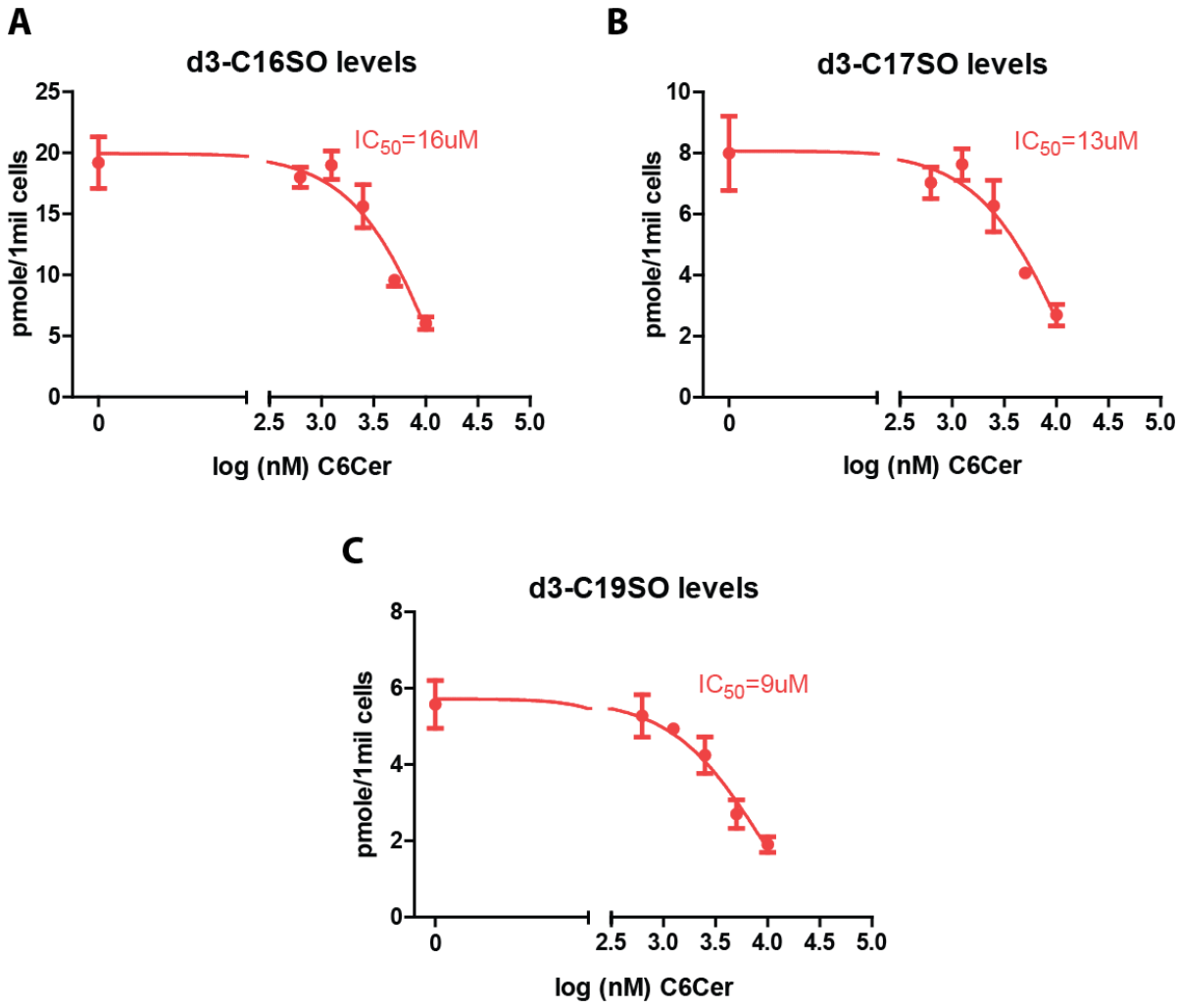

Figure 4. The effect of increasing amount of C6Cer on SPT activity. Scatter plots show A) d3-C16SO, B) d3-C17SO and C) d3-C19SO levels in HEK293 cells overexpressing SPTLC3 treated with C6Cer (0.625µM-10µM). The fitted line was done using log (inhibitor) vs. response function. The values are shown as mean of triplicates ± SD.

C6Cer-mediated inhibition of SPT in HSAN1 mutant cells

Certain HSAN1 SPT mutants (e.g. SPTLC1 p.C133W) were shown to have a reduced activity *in vitro* [33, 34]; however, the metabolic labeling assay did not show significant difference in SL *de novo* synthesis for SPTLC1wt and p.C133W expressing cells. This indicates that the residual activity of the C133W mutant is still sufficient to

meet the requirements of SL *de novo* synthesis under physiological conditions [17]. In contrast, cells expressing the SPTLC1 p.S331F mutant, which is associated with an exceptionally severe HSAN1 form, showed higher canonical SPT activity in the metabolic labeling assay [17].

We therefore wanted to see if this increased SL formation is caused by impaired feedback regulation of the mutant. For that we compared the inhibitory effect of C6Cer in HEK293 cells overexpressing SPTLC1wt, SPTLC1 p.C133W and p.S331F. The uptake of lipids was confirmed by increased intracellular C18SO levels in response to the exogenously added C6Cer (Fig. 5A). As before, with increasing concentrations of C6Cer *de novo* formation of C18SLs was suppressed in all mutant expressing cells (Fig. 5B). However, higher C6Cer levels were needed to obtain the same inhibitory effect in S331F expressing cells as it was seen for WT or C133W expressing cells (Fig. 5B, D). This is also reflected by a significantly higher IC_{50} value for this mutant (20uM vs 2uM for the WT).

HSAN1 related mutations in SPT cause a permanent shift in the substrate specificity from L-serine to L-alanine, which results in increased 1-deoxySLs formation [9, 11, 16]. Cells overexpressing HSAN1 mutations SPTLC1 p.C133W and SPTLC1 p.S331F form significantly more 1-deoxySLs compared to the WT cells [17]. Similar to the canonical C18SO, *de novo* formation of 1-deoxySA was also reduced when supplementing C6Cer to these cells (Fig. 5C). This indicated that C18SO and 1-deoxySL formation are not independent and appear to be co-regulated by the same mechanism.

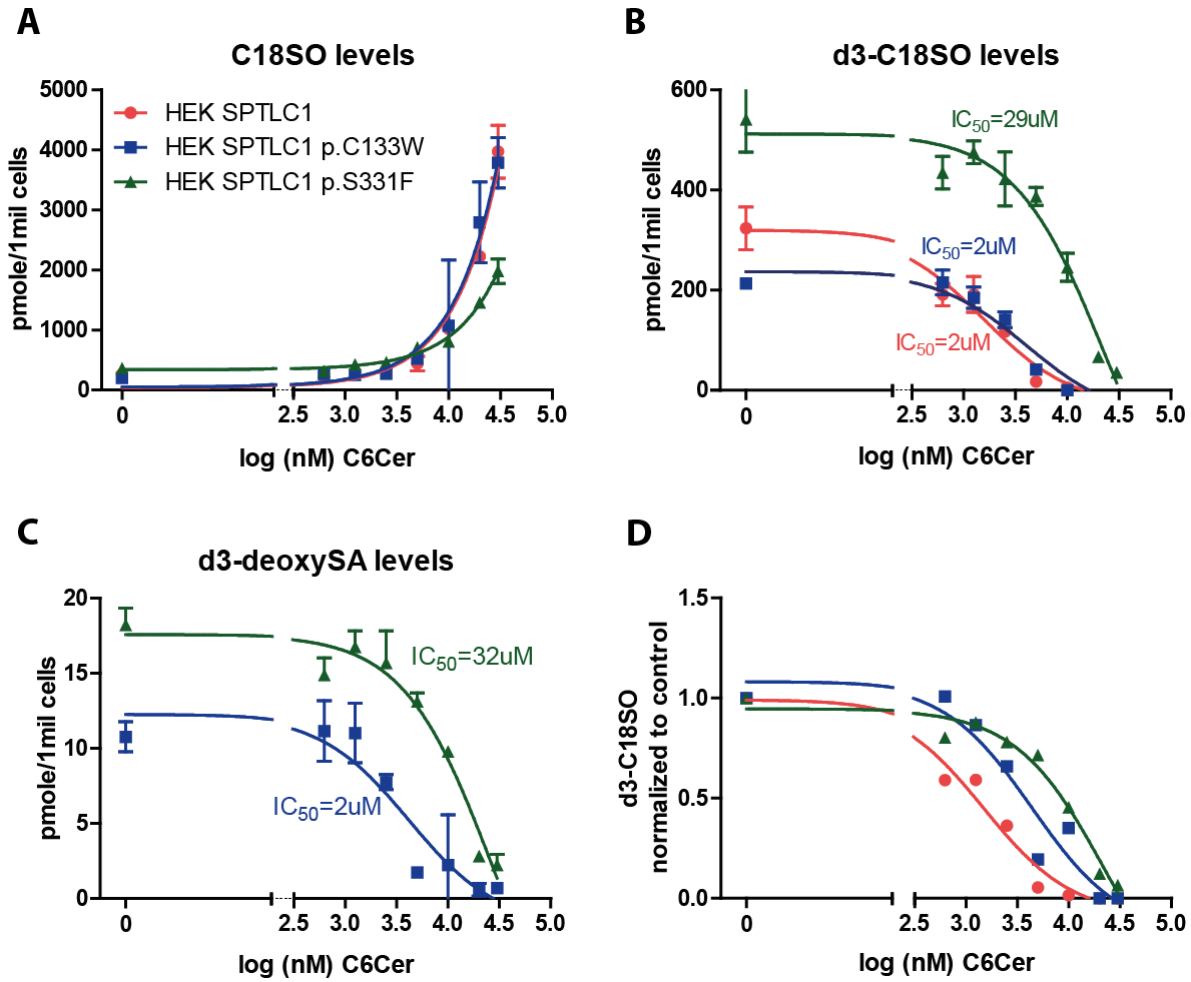

Figure 5. The effect of increasing concentration of C6Cer (0.625μM-30μM) on SPT activity in HEK293 cells overexpressing SPTLC1wt, SPTLC1 p.C133W and SPTLC1 p.S331F. Scatter plots show an inverse relationship between increasing amounts of A) C18SO coming from addition of C6Cer; B) d3-C18SO levels and C) d3-1-deoxySA levels; D) d3-C18SO values normalized to EtOH control. In red are the values for HEK SPTLC1wt cells, in blue – HEK SPTLC1 p.C133W cells, in green – HEK SPTLC1 p.S331F cells. The fitted line was done using log (inhibitor) vs. response function. The values are shown as mean of triplicates ± SD.

We also investigated the effect of C6Cer on the SPTLC2 p.I504F HSAN1 mutation, which showed similar biochemical features as the SPTLC1 p.S331F [17]. Overexpression of wildtype SPTLC2 in HEK293 cells was shown to result in increased SPT activity [17]. Despite the initial higher SPT activity, an inverse relationship between increasing amounts of C6Cer and *de novo* d3-C18SO levels was observed for cells overexpressing the SPTLC2 p.I504F mutant (Fig. 6B). As SPTLC1 p.S331F this mutant also showed a reduced *de novo* synthesized 1-deoxySA with increasing C6Cer (Fig. 6C).

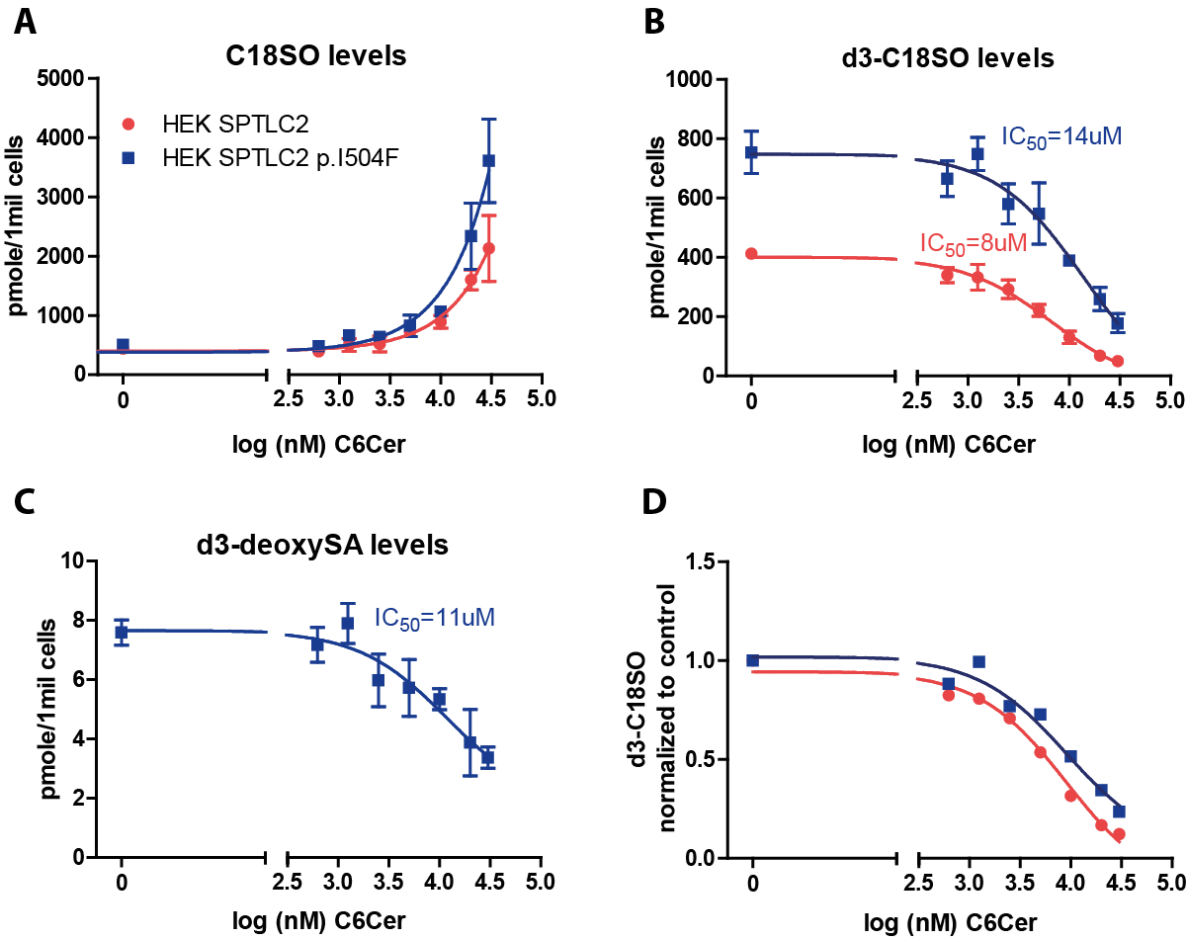

Figure 6. The effect of increasing concentration of C6Cer (0.625μM-30μM) on SPT activity in HEK293 cells overexpressing SPTLC2wt and SPTLC2 p.I504F. Scatter plots show A) C18SO levels, B) *de novo* d3-C18SO levels and C) *de novo* d3-1-deoxySA levels, D) d3-C18SO values normalized to EtOH control in HEK293 cells overexpressing SPTLC2wt and SPTLC2 p.I504F treated with increasing amount of C6Cer. In red are the values for HEK SPTLC2wt cells, in blue – HEK SPTLC2 p.I504F cells. The fitted line was done using log (inhibitor) vs. response function. The values are shown as a mean of triplicates ± SD.

Discussion

In yeast, *de novo* sphingolipid synthesis is regulated by a negative feedback loop mediated by Orm 1 and 2 proteins [19]. However, it is not clear if the same mechanism also applies to mammalian cells. In contrast to yeast, mammalian cells express three ORM orthologues – ORMDL1-3, but the phosphorylation sites reported in yeast are not conserved [25]. However, exogenous supplementation with sphingosine was shown to decrease *de novo* sphingolipid synthesis [28, 29] and Siow et al reported decreased ceramide biosynthesis in HeLa cells upon treatment with C6Cer [30, 31]. Here, we wanted to test whether such feedback inhibition also applies when supplementing mammalian cells with other types of exogenous sphingolipids and whether this regulation affects the formation of typical and atypical sphingoid bases to the same extent. We therefore supplemented HEK293 cells with C6Cer, D7SO, D7SA and SM. The uptake of exogenously added SLs was controlled by an increase in total intracellular SO levels in hydrolyzed lipid extracts. SPT activity was analyzed by incorporation of d4-serine and d4-alanine into the *de novo* formed sphingoid bases. We observed significant reduction in SL *de novo* synthesis upon adding C6Cer, D7SO and D7SA, but not with SM.

In contrast to cell membrane-permeable C6Cer and free sphingoid bases, SM is believed to be not efficiently taken up by the cells. However, when supplementing cells with SM we observed a very strong and dose dependent increase in intracellular SO levels indicating that added SM was taken up. However, despite this strong rise in intracellular SO levels we observed only a minor inhibitory effect on SPT activity compared to the cells treated with the free bases (D7SA, D7SO) or C6Cer. Exogenously added sphingolipids in general are taken up via endocytosis. Free sphingoid bases could flip-flop across the cell membrane. However, the metabolic fate of these sphingolipids may differ. Following the uptake into the cells, SM is perhaps trapped in lysosomes and is not metabolized well by the cells or sphingosine resulted from degradation of SM is preferentially phosphorylated by sphingosine kinases into sphingosine-1-phosphate, which ends up at the plasma membrane (PM). Alternatively, SM could be degraded by the actions of sphingomyelinase (SMase) at the PM and resulting ceramides could be recycled again. An ER localized SPT therefore might not sense the increase in SM levels. On the contrary, C6Cer and free sphingoid bases upon entry to the cell can be degraded to sphingosine (primarily in lysosomes) and can be recycled into ceramides in the ER by

ceramide synthase (CerS). Therefore, it appears that sphingolipid trafficking and compartmentalization seems to affect the way the lipids are sensed. Due to limitation of our method we cannot tell whether the total free sphingoid bases after the hydrolysis of lipids that we measure are actually coming from SM or SO. A broader method to measure SM, Cer and SO would be ideal to see the difference in these sphingolipids and to confirm that the increase in SO levels is indeed coming from SM addition.

We also observed that an increase in C_{18}-based sphingolipids (by addition of C6Cer) resulted in a decreased *de novo* formation of not only canonical sphingoid bases, but also of atypical C_{16}/C_{17}/C_{19}-based sphingoid bases. This indicates that C6Cer-mediated regulation is independent of acyl-CoA levels in the cell.

The expression of SPT mutants SPTLC1 p.S331F and SPTLC2 p.I504F was shown to be associated with increased SPT activity compared to SPTLC1 and 2wt expressing cells [17]. A possible explanation might be that these mutants bypass the inhibition by the ORMDL proteins or some other regulatory factors. In fact, in a homology model of the human SPTLC1-SPTLC2 dimer, the two residues SPTLC1-S331 and SPTLC2-I504 were found to be located on the surface of the protein [17], whereas most of the other HSAN1 mutation clustered around the active site of the protein. This suggests that the mutation might interfere with the binding of a regulatory element or interaction partner of SPT. However, SPT activity in cells expressing SPTLC1 p.S331F and SPTLC2 p.I504F was still suppressed by increasing amount of C6Cer, but at a significantly higher IC_{50} as it is seen for SPTLC1 and 2 wt expressing cells (Fig 3B). The difference in the IC_{50} values indicated that regulation is not the same in S331F (IC_{50}=29uM) compared to C133W (IC_{50}=2uM) and SPTLC1wt (IC_{50}=2uM) and I504F (IC_{50}=14uM) to SPTLC2wt (IC_{50}=8uM). Hence, S331F and I504F mutants are also regulated by the addition of exogenous SLs, although they seem to be less responsive to C6Cer treatment in comparison to the wildtype.

Overall, treatment with C6Cer resulted in decreased *de novo* production of both canonical C18SLs and atypical 1-deoxySLs. The fact that increasing amounts of C6Cer could lower *de novo* produced 1-deoxySA levels indicated that the regulation is independent of serine or alanine availability. This implies that an allosteric regulation of the SPT enzyme modifies the substrate binding pocket of the active site to turn off the enzyme activity independent of the provided substrates. A possible significance of this observation could be the use of C6Cer to inhibit 1-deoxySLs formation as a treatment in HSAN1. However, C6Cer is not a better alternative to L-serine supplementation, which

was shown to lower 1-deoxySLs [35] in particular as a permanent suppression of SL formation at elevated C6Cer levels likely to have severe consequences for the cell.

However, it is not clear how the regulation affects the composition of the SPT complex and which of the SPT subunits is primarily affected by the regulation. The structure of mammalian SPT is not solved yet. However, earlier data showed that SPT is a multimeric complex with molecular weight of 480 kDa and composed of either four SPTLC1-SPTLC2 or SPTLC1-SPTLC3 [36] dimers thereby forming a functional octamer. Hence, C6Cer-mediated inhibition could primarily act on SPTLC1, which is the main subunit and a core binding partner for both, SPTLC2 and 3 subunit. Hereby SPTLC1 and SPTLC2 (likely also SPTLC1 and SPTLC3) form a functional dimer in which the active site is located at the monomer-monomer interface. The two mutations – SPTLC1p.C133W and p.V144D, were shown to be located close to PLP-binding site of the opposing SPTLC2 subunit thereby influencing the formation of active catalytic site [17].

In conclusion, we found that exogenous supplementation with C6Cer and the free LCB (SA and SO), but not with SM inhibited SPT activity. This regulation was shown to be similar in SPTLC1, 2 and 3 overexpressing cells. Moreover, we showed that also the HSAN1 mutants SPTLC1p.S331 and SPTLC2p.I504F were regulated, but at higher IC_{50} values requiring greater amount of C6Cer to obtain the same inhibitory effect. This indicates that *de novo* SL synthesis is switched off later in the HSAN1 mutants than in normal cells.

References

1. Hanada, K., et al., *A mammalian homolog of the yeast LCB1 encodes a component of serine palmitoyltransferase, the enzyme catalyzing the first step in sphingolipid synthesis.* Journal of Biological Chemistry, 1997. **272**(51): p. 32108-32114.
2. Hanada, K., *Serine palmitoyltransferase, a key enzyme of sphingolipid metabolism.* Biochim Biophys Acta, 2003. **1632**(1-3): p. 16-30.
3. Hornemann, T., et al., *The SPTLC3 subunit of serine palmitoyltransferase generates short chain sphingoid bases.* J Biol Chem, 2009. **284**(39): p. 26322-30.
4. Hornemann, T., et al., *Cloning and initial characterization of a new subunit for mammalian serine-palmitoyltransferase.* J Biol Chem, 2006. **281**(49): p. 37275-81.
5. Bejaoui, K., et al., *SPTLC1 is mutated in hereditary sensory neuropathy, type 1.* Nat Genet, 2001. **27**(3): p. 261-2.
6. Dawkins, J.L., et al., *Mutations in SPTLC1, encoding serine palmitoyltransferase, long chain base subunit-1, cause hereditary sensory neuropathy type I.* Nature genetics, 2001. **27**(3): p. 309-312.
7. Auer-Grumbach, M., et al., *Molecular genetics of hereditary sensory neuropathies.* Neuromolecular Med, 2006. **8**(1-2): p. 147-58.
8. Rotthier, A., et al., *Genes for hereditary sensory and autonomic neuropathies: a genotype-phenotype correlation.* Brain, 2009. **132**(Pt 10): p. 2699-711.
9. Rotthier, A., et al., *Mutations in the SPTLC2 Subunit of Serine Palmitoyltransferase Cause Hereditary Sensory and Autonomic Neuropathy Type I.* American Journal of Human Genetics, 2010. **87**(4): p. 513-522.
10. Murphy, S.M., et al., *Hereditary sensory and autonomic neuropathy type 1 (HSANI) caused by a novel mutation in SPTLC2.* Neurology, 2013. **80**(23): p. 2106-11.
11. Ernst, D., et al., *Novel HSAN1 Mutation in Serine Palmitoyltransferase Resides at a Putative Phosphorylation Site That Is Involved in Regulating Substrate Specificity.* Neuromolecular Medicine, 2015. **17**(1): p. 47-57.
12. Suriyanarayanan, S., et al., *The Variant p.(Arg183Trp) in SPTLC2 Causes Late-Onset Hereditary Sensory Neuropathy.* NeuroMolecular Medicine, 2015. **18**(1): p. 81-90.
13. Fridman, V., et al., *Natural history and biomarkers in hereditary sensory neuropathy type 1.* Muscle & Nerve, 2015. **51**(4): p. 489-495.
14. Auer-Grumbach, M., *Hereditary sensory neuropathy type I.* Orphanet Journal of Rare Diseases, 2008. **3**.
15. Houlden, H., et al., *Clinical, pathological and genetic characterization of hereditary sensory and autonomic neuropathy type 1 (HSAN I).* Brain, 2006. **129**: p. 411-425.
16. Penno, A., et al., *Hereditary sensory neuropathy type 1 is caused by the accumulation of two neurotoxic sphingolipids.* J Biol Chem, 2010. **285**(15): p. 11178-87.
17. Bode, H., et al., *HSAN1 mutations in serine palmitoyltransferase reveal a close structure-function-phenotype relationship.* Hum Mol Genet, 2015.
18. Auer-Grumbach, M., et al., *Mutations at Ser331 in the HSN type I gene SPTLC1 are associated with a distinct syndromic phenotype.* Eur J Med Genet, 2013. **56**(5): p. 266-9.
19. Breslow, D.K., et al., *Orm family proteins mediate sphingolipid homeostasis.* Nature, 2010. **463**(7284): p. 1048-53.
20. Han, S., et al., *Orm1 and Orm2 are conserved endoplasmic reticulum membrane proteins regulating lipid homeostasis and protein quality control.* Proc Natl Acad Sci U S A, 2010. **107**(13): p. 5851-6.
21. Roelants, F.M., et al., *Protein kinase Ypk1 phosphorylates regulatory proteins Orm1 and Orm2 to control sphingolipid homeostasis in Saccharomyces cerevisiae.* Proc Natl Acad Sci U S A, 2011. **108**(48): p. 19222-7.
22. Tafesse, F.G. and J.C. Holthuis, *Cell biology: A brake on lipid synthesis.* Nature, 2010. **463**(7284): p. 1028-9.
23. Walther, T.C., *Keeping sphingolipid levels nORMal.* Proc Natl Acad Sci U S A, 2010. **107**(13): p. 5701-2.
24. Shimobayashi, M., et al., *TORC1-regulated protein kinase Npr1 phosphorylates Orm to stimulate complex sphingolipid synthesis.* Mol Biol Cell, 2013. **24**(6): p. 870-81.
25. Hjelmqvist, L., et al., *ORMDL proteins are a conserved new family of endoplasmic reticulum membrane proteins.* Genome Biol, 2002. **3**(6): p. RESEARCH0027.

26. Ogretmen, B., et al., *Biochemical mechanisms of the generation of endogenous long chain ceramide in response to exogenous short chain ceramide in the A549 human lung adenocarcinoma cell line. Role for endogenous ceramide in mediating the action of exogenous ceramide.* J Biol Chem, 2002. **277**(15): p. 12960-9.
27. Takeda, S., et al., *Apoptosis occurs via the ceramide recycling pathway in human HaCaT keratinocytes.* J Biochem, 2006. **139**(2): p. 255-62.
28. van Echten, G., et al., *Modulation of sphingolipid biosynthesis in primary cultured neurons by long chain bases.* J Biol Chem, 1990. **265**(16): p. 9333-9.
29. Mandon, E.C., et al., *Sphingolipid biosynthesis in cultured neurons. Down-regulation of serine palmitoyltransferase by sphingoid bases.* Eur J Biochem, 1991. **198**(3): p. 667-74.
30. Siow, D.L. and B.W. Wattenberg, *Mammalian ORMDL proteins mediate the feedback response in ceramide biosynthesis.* J Biol Chem, 2012. **287**(48): p. 40198-204.
31. Siow, D., et al., *Regulation of de novo sphingolipid biosynthesis by the ORMDL proteins and sphingosine kinase-1.* Adv Biol Regul, 2015. **57**: p. 42-54.
32. Othman, A., et al., *Plasma deoxysphingolipids: a novel class of biomarkers for the metabolic syndrome?* Diabetologia, 2012. **55**(2): p. 421–431.
33. Bejaoui, K., et al., *Hereditary sensory neuropathy type 1 mutations confer dominant negative effects on serine palmitoyltransferase, critical for sphingolipid synthesis.* Journal of Clinical Investigation, 2002. **110**(9): p. 1301-1308.
34. Gable, K., et al., *Mutations in the yeast LCB1 and LCB2 genes, including those corresponding to the hereditary sensory neuropathy type I mutations, dominantly inactivate serine palmitoyltransferase.* J Biol Chem, 2002. **277**(12): p. 10194-200.
35. Garofalo, K., et al., *Oral L-serine supplementation reduces production of neurotoxic deoxysphingolipids in mice and humans with hereditary sensory autonomic neuropathy type 1.* J Clin Invest, 2011. **121**(12): p. 4735-45.
36. Hornemann, T., Y. Wei, and A. von Eckardstein, *Is the mammalian serine palmitoyltransferase a high-molecular-mass complex?* Biochem J, 2007. **405**(1): p. 157-64.

Chapter 3:

STUDIES ON THE MECHANISM BEHIND CERAMIDE MEDIATED INHIBITION OF SPT

Assem Zhakupova, Arnold von Eckardstein, Thorsten Hornemann

Author contributions

AZ – acquired, analyzed and interpreted data, wrote the manuscript

AvE – revised the manuscript, supervised the study

TH – interpreted data, revised the manuscript, supervised the study

Abstract

Objective: Sphingolipid *de novo* synthesis is tightly controlled by a metabolic feedback mechanism that regulates the activity of the rate limiting enzyme serine palmitoyltransferase (SPT). We and others have demonstrated that sphingolipid *de novo* synthesis is suppressed with increasing intracellular sphingolipid levels by adding either sphingosine (SO) or synthetic membrane-permeable C6-ceramide (C6Cer). However, the underlying mechanism of this regulation is not fully understood. In yeast it was demonstrated that SPT activity is controlled by two proteins (Orm1 and 2), which bind and regulate the activity in a phosphorylation dependent manner. However, it is not clear yet to which extent the same mechanism also applies to mammalian cells. Additionally, it is unknown how the cell senses intracellular SL levels. We aimed to study the functional connection between intracellular ceramide (Cer) metabolism and SPT activity in more detail.

Methods: Cells were supplemented with exogenous sphingolipids while modulating key enzymes of the SL metabolism using specific chemical inhibitors. SPT activity and SL *de novo* synthesis was measured by the incorporation of isotope labeled substrates (d3-N15-L-serine and d4-L-alanine). Ceramides and total sphingoid base profiles were quantified by LC-MS.

Results: We found that the supplemented C6Cer was almost exclusively converted to monohexosylceramide (MHCer), but not to sphingomyelins (SM). However, the inhibitory effect of C6Cer on SPT was independent of this conversion. The C6Cer mediated inhibition of SPT was partly reversed in the presence of the ceramide synthase (CerS) inhibitor FB1 and the ceramidase inhibitor NOE. This effect was even more pronounced when supplementing SO in the presence of FB1. The inhibition of other key enzymes in the SL metabolism had no effect.

Conclusion: Increasing intracellular Cer levels inhibits SPT, which results in reduced SL *de novo* synthesis. Selective inhibition of CerS or ceramidase partly reversed this effect. We therefore concluded that the formation of Cer either by reacylation of C6Cer via the salvage pathway or by N-acylation of SO is essential for the inhibition of SPT.

Abbreviations: C6-ceramide – C6Cer; SO – sphingosine; SM – sphingomyelin; MHCer – monohexosylceramide; SLs – sphingolipids; glycoSLs – glycosphingolipids; D7SO – D-erythro-sphingosine-d7.

Introduction

Serine palmitoyltransferase (SPT) catalyzes the condensation of palmitoyl-CoA and L-serine to form long chain base C_{18}-sphinganine (SA) [1-3]. SA is then converted to ceramides by the consecutive actions of ceramide synthases (CerS1-6) and dihydroceramide desaturase (DES1). Ceramide itself serves as a building block of complex sphingolipids such as sphingomyelin (SM) and glycosphingolipids (glycoSLs). Ceramide biosynthesis starts in the endoplasmic reticulum (ER) from where the *de novo* formed ceramides are transported to the Golgi for the synthesis of complex sphingolipids. This transport is mediated either via vesicular or non-vesicular transport mediated by the ceramide transfer protein (CERT) [4]. CERT-mediated transport of ceramides from ER to the Golgi targets ceramides primarily for SM synthesis. Because of their crucial role in cell growth and viability, cells maintain a close balance between ceramide and phosphorylated sphingoid bases by keeping total intracellular sphingolipids in homeostasis [5, 6].

C6Cer is a synthetic short-chain ceramide that can cross the cell-membrane [7]. It is commonly used to increase intracellular Cer levels in investigational cancer therapy [8-10]. C6Cer, but not C2-ceramide, was shown to undergo reacylation via the salvage pathway, where ceramidase degrades C6-ceramides to sphingosine (SO), which is then converted to long-chain ceramides by CerS [11-14]. Raising intracellular ceramide levels by supplementing cells with C6Cer strongly suppresses SPT activity by blocking *de novo* SL synthesis (see chapter 2).

However, the mechanisms that are responsible for sensing and maintaining intracellular SL levels are not yet understood. Interestingly, recently sphingomyelin synthase-related protein (SMSr) was shown to be a sensor of ceramide levels in the ER [15]. It hypothesized that SMSr acts in coordination with CERT to maintain ceramide homeostasis in the cell. However, this hypothesis was not confirmed.

Here, we further explored the metabolic effects of C6Cer to better understand the mechanism behind C6Cer-mediated SPT inhibition in mammalian cells. We used a set of chemical inhibitors to block key enzymes in the sphingolipid pathway and to test whether the C6Cer itself or specific downstream metabolites are essential for the inhibitory effect on SPT.

Methods

General

All chemicals were purchased from Sigma Aldrich unless otherwise stated. D7-sphingosine, d7-sphinganine and sphingomyelin were from Avanti Polar Lipids. Myriocin was from Cayman Chemical.

Inhibitors

All inhibitors were dissolved in ethanol (except myriocin, which was dissolved in methanol and NVP-231 – in DMSO) and stored at -20°C. Effective concentration for each inhibitor was chosen based on their IC_{50} reported earlier [16, 17].

Stable isotope labelling assay to measure SPT activity

HEK293 cells were grown to 60-70% confluency in DMEM (Sigma Aldrich) containing 10% fetal bovine serum (Gibco, Life Technologies) and 1% penicillin/streptomycin (100 U/ml, Sigma Aldrich). Medium was changed to L-serine and L-alanine free DMEM (Genaxxon, Ulm, Germany) containing 10% delipidated FCS (Sigma Aldrich). Four hours later the cells were treated with isotope-labeled deuterated substrates 1mM L-serine (2,3,3-D3, 15N) and 2mM L-alanine (2,3,3,3-D4) (Cambridge Isotopes). After 24h incubation, cells were washed once with PBS, collected with 900ul of PBS and counted (Z2 Coulter Counter, Beckman Coulter, CA). Cell pellets were collected by centrifugation (1200g x 5min, at 4°C) and stored at -20°C.

SPT activity was quantified by incorporation of isotopically labeled substrates (d3-N15-L-serine and d4-L-alanine) into *de novo* synthesized sphingolipids, which were then measured by a shift in mass over charge (m/z) of +3Da detected on the MS. Because one deuterium is replaced by hydrogen during the condensation reaction with palmitoyl-CoA, SPT activity was measured by quantifying *de novo* formed sphinganines (d3-C18SA) and sphingosines (d3-C18SO) after acid-base hydrolysis of total sphingolipids. Therefore, it reflects the SPT activity.

Analysis of sphingoid bases

Cell pellets were dissolved in 100uL of PBS. Two-hundred pmol of internal standards (d7-sphinganine and d7-sphingosine, Avanti Polar Lipids) in 500uL of methanol

(Honeywell) were added to the cells. The samples were agitated on a shaker (Thermomixer comfort, Eppendorf; Hamburg, Germany) at 37°C and 1400 rpm for 1 hour. Followed by centrifugation at 16,000g x 5min protein precipitate was formed and the supernatant was transferred to a new 2mL Eppendorf tube. HCL (≥32%, Sigma-Aldrich) was added and lipids were hydrolyzed for 16h at 65°C and afterwards neutralized with 10M KOH. Free sphingoid bases were then extracted by adding chloroform (99.8%, Sigma-Aldrich) in basic condition containing 2N ammoniac (Sigma-Aldrich). The sphingoid bases were analyzed using TSQ Quantum Ultra and QExactive liquid chromatography-mass spectrometers (LC-MS) as previously described [18, 19].

Extraction and analysis of ceramide species

Cell pellets were resuspended in 100uL of PBS. The extraction mix containing 1mL of methanol and chloroform (in 1:2 ratio) including 200pmol of C12-Ceramide (d18:1/12:0) was added to the cells. The samples were kept on a shaker at 37°C for 1h (Thermomixer comfort, Eppendorf; Hamburg, Germany). Following that 500uL of chloroform (99.8%, Sigma-Aldrich) and 200uL of alkaline water (500uL NH_4OH (25%) in 250 mL H_2O and 20uL Bromphenol blue (2.5%)) were added to the tubes. Afterwards, the samples were centrifuged at 16,000g for 5 min. The lower phase was washed three times with alkaline water. Dried samples were stored at -20°C until further analysis. The lipids were then analyzed by using QExactive LC-MS as published earlier [19].

Statistical analysis

Statistical analysis was done using GraphPad Prism 5. All values are reported as mean ± standard deviations.

Results

Increasing intracellular ceramide levels inhibit SPT activity

We (Chapter 2) and others [20, 21] showed that supplementing HEK293 or HeLa cells with membrane permeable C6Cer significantly decreased ceramide *de novo* biosynthesis. In continuation, we were interested to study the dynamics of C6Cer-mediated inhibition of SPT in more detail. For that we treated HEK293 cells with C6Cer over a period of 24h and analyzed the impact on SPT activity over time. The goal was to analyze the kinetics of SPT inhibition during which the C6Cer is taken up and metabolized. To exclude a bias by external sphingolipids in the medium, the assay was carried out in DMEM containing 10% delipidated serum.

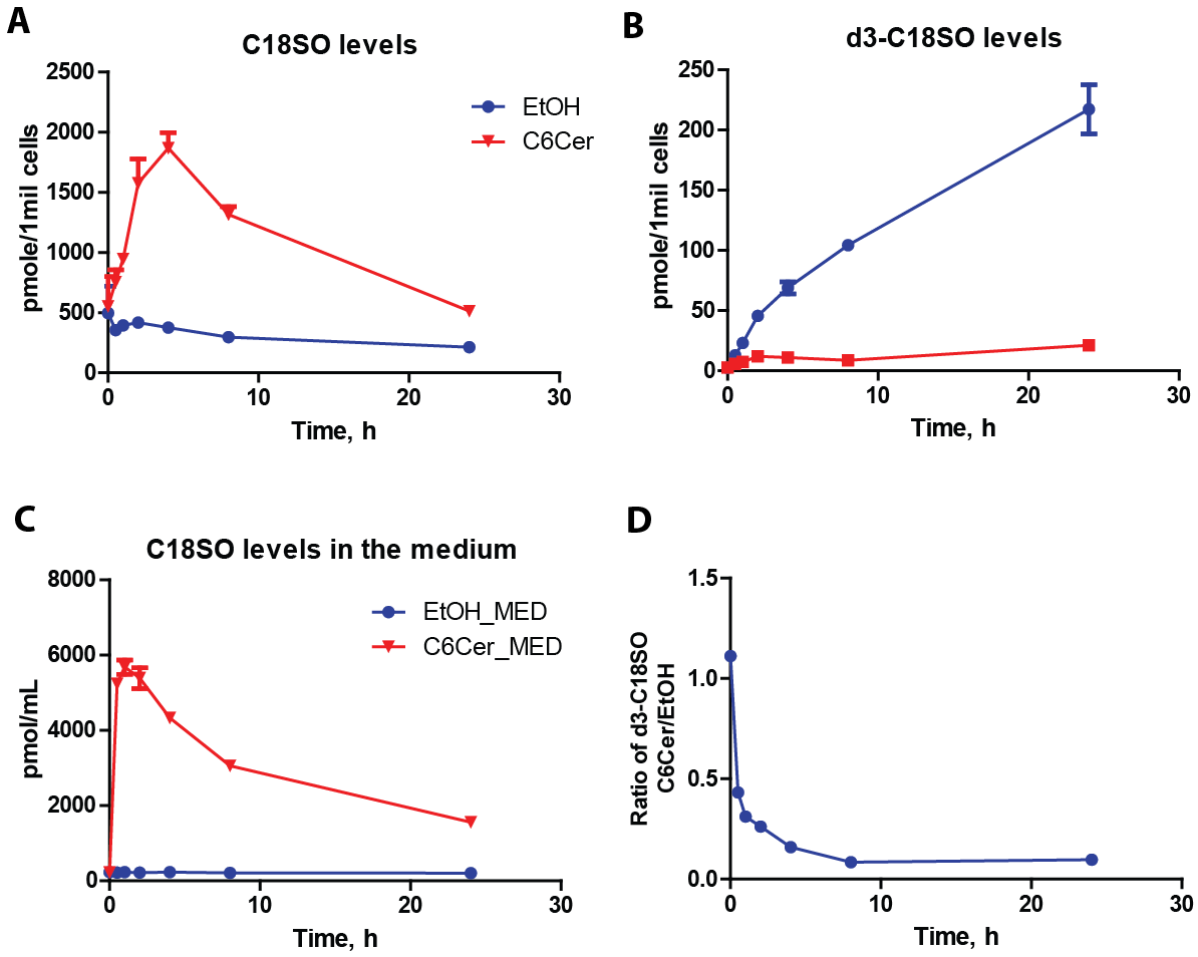

Figure 1. HEK293 cells treated with ethanol (blue) and C6Cer 10µM (red) over time (0-24h). A) C18SO levels in the cells; B) *de novo* formed C18SO (d3-C18SO); C) C18SO levels in the medium; D) the ratio of d3-C18SO C6Cer over ethanol control. Data are shown as mean ±SD (n=3).

Upon addition of C6Cer, we observed a rapid increase in C18SO levels (reflecting intracellular C6Cer levels) already after 30 min. SO levels peaked at 4h and then

decreased over time (shown in red in Fig. 1A). In parallel, C18SO levels in the medium started to significantly decrease after 2h. Approximately a third of the added C6Cer was still present in the medium after 24h. However, the C18SO levels in ethanol treated controls remained constant at low levels throughout the time (shown in blue in Fig. 1A).

In contrast, the levels of *de novo* formed d3-C18SO increased over time in control cells (Fig. 1B), but not in cells treated with C6Cer. *De novo* formed d3-C18SO remained low over the entire 24h in these cells (Fig. 1B, D). The peak of intracellular C18SO after 4h was not associated with a further decrease in d3-C18SO formation at that time point. Interestingly, although intracellular C18SO levels were back to baseline after 24h, SPT activity remained still inhibited.

C6Cer treatment results in enrichment of primarily glycosphingolipids

Next, we wanted to see if C6Cer itself or rather one of its downstream metabolites was responsible for the inhibitory effect. We therefore examined the metabolic conversion of the added C6Cer in more detail.

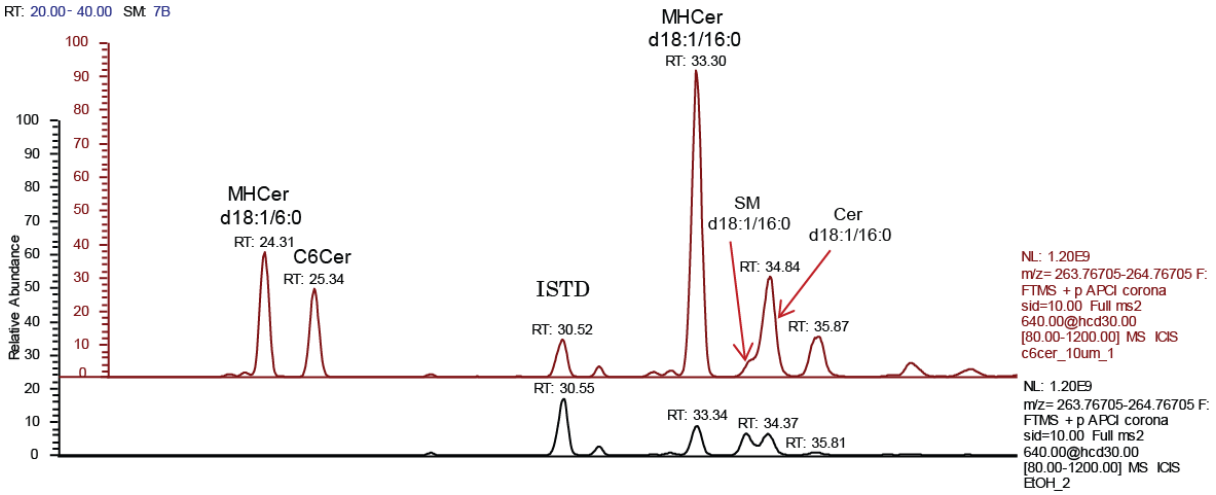

Figure 2. Comparison of chromatograms in full scan AIF containing C18SO (fragment 264.26705) sphingolipids; relative abundance is shown with the intensity of $1.2x10^9$. Top panel depicts the peaks in HEK293 cells treated with C6Cer (10µM), lower one – with EtOH. Identity of each peak was confirmed by the exact mass of the full compound. ISTD – internal standard, MHCer – monohexosylceramide, SM – sphingomyelin, Cer – ceramide. We observed a selective increase of monohexosylceramide (especially MHCer d18:1/16:0) species in C6Cer treated cells.

Chromatograms of sphingolipids containing C18SO (indicator fragment 264.26705) are shown in Fig. 2. The MS analysis revealed that C6Cer was readily taken

up by the cells (peak corresponding to C6Cer), but then almost exclusively converted to a metabolite with m/z 699.57096. This metabolite increased 10 fold in C6Cer treated cells compared to ethanol control. Surprisingly, sphingomyelin (SM) did not increase after adding C6Cer. Using the LIPID MAPS database the metabolite was identified as a monohexosylceramide (MHCer), being either d18:1/16:0 glucosylceramide (GlcCer) or galactosylceramide (GalCer).

To confirm whether the formation of this MHCer metabolite is essential for SPT inhibition, we used the glucosylceramide synthase (GCS) inhibitor PDMP to block the conversion of Cer into GlcCer. HEK293 cells were treated with different concentration of PDMP (1µM and 10µM) in combination with or without C6Cer (10µM). C6- and C16-glucosylceramide levels decreased in PDMP treated samples in a dose-dependent manner (Fig. 3D) suggesting that the observed MHCer peak is GlcCer rather than GalCer. Unfortunately, no inhibitor for galactosylceramide synthase was available for comparison. In parallel, we observed a significant reacylation of the C6Cer into C16-Cer and C16-GlcCer (Fig. 3C, D). However, also in the presence of PDMP, C6Cer was still able to efficiently suppress SPT activity and SL *de novo* synthesis (Fig. 3B) indicating that the conversion of C6Cer into GlcCer is not directly responsible for the inhibitory effect on SPT.

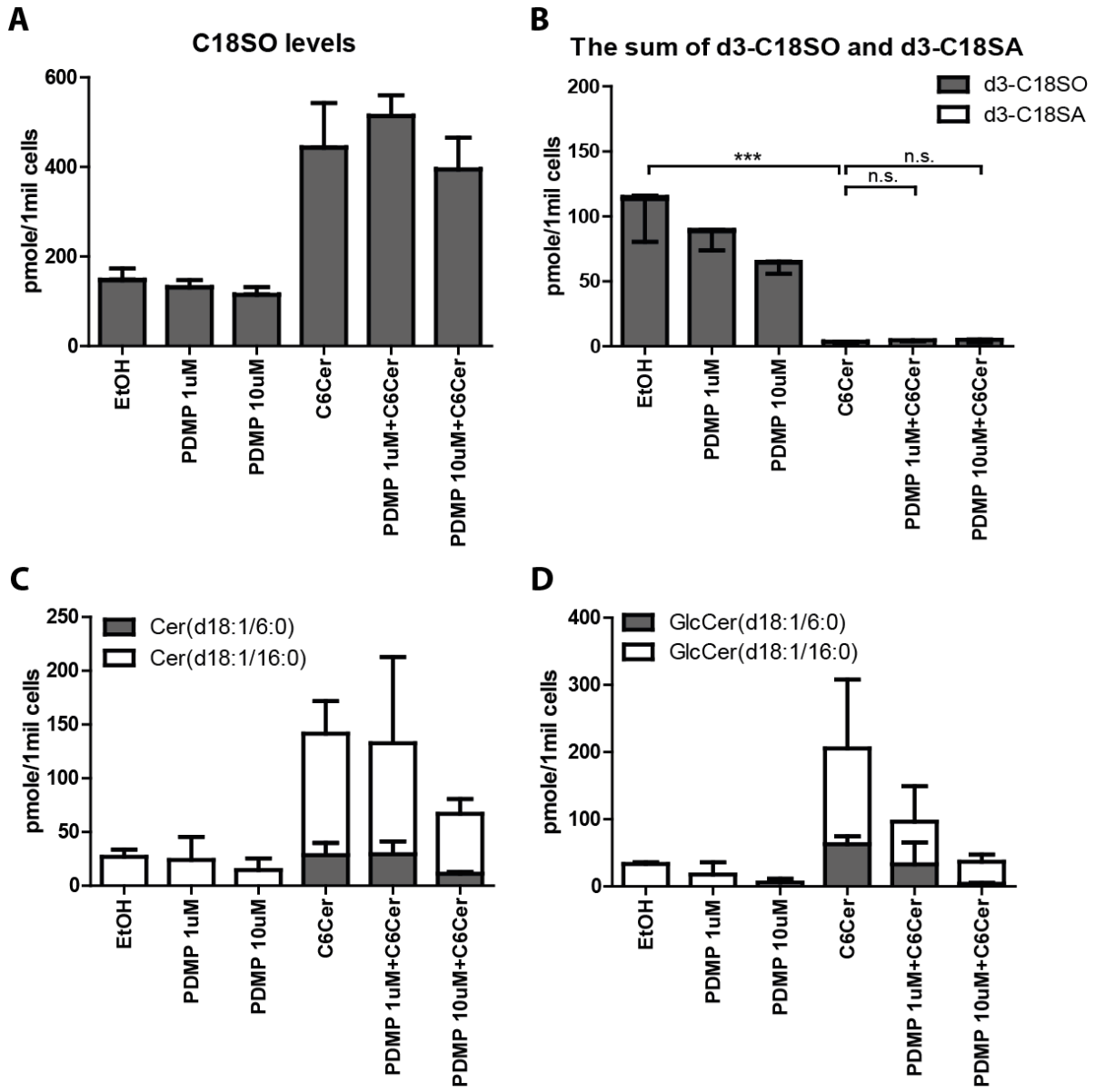

Figure 3. Stacked bar plots show A) C18SO levels; B) the sum of *de novo* C18SLs (d3-C18SO and d3-C18SA); C) C6-/C16-ceramide and D) C6-/C16-glucosylceramide levels in HEK 293 cells treated with PDMP (1μM, 10μM), C6Cer (10μM) and ethanol control. HEK293 cells were incubated with the inhibitors in combination with or without C6Cer for 24h. Data are shown as mean ±SD (n=3). The significance was calculated for the sum of d3-C18SO and d3-C18SA using one-way ANOVA, post-test: Newman-Keuls Multiple Comparison Test, ***$p<0.001$.

Inhibiting the key enzymes in sphingolipid metabolism pathway

To see whether other downstream metabolites are responsible for SPT inhibition, we used a set of defined chemical inhibitors to block distinct key enzymes in the sphingolipid pathway. The characteristics of the inhibitors used are presented in Table 1 and Fig. 4 [16, 17].

Table 1. The list of the inhibitors.

Inhibitor	Targeting Enzyme	Concentration used, uM	Reference
Myriocin	SPT	2μM	[22, 23]
Fumonisin B1 (FB1)	Ceramide synthase (CerS)	35μM	[24, 25]
Fenretinide (4-HPR)	Desaturase (DES)	2μM	[26, 27]
N-oleoylethanolamine (NOE)	(Acid) Ceramidase	20μM	[28-30]
N,N-Dimethylsphingosine (DMS)	Sphingosine kinase	5μM	[31, 32]
4-[[4-(4-Chlorophenyl)-2-thiazolyl]amino]phenol (SKI-II)	Sphingosine kinase	10μM, 20μM	[33-36]
2-Acetyl-4-tetrahydroxybutyl imidazole (THI)	S1P lyase	2μM, 10μM	[37]
NVP-231	Ceramide kinase	10nM, 100nM, 1000nM	[38-40]
d,l-threo-1-phenyl-2-decanoylamino-3-morpholino-1-propanolhydrochloride (PDMP)	Glucosylceramide synthase	1μM, 10μM	[41, 42]

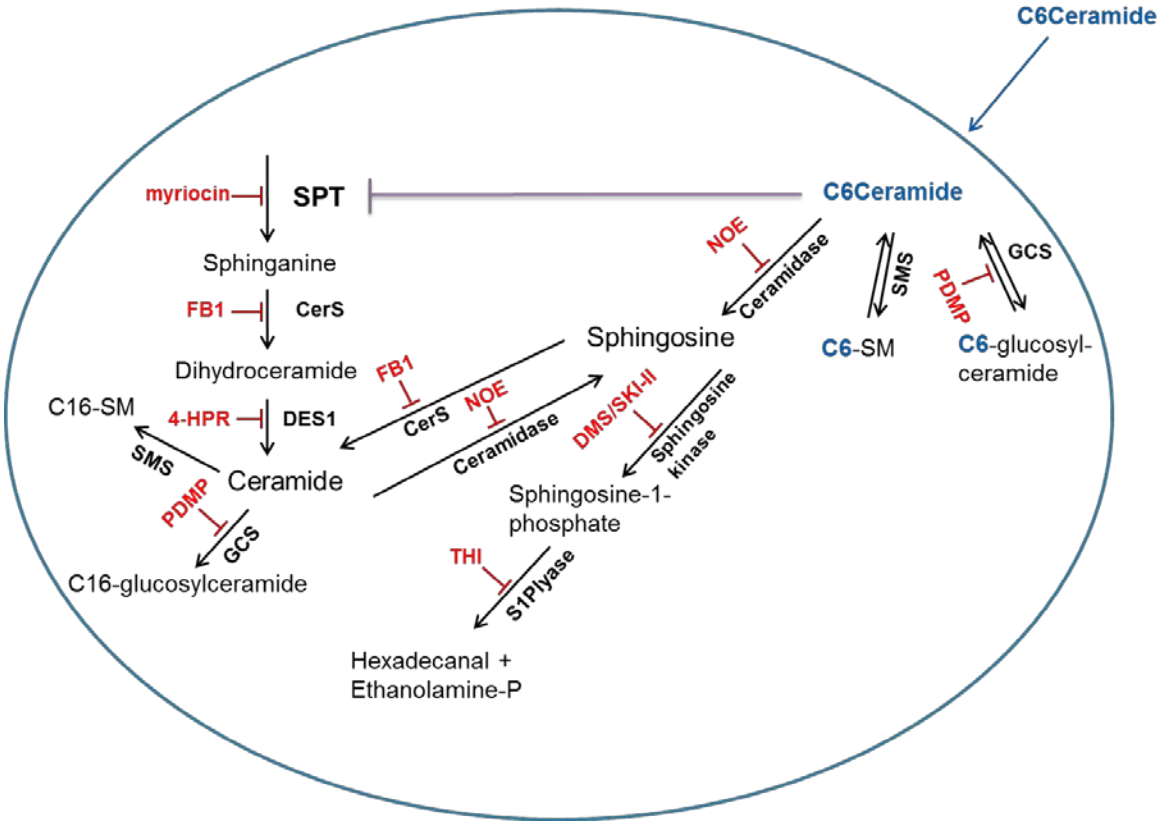

Figure 4. Schematic view of the sphingolipid metabolic pathway showing the inhibitors in red and corresponding enzymes in bold. CerS – ceramide synthase, DES1 – desaturase, SMS – sphingomyelin synthase, GCS – glucosylceramide synthase, S1P lyase – sphingosine-1-phosphate lyase, SM – sphingomyelin.

HEK293 cells were incubated for 24h with the inhibitors in the given concentration (Table 1 and Fig. 4) either with or without C6Cer (10µM). The efficacy of the inhibitors was confirmed by showing for the accumulation of the metabolite upstream of the targeted enzyme. However, not all of the inhibitors could be confirmed that way, as our method did not allow to directly measure S1P and Cer-1P levels. In parallel, the impact of the inhibitor on SPT activity was assessed by quantifying *de novo* formed sphingoid bases and by checking whether in presence of the inhibitor C6Cer was still capable to inhibit SPT activity.

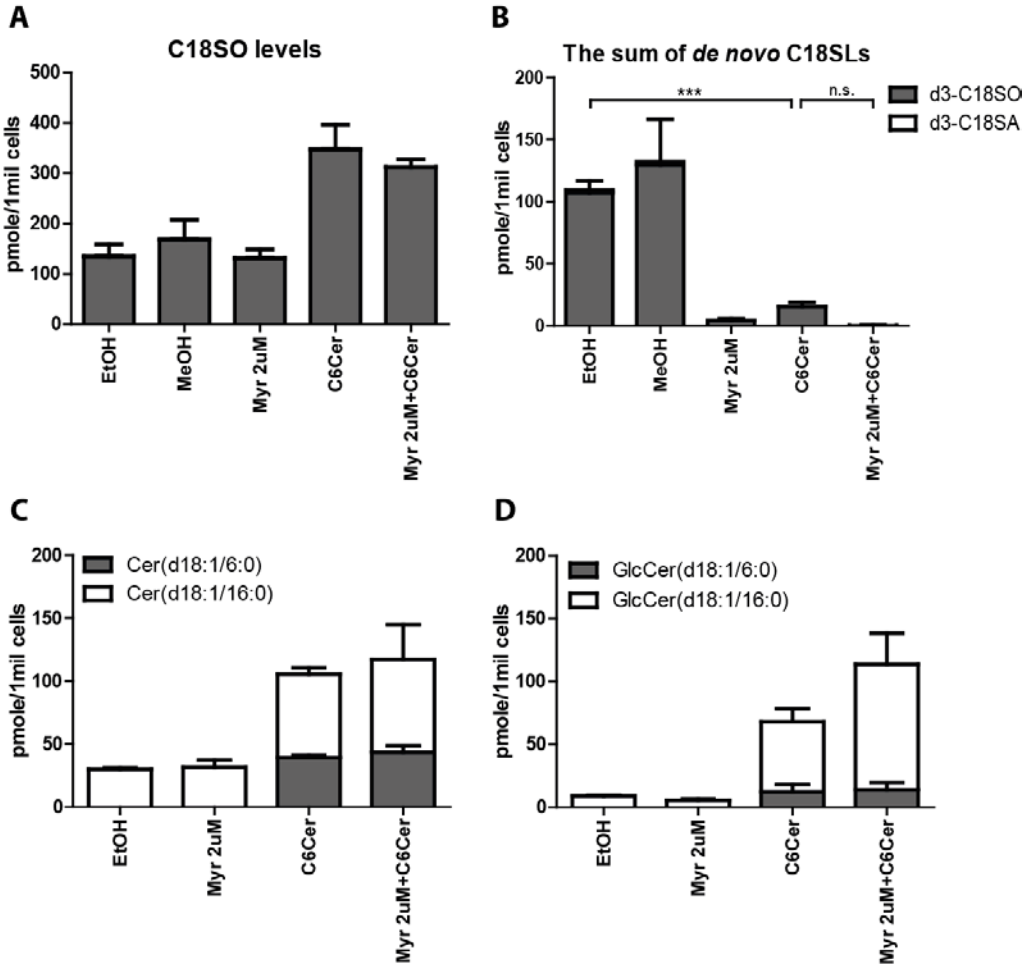

Figure 5. Stacked bar plots show A) C18SO levels, B) the sum of *de novo* C18SLs (d3-C18SO and d3-C18SA), C) C6-/C16-ceramide and D) C6-/C16-glucosylceramide levels in HEK 293 cells treated with myriocin (2µM), C6Cer (10µM), ethanol and methanol control, and incubated with the inhibitor in combination with C6Cer for 24h. Data are shown as mean ±SD (n=3). The significance was calculated for the sum of d3-C18SO and d3-C18SA using one-way ANOVA, post-test: Newman-Keuls Multiple Comparison Test, ***p<0.001.

Myriocin was used as a negative control to determine SL background levels in the absence of SPT activity. In the presence of myriocin (2µM) *de novo* C18SLs formation was almost completely suppressed (Fig. 5B) and even further reduced in the presence of

C6Cer. Interestingly, C16-glucosylceramide levels were higher upon treatment with Myr+C6Cer (Fig. 5D) compared to C6Cer alone.

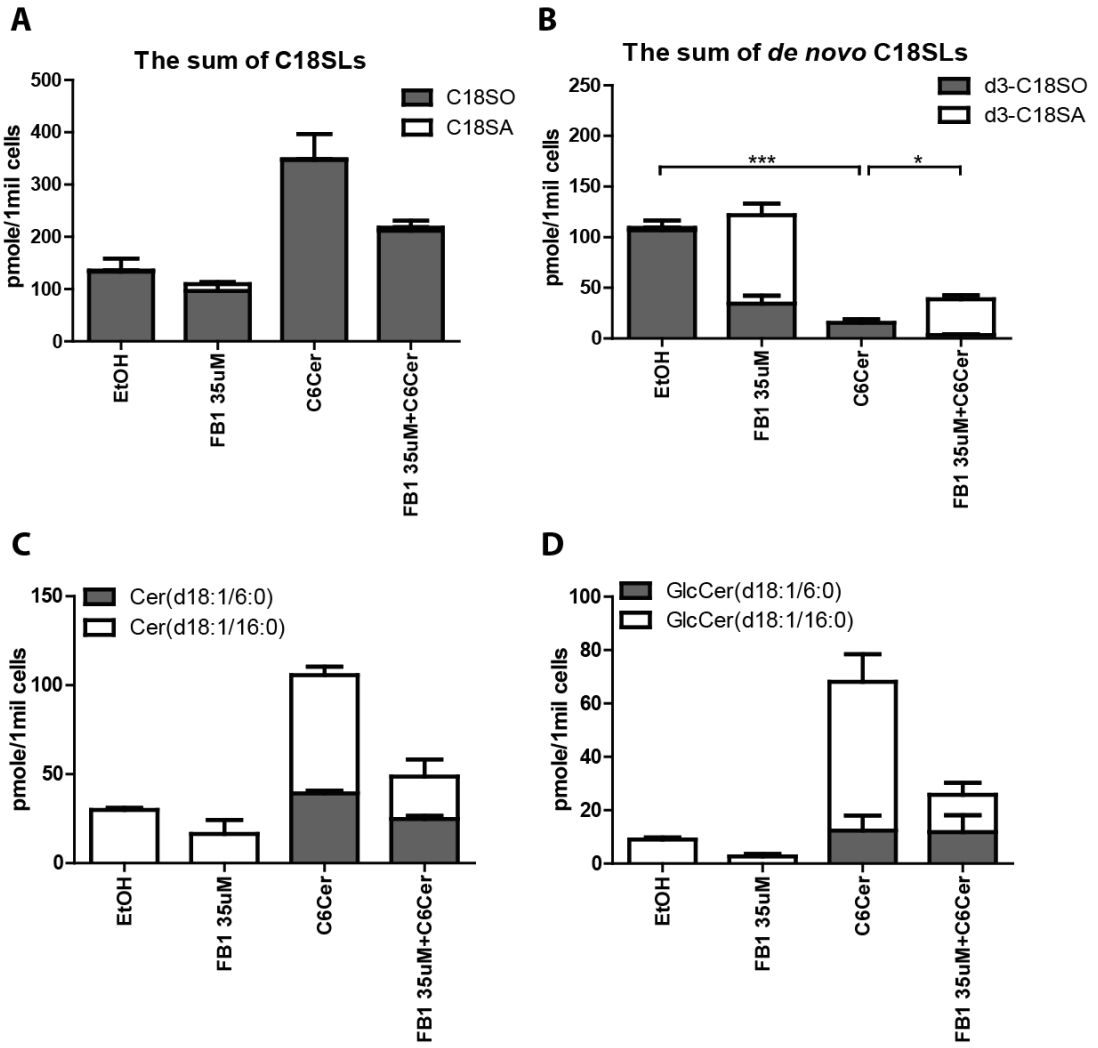

Figure 6. Stacked bar plots showing A) the sum of C18SLs (C18SO and C18SA), B) the sum of *de novo* C18SLs (d3-C18SO and d3-C18SA), C) C6-/C16-ceramide and D) C6-/C16-glucosylceramide levels in HEK293 cells treated with FB1 (35µM), C6Cer (10µM) and ethanol control, and incubated for 24h. Data are shown as mean ±SD (n=3). The significance was calculated for the sum of d3-C18SO and d3-C18SA using one-way ANOVA, post-test: Newman-Keuls Multiple Comparison Test, *p<0.05, ***p<0.001.

Inhibition of ceramide synthase (CerS) by FB1 blocks the formation of dihydroceramide (DHCer) and leads to the accumulation of its precursor sphinganine (SA). HEK293 cells treated with FB1 showed considerably more C18SA levels compared to controls (Fig. 6B). Total C16-ceramides and C16-GlcCer were strongly reduced in FB1+C6Cer cells (Fig. 6D). This is explained by the fact that also the reacylation of SO is inhibited by FB1, which leads to increased degradation of SO through the catabolic pathway. Like before, adding C6Cer resulted in decreased *de novo* formed d3-C18SLs

compared to controls. In combination with FB1, the inhibitory effect was reduced compared to the cells treated with C6Cer alone (Fig. 6B). This indicates that the inhibition of ceramide synthase by FB1 in combination with C6Cer partly reverses C6Cer mediated inhibition.

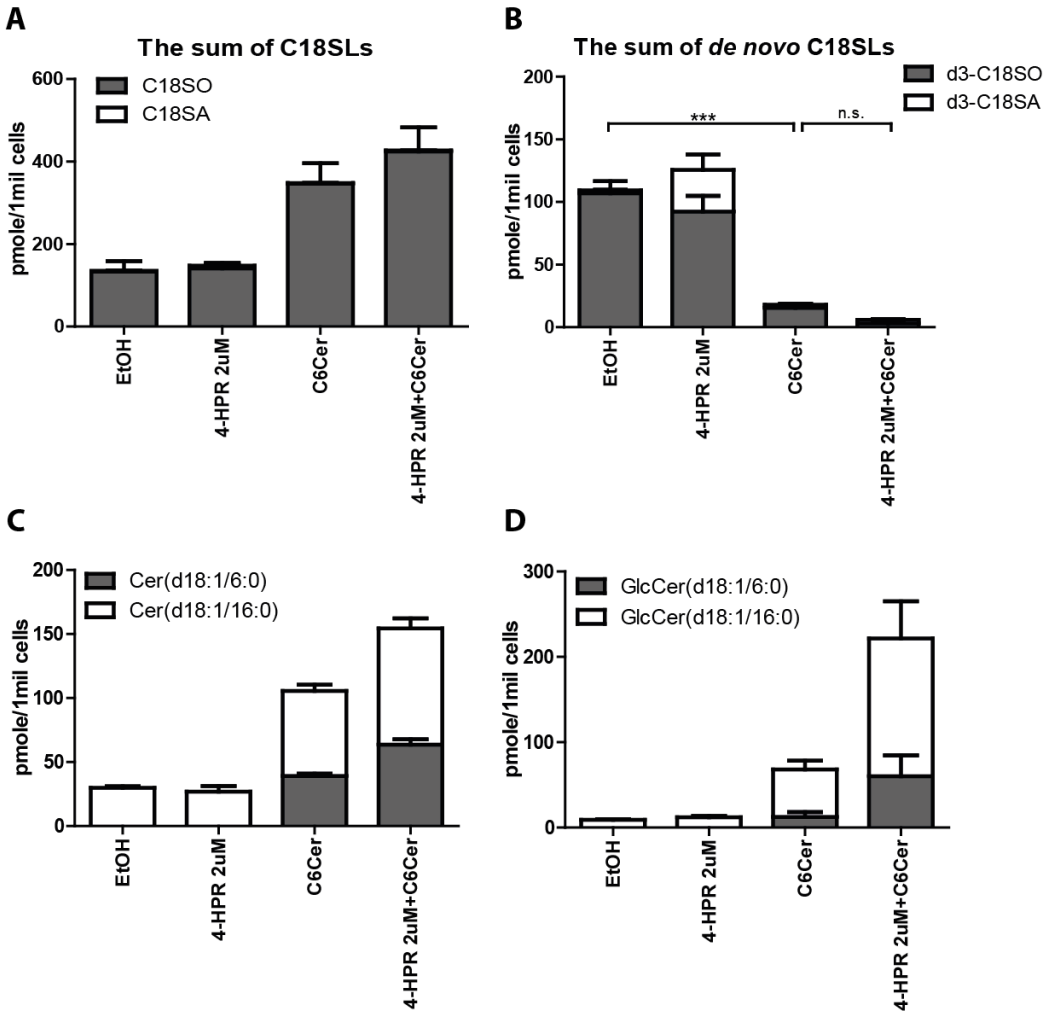

Figure 7. Stacked bar plots show A) the sum of C18SLs, B) the sum of *de novo* C18SLs (d3-C18SO and d3-C18SA), C) C6-/C16-ceramide and D) C6-/C16-glucosylceramide levels in HEK293 cells treated with 4-HPR (2µM), C6Cer (10µM) and ethanol control and incubated with the inhibitor in combination with C6Cer for 24h. Data are shown as mean ±SD (n=3). The significance was calculated for the sum of d3-C18SO and d3-C18SA using one-way ANOVA, post-test: Newman-Keuls Multiple Comparison Test, ***p<0.001.

The inhibition of dihydroceramide desaturase-1 (DES1) by 4-HPR blocks the conversion of DHCer to Cer and leads to the accumulation of DHCer (which is reflected by increased C18SA levels after hydrolysis). Thus, cells treated with 4-HPR had higher levels of *de novo* formed C18SA compared to ethanol control (Fig. 7B). The levels of C16-ceramide in 4-HPR treated cells were similar to controls (Fig. 7C). However, the levels of C6-/C16-glucosylceramide were much higher upon co-treatment of 4-HPR and C6Cer

(Fig. 7D). The minor raise of SA indicated that the inhibition of DES1 by 4-HPR was not complete and probably higher concentrations of 4-HPR are needed for complete inhibition. However, the concentration of 2µM was chosen to avoid the cytotoxic effects of 4-HPR at higher concentration. By trend SPT activity was increased in the presence of 4-HPR, but the addition of C6Cer+4-HPR blocked the activity similar to that of C6Cer alone (decreased sum of *de novo* d3-C18SLs) (Fig. 7B). The inhibition of DES1 by 4-HPR therefore does not reverse the inhibition of SPT by C6Cer.

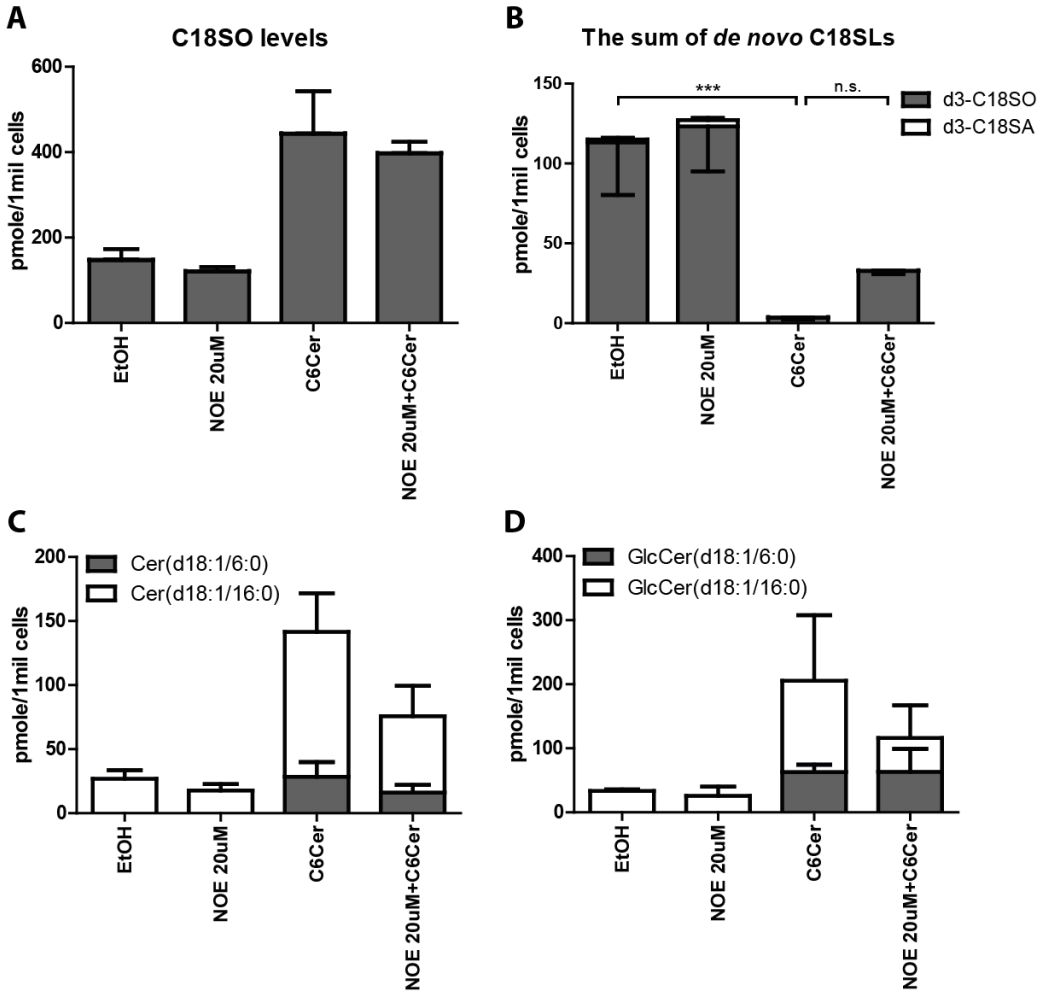

Figure 8. Stacked bar plots show A) C18SO levels, B) the sum of *de novo* C18SLs (d3-C18SO and d3-C18SA), C) C6-/C16-ceramide and D) C6-/C16-glucosylceramide levels in HEK 293 cells treated with NOE (20µM), C6Cer (10µM) and ethanol control and incubated with the inhibitor in combination with C6Cer for 24h. Data are shown as mean ±SD (n=3). The significance was calculated for the sum of d3-C18SO and d3-C18SA using one-way ANOVA, post-test: Newman-Keuls Multiple Comparison Test, ***p<0.001.

Next, we used NOE to inhibit ceramidase, which is expected to increase intracellular ceramide levels as the conversion from ceramide to sphingosine is blocked. However, we did not see any significant increase in total ceramide levels in the presence

of NOE, which indicates that the inhibitor might not have worked efficiently under the chosen conditions. The levels of C18SO were comparable between C6Cer and C6Cer+NOE treated cells (Fig. 8A). In the cells treated with NOE alone, levels of *de novo* formed d3-C18SLs were similar to control cells indicating that NOE itself has no effect on SPT activity (Fig. 8B). Like with FB1, cells treated with NOE+C6Cer showed a reduced inhibition compared to cells treated with C6Cer alone (Fig. 8B). However, as we could not confirm that NOE worked under these conditions, the observed effect on SPT activity is uncertain and might also be related to potential off-target effects of NOE.

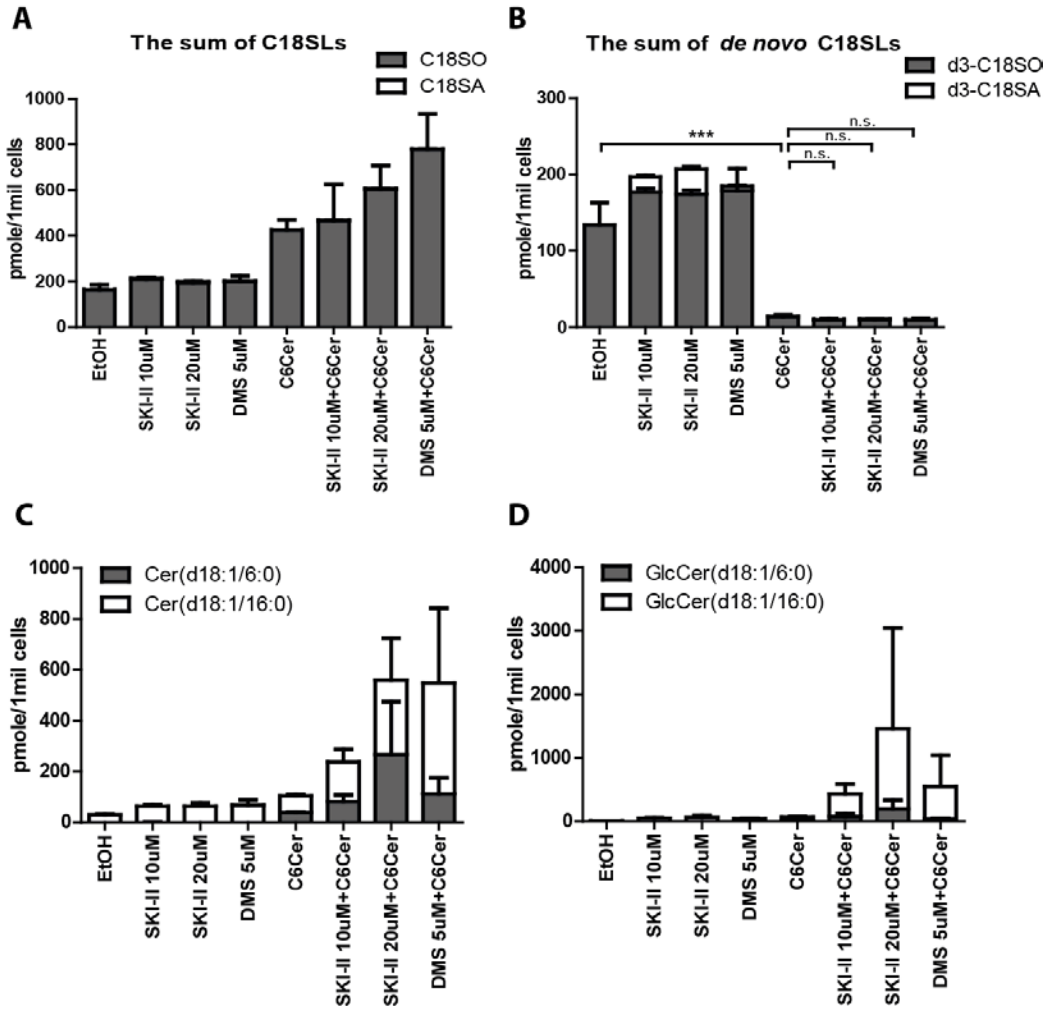

Figure 9. Stacked bar plots show A) the sum of C18SLs, B) the sum of *de novo* C18SLs (d3-C18SO and d3-C18SA), C) C6-/C16-ceramide and D) C6-/C16-glucosylceramide levels in HEK293 cells treated with SKI-II (10µM, 20µM), DMS (5µM), C6Cer (10µM) and ethanol control and incubated with the inhibitor in combination with C6Cer for 24h. Data are shown as mean ±SD (n=3). The significance was calculated for the sum of d3-C18SO and d3-C18SA using one-way ANOVA, post-test: Newman-Keuls Multiple Comparison Test, ***p<0.001.

Next, we tested the effect of two sphingosine kinase (SK) inhibitors – SKI-II and DMS. Inhibition of SK is expected to completely block SL degradation as the essential

catabolic intermediate S1P cannot be formed. In our analysis we could not directly confirm reduced S1P levels as this metabolite is lost upon extraction. The inhibitors had no effect on basal C18SO levels, but for the C6Cer treated cells total C18SO levels increased upon co-treatment with SKI-II or DMS, indicating that degradation of Cer was reduced in the presence of the inhibitor (Fig. 9A). Also, C6-/C16-ceramide and interestingly C6-/C16-glucosylceramide levels were increased in cells co-treated with SKI-II or DMS (Fig. 9C, D). However, neither SKI-II nor DMS had any effect on the C6Cer-mediated inhibition of SPT (Fig. 9B) indicating that the inhibition is independent of S1P formation.

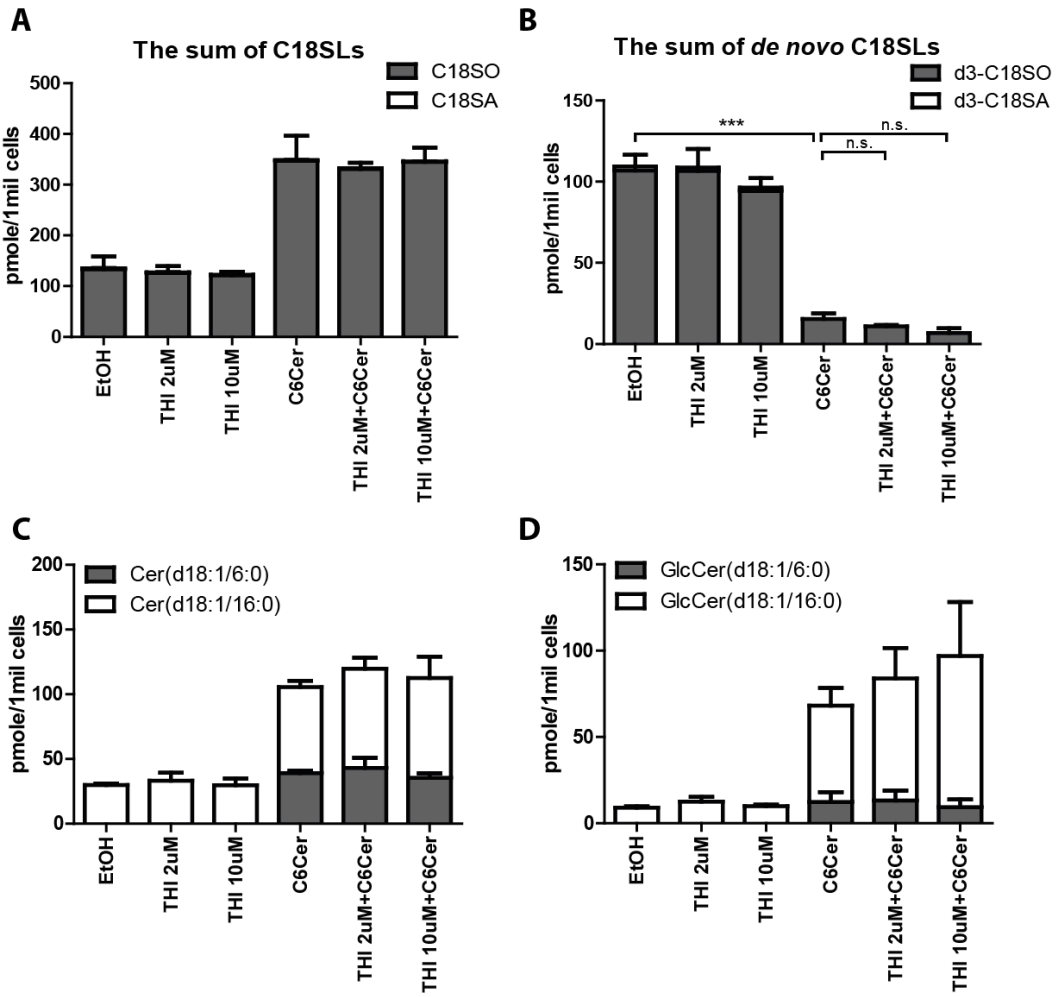

Figure 10. Stacked bar plots show A) the sum of C18SLs, B) the sum of *de novo* C18SLs (d3-C18SO and d3-C18SA), C) C6-/C16-ceramide and D) C6-/C16-glucosylceramide levels in HEK293 cells incubated with THI (2µM, 10µM) in combination with C6Cer (10µM) and ethanol control for 24h. Data are shown as mean ±SD (n=3). The significance was calculated for the sum of d3-C18SO and d3-C18SA using one-way ANOVA, post-test: Newman-Keuls Multiple Comparison Test, ***p<0.001.

THI inhibits sphingosine-1-phosphate lyase (S1P lyase) thereby blocking the very last step in the catabolic pathway which terminally degrades S1P into hexadecenal and ethanolamine-phosphate. Blocking S1P lyase should therefore result in increased S1P levels. However, for the reasons mentioned above we were not able to measure S1P levels directly and we therefore could not directly confirm the efficacy of the added THI. However, C18SO levels in cells treated with THI were not different from controls (Fig. 10A). Like for the SK inhibitors the total amount of C6- and C16-glucosylceramides increased in cells treated with C6Cer+THI (Fig. 10D). However, SPT activity was not affected by THI (Fig. 10B) indicating that S1P lyase is not involved in the inhibitory effect on SPT activity.

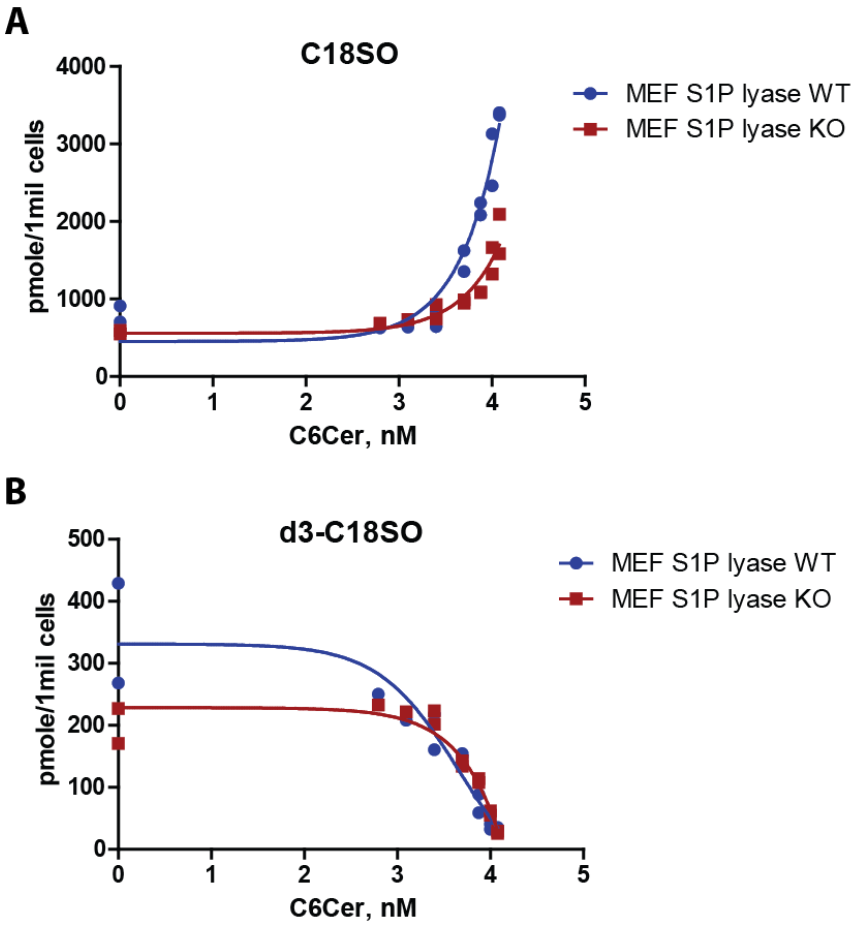

Figure 11. A) C18SO and B) *de novo* d3-C18SO levels in S1P lyase KO MEF cells compared to WT treated with increasing amounts of C6Cer (0.625-10µM) and incubated for 24h.

As we could not directly verify the effect of THI, we aimed to confirm these results by comparing SPT activity in MEF cells from WT and S1P lyase KO mice. Cells

were treated with increasing concentration of C6Cer (0.625-10µM), which corresponds to an increase in intracellular C18SO levels (Fig. 11A). The inhibitory effect of C6Cer on SPT activity in S1P lyase KO cells was comparable to the WT cells confirming that S1Plyase is not involved in the inhibition (Fig. 11B).

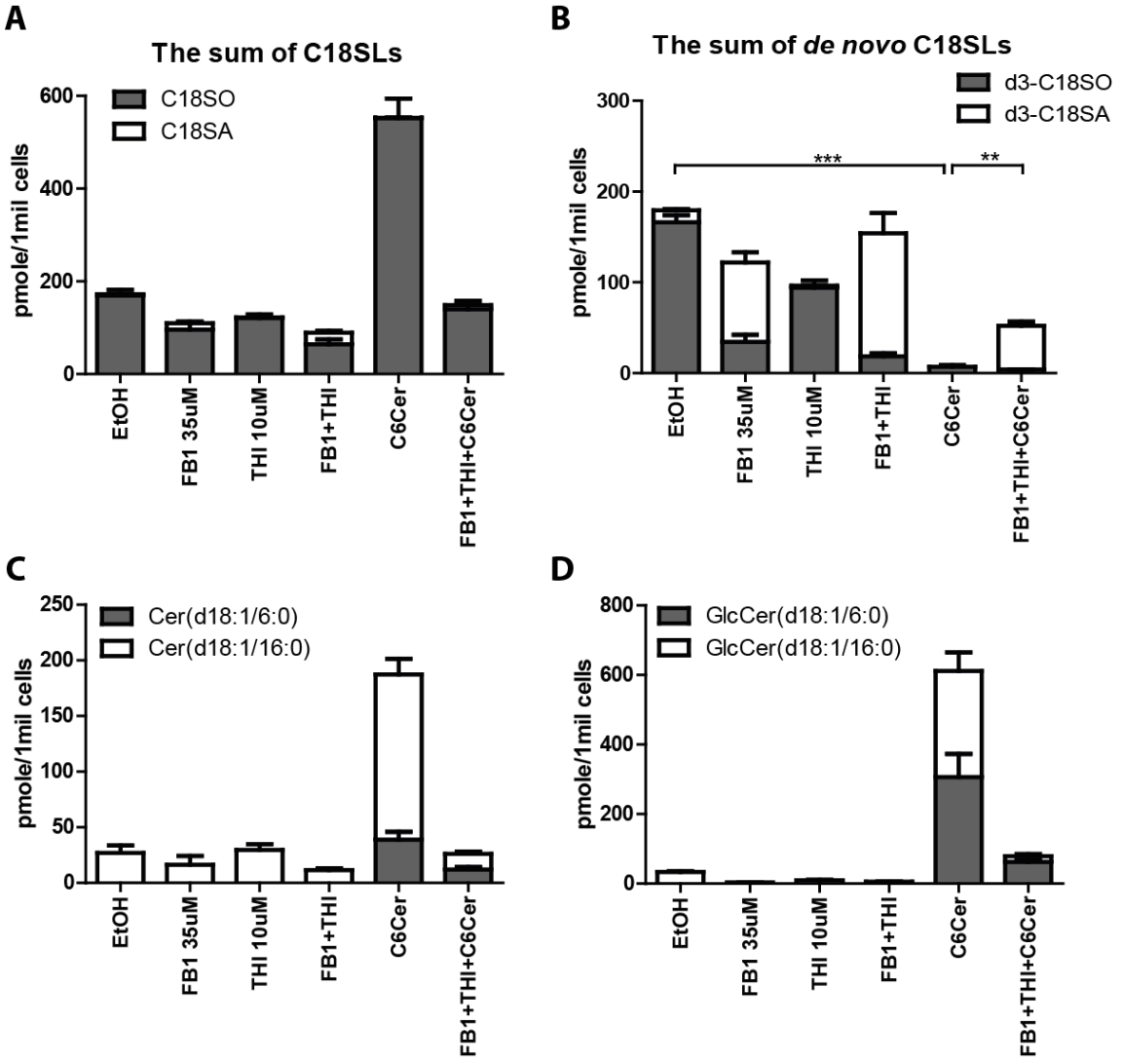

Figure 12. Stacked bar plots show A) the sum of C18SLs (C18SO and C18SA), B) the sum of *de novo* C18SLs (d3-C18SO and d3-C18SA), C) C6-/C16-ceramide and D) C6-/C16-glucosylceramide levels in HEK293 cells treated with FB1 (35µM) and THI (10µM) alone or FB1 together with THI, C6Cer (10µM); ethanol was used as a control and the cells were incubated with the inhibitors in combination with C6Cer for 24h. Data are shown as mean±SD (n=3). The significance was calculated for the sum of d3-C18SO and d3-C18SA using one-way ANOVA, post-test: Newman-Keuls Multiple Comparison Test, **p<0.01, ***p<0.001.

Since the inhibition of CerS by FB1 in combination with C6Cer could partly reverse the C6Cer mediated inhibition of SPT, we decided to explore this effect in more detail. When using FB1 it has to be considered that the accumulated SA can get partly converted to sphinganine-1-phosphate (SA1P) to be degraded by the subsequent

cleavage by S1P lyse. This might lead to an underestimate the amount of free SA that is formed in the presence of FB1. To control for this bypass reaction we used FB1 in combination with THI to block CerS and S1P lyase in parallel. Also cells treated with FB1+THI showed a significant increase in *de novo* formed d3-C18SA, however it was only slightly higher compared to FB1 alone (Fig. 12B) indicating that there is no significant degradation of SA. The levels of C6-/C16-ceramide and glucosylceramide in C6Cer treated cells were reduced in the presence of FB1+THI (Fig. 12C, D), which is explained by the fact that SO formed from C6Cer is not reacylated due to inhibition of CerS. Like for FB1 alone, also the combination of FB1+THI resulted in a partial recovery of SPT activity in presence of C6Cer (Fig. 12B). However, this recovery seems to be independent of THI, as the effect is the same as for FB1+C6Cer alone (Fig. 6B).

Finally, we tested the ceramide kinase inhibitor NVP-231, which blocks the formation of ceramide-1-phosphate and should increase ceramide levels. We tested different concentration of NVP-231 and observed a significant increase in Cer levels only at elevated NVP-231 concentrations (100 and 1000nM) (Fig. 13C, D). This indicated that the inhibitor worked, although we did not measure Cer1P levels directly. We did not see any clear dose response between NPV-231 and the increase in Cer. However, also in the presence of NVP-231, SPT was still suppressed by adding C6Cer (Fig. 13B) indicating the ceramide kinase is also not involved in this mechanism.

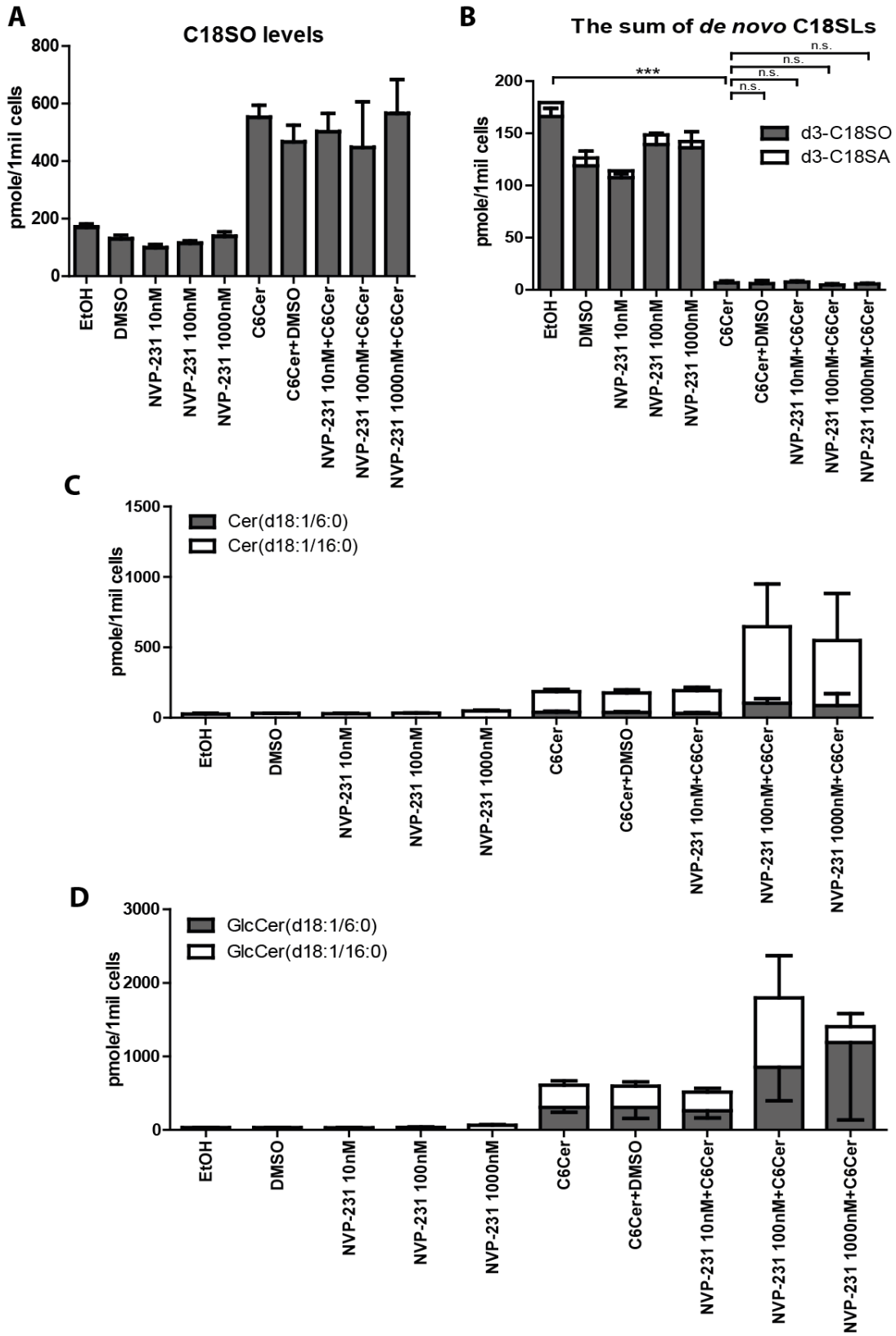

Figure 13. Bar plots show A) C18SO levels, B) the sum of *de novo* C18SLs (d3-C18SO and d3-C18SA), C) C6-/C16-ceramide and D) C6-/C16-glucosylceramide levels in HEK 293 cells treated with NVP-231 (10nM, 100nM, 1000nM) with or without C6Cer (10µM) and incubated with the inhibitor in combination with C6Cer for 24h. DMSO was used as a control for NVP-231 and ethanol for C6Cer. Data are shown as mean ± SD (n=3). The significance was calculated for the sum of d3-C18SO and d3-C18SA using one-way ANOVA, post-test: Newman-Keuls Multiple Comparison Test, ***p<0.001.

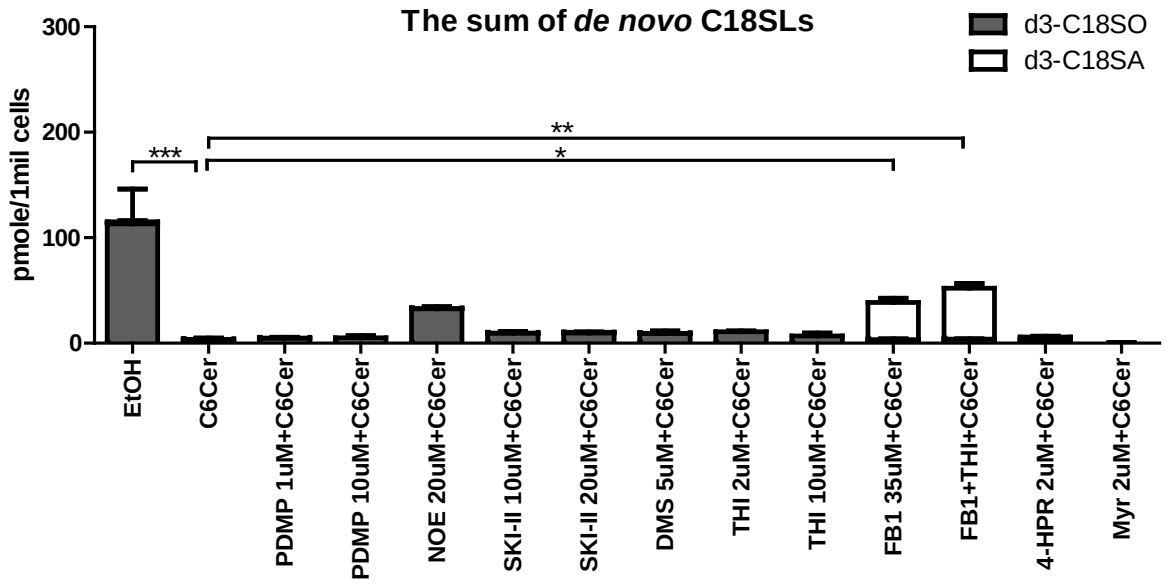

Figure 14. Summary of the various inhibitors tested and their effect on SL *de novo* synthesis in HEK293 cells treated with either C6Cer alone or inhibitor in combination with C6Cer. Stacked bar plots show the sum of *de novo* C18SLs (d3-C18SO and d3-C18SA). Data are shown as mean ±SD (n=3). The significance was calculated for the sum of d3-C18SO and d3-C18SA using one-way ANOVA, post-test: Newman-Keuls Multiple Comparison Test, *p<0.05, ***p<0.001.

The effect of all tested inhibitors on SPT activity in the presence of C6Cer is summarized in Fig.14. Among the tested compounds only FB1 and NOE could partly reverse the C6Cer mediated inhibition of SPT. However, the increase in activity that we observed with NOE was not significant after correction and as we could not verify the efficacy of NOE the effect of this inhibitor is uncertain. Nonetheless, the presence of FB1 resulted in a significantly gain in SPT activity compared to cells treated with C6Cer alone.

We already demonstrated in chapter 2 that also the addition of SO leads to a significant suppression of SPT activity. We therefore tested the effect of FB1 in cells supplemented with SO (D7SO).

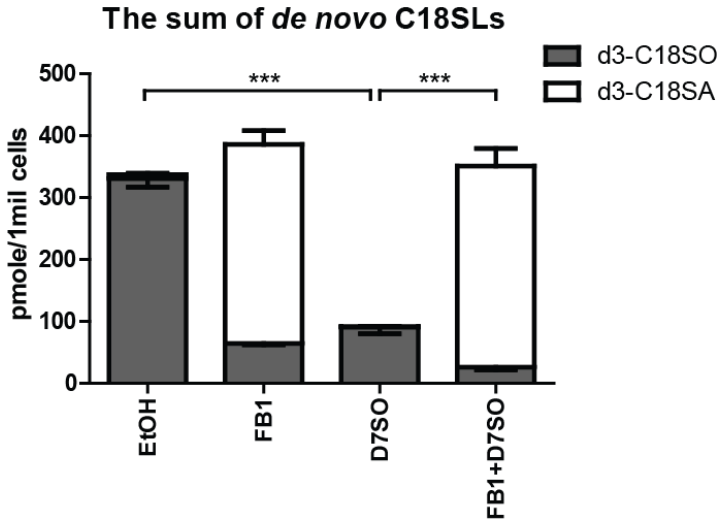

Figure 15. The sum of *de novo* C18SLs (d3-C18SO and d3-C18SA) in HEK293 cells treated with D7SO (5μM), FB1 (35 μM), FB1 (35μM) + D7SO (5μM) and ethanol control. The cells were incubated for 24h. Data are shown as mean ± SD (n=3). The significance was calculated for the sum of d3-C18SO and d3-C18SA using one-way ANOVA, post-test: Newman-Keuls Multiple Comparison Test, ***p<0.001.

Like already demonstrated in chapter 2, the addition of D7SO also decreased SPT activity although less efficiently than C6Cer (Fig. 15). However, this inhibition was completely reversed in the presence of FB1 indicating that the conversion of D7SO to Cer is essential for the observed inhibitory effect on SPT.

Discussion

We previously showed (Chapter 2) that increasing intracellular ceramide levels either by exogenously added C6Cer or free LCBs – D7SO and D7SA resulted in a significant inhibition of SPT activity. Here, we further explored the factors by which addition of C6Cer suppresses *de novo* SL synthesis. Inhibition of SPT occurs rapidly within 30 min after adding of C6Cer. Interestingly, SPT activity was fully inhibited even before the highest SO concentration was reached (Fig. 1). We also showed that the supplemented C6Cer was primarily converted into C6-glucosylceramides, but not into sphingomyelin. This is consistent with previous reports, which showed that in several cancer cell lines C6Cer is primarily converted to C6-glucosylceramides, but not to C6-SM [13]. However, this conversion does not seem to be primarily relevant for the inhibitory effect on SPT as blocking GCS with the rather specific inhibitor PDMP had no effect on SPT. Furthermore, we investigated whether the effect of C6Cer on SPT activity depended on the formation of a particular sphingolipid downstream metabolite. We used a set of chemical inhibitors to see whether blocking SL metabolism at distinct steps reverses the inhibitory effect of C6Cer on SPT activity. We found that blocking the CerS by FB1 and ceramidase by NOE slightly restored SPT activity in the presence of C6Cer. This is in a way contradictory as FB1 would prevent the formation of Cer leading to lower levels, whereas NOE should result in increased Cer levels as the degradation by ceramidase is blocked. Surprisingly, we observed the opposite. Cer and also GlcCer levels were reduced in NOE treated cells. This might explain why we see a rescue in the presence of NOE, but also indicates that NOE did not efficiently inhibit Cer degradation. However, it indicates that ceramide itself is responsible for the inhibitory effect on SPT. This is further supported by the fact that the inhibitory effect of SO was completely reversed when the conversion to Cer by FB1 was blocked. However, it is not clear yet whether ceramides in general or rather specific ceramide subspecies are responsible for this effect. Ogretmen et al reported that C6Cer is converted to endogenous C16Cer via the recycling or salvage pathway [11-14]. Upon entry in the cell C6Cer is first deacylated by ceramidase to sphingosine and then reacylated to endogenous C16-ceramides by ceramide synthase (CerS). However, due to the limitations of our analytical method, we were not able to simultaneously measure all relevant metabolites (including SM, Cer, S1P, free SBs – SO and SA) at the same time to see the interconversion of these sphingolipids species after supplementing C6Cer.

In addition, it appears a general principle in SL metabolism that not the global concentration, but rather the spatial distribution determine the metabolic fate of the lipids, indicating that the local changes in the concentration of certain lipids are responsible for the feedback inhibition. This aspect is experimentally difficult to address. Subcellular fractionation to analyze SL levels in individual cell organelles turned out to be unattainable. However, the data on FB1 (which prevents reacylation of ceramides, thereby reversing the SPT inhibition by C6Cer) suggests that it is the local increase in ceramide levels that is triggering the inhibition of SPT. And since CerS, and also other enzymes of the SL *de novo* synthesis are located in the ER, Cer levels in the ER could be the relevant factor for inhibiting SPT. Ceramides are either synthesized via the *de novo* pathway or generated by the breakdown of complex SLs like SM, S1P, glycoSLs via the salvage pathway. Interconnectedness of synthesis and degradation pathways makes ceramide ideal metabolite for being recognized as a surrogate marker for total SL levels in the cell.

The distribution of lipids in particular of sphingolipids in the cells is highly controlled and certain lipid species are only found in specific membranes of the cellular organelles, where they were either synthesized locally or transported by specific lipid transfer proteins like the ceramide transfer protein (CERT). In that context SL metabolism is highly compartmentalized. This is also reflected by the specific location of sphingolipid metabolizing enzymes in various organelles, such as Golgi, lysosomes, mitochondria, PM and ER. Besides being produced in the ER, ceramides can also be generated at the PM by the actions of SMases. Alterations in lipid composition of organelle membranes like in the ER might therefore locally influence the properties of metabolic enzymes located in these compartments [43-45].

Ceramide levels in the cell appear to be tightly controlled, but it is not clear how the cell is capable to sense intracellular Cer levels. A recently identified ER protein (SMSr), which shows structural similarity to sphingomyelin synthases (SMS), was suggested to be a ceramide sensor in the ER [15]. Reducing SMSr expression leads to ceramide accumulation in the ER [15]. Moreover, SMSr acts in coordination with CERT to maintain ceramide homeostasis in the cell [15]. However, a role of SMSr in regulating SPT activity has not been confirmed as Wattenberg and colleagues demonstrated that the knockdown of SMSr in HeLa cells did not result in increased *de novo* formed SLs [20].

Another potential candidate for sensing the ceramide levels in the ER is the phosphoinositide-4-phosphatase (PI4P) Sac1. Upon nutrient limitation Sac1 was shown

to move from the ER to the Golgi where it depletes PI4P levels to PI [46]. The PH domain of the CERT recognizes PI4Ps, which allows it to bind to the Golgi. Therefore, depletion of PI4P levels in the Golgi disrupts the ceramide transport from the ER to the Golgi. And since Sac1 was shown to form a complex with SPT in yeast (SPOTS) [47], it is feasible that Sac1 could be involved in sensing ceramide levels in the ER and regulating SPT activity in mammals as well. However, overexpression of Sac1 in HEK293 cells did not show a significant effect on SPT activity (data not shown).

In conclusion, we showed that increasing intracellular ceramide levels in the cell decreases the *de novo* formation of SLs, which is mediated by metabolic inhibition of SPT. Based on our results we hypothesize that a local increase in ceramides levels, likely in the ER, triggers this inhibition of SPT. However, the molecular basis underlying this regulatory process is still a matter of further investigation.

References

1. Hanada, K., et al., *A mammalian homolog of the yeast LCB1 encodes a component of serine palmitoyltransferase, the enzyme catalyzing the first step in sphingolipid synthesis.* Journal of Biological Chemistry, 1997. **272**(51): p. 32108-32114.
2. Hanada, K., *Serine palmitoyltransferase, a key enzyme of sphingolipid metabolism.* Biochim Biophys Acta, 2003. **1632**(1-3): p. 16-30.
3. Williams, R.D., E. Wang, and A.H. Merrill, Jr., *Enzymology of long-chain base synthesis by liver: characterization of serine palmitoyltransferase in rat liver microsomes.* Arch Biochem Biophys, 1984. **228**(1): p. 282-91.
4. Hanada, K., et al., *Molecular machinery for non-vesicular trafficking of ceramide.* Nature, 2003. **426**(6968): p. 803-809.
5. Kobayashi, S.D. and M.M. Nagiec, *Ceramide/long-chain base phosphate rheostat in Saccharomyces cerevisiae: regulation of ceramide synthesis by Elo3p and Cka2p.* Eukaryot Cell, 2003. **2**(2): p. 284-94.
6. Mandala, S.M., et al., *Sphingoid base 1-phosphate phosphatase: a key regulator of sphingolipid metabolism and stress response.* Proc Natl Acad Sci U S A, 1998. **95**(1): p. 150-5.
7. Ridgway, N.D. and D.L. Merriam, *Metabolism of short-chain ceramide and dihydroceramide analogues in Chinese hamster ovary (CHO) cells.* Biochim Biophys Acta, 1995. **1256**(1): p. 57-70.
8. Flowers, M., et al., *C6-ceramide and targeted inhibition of acid ceramidase induce synergistic decreases in breast cancer cell growth.* Breast Cancer Res Treat, 2012. **133**(2): p. 447-58.
9. Watters, R.J., et al., *Targeting glucosylceramide synthase synergizes with C6-ceramide nanoliposomes to induce apoptosis in natural killer cell leukemia.* Leuk Lymphoma, 2013. **54**(6): p. 1288-96.
10. Chapman, J.V., et al., *P-glycoprotein antagonists confer synergistic sensitivity to short-chain ceramide in human multidrug-resistant cancer cells.* Exp Cell Res, 2011. **317**(12): p. 1736-45.
11. Takeda, S., et al., *Apoptosis occurs via the ceramide recycling pathway in human HaCaT keratinocytes.* J Biochem, 2006. **139**(2): p. 255-62.
12. Ogretmen, B., et al., *Biochemical mechanisms of the generation of endogenous long chain ceramide in response to exogenous short chain ceramide in the A549 human lung adenocarcinoma cell line. Role for endogenous ceramide in mediating the action of exogenous ceramide.* J Biol Chem, 2002. **277**(15): p. 12960-9.
13. Chapman, J.V., et al., *Metabolism of short-chain ceramide by human cancer cells--implications for therapeutic approaches.* Biochem Pharmacol, 2010. **80**(3): p. 308-15.
14. Morad, S.A., et al., *Ceramide-tamoxifen regimen targets bioenergetic elements in acute myelogenous leukemia.* J Lipid Res, 2016.
15. Vacaru, A.M., et al., *Sphingomyelin synthase-related protein SMSr controls ceramide homeostasis in the ER.* Journal of Cell Biology, 2009. **185**(6): p. 1013-1027.
16. Delgado, A., et al., *Inhibitors of sphingolipid metabolism enzymes.* Biochim Biophys Acta, 2006. **1758**(12): p. 1957-77.
17. Albi, E.M., M.V. , *Sphingolipid Metabolism Inhibitors and Cell Function.* The Open Enzyme Inhibition Journal, 2008: p. 72-79.
18. Othman, A., et al., *Plasma deoxysphingolipids: a novel class of biomarkers for the metabolic syndrome?* Diabetologia, 2012. **55**(2): p. 421–431.
19. Ziv, C., et al., *Viral serine palmitoyltransferase induces metabolic switch in sphingolipid biosynthesis and is required for infection of a marine alga.* Proceedings of the National Academy of Sciences, 2016.
20. Siow, D.L. and B.W. Wattenberg, *Mammalian ORMDL proteins mediate the feedback response in ceramide biosynthesis.* J Biol Chem, 2012. **287**(48): p. 40198-204.
21. Siow, D., et al., *Regulation of de novo sphingolipid biosynthesis by the ORMDL proteins and sphingosine kinase-1.* Adv Biol Regul, 2015. **57**: p. 42-54.
22. Miyake, Y., et al., *Serine Palmitoyltransferase Is the Primary Target of a Sphingosine-Like Immunosuppressant, Isp-1/Myriocin.* Biochemical and Biophysical Research Communications, 1995. **211**(2): p. 396-403.
23. Wadsworth, J.M., et al., *The chemical basis of serine palmitoyltransferase inhibition by myriocin.* J Am Chem Soc, 2013. **135**(38): p. 14276-85.

24. Merrill, A.H., Jr., et al., *Fumonisin B1 inhibits sphingosine (sphinganine) N-acyltransferase and de novo sphingolipid biosynthesis in cultured neurons in situ.* J Biol Chem, 1993. **268**(36): p. 27299-306.
25. Desai, K., et al., *Fumonisins and fumonisin analogs as inhibitors of ceramide synthase and inducers of apoptosis.* Biochim Biophys Acta, 2002. **1585**(2-3): p. 188-92.
26. Wang, H., et al., *N-(4-Hydroxyphenyl)retinamide increases dihydroceramide and synergizes with dimethylsphingosine to enhance cancer cell killing.* Mol Cancer Ther, 2008. **7**(9): p. 2967-76.
27. Rahmaniyan, M., et al., *Identification of dihydroceramide desaturase as a direct in vitro target for fenretinide.* J Biol Chem, 2011. **286**(28): p. 24754-64.
28. Sugita, M., et al., *Ceramidase and ceramide synthesis in human kidney and cerebellum. Description of a new alkaline ceramidase.* Biochim Biophys Acta, 1975. **398**(1): p. 125-31.
29. Payne, S.G., D.N. Brindley, and L.J. Guilbert, *Epidermal growth factor inhibits ceramide-induced apoptosis and lowers ceramide levels in primary placental trophoblasts.* J Cell Physiol, 1999. **180**(2): p. 263-70.
30. Strelow, A., et al., *Overexpression of acid ceramidase protects from tumor necrosis factor-induced cell death.* J Exp Med, 2000. **192**(5): p. 601-12.
31. Yatomi, Y., et al., *N,N-dimethylsphingosine inhibition of sphingosine kinase and sphingosine 1-phosphate activity in human platelets.* Biochemistry, 1996. **35**(2): p. 626-33.
32. Edsall, L.C., et al., *N,N-Dimethylsphingosine is a potent competitive inhibitor of sphingosine kinase but not of protein kinase C: modulation of cellular levels of sphingosine 1-phosphate and ceramide.* Biochemistry, 1998. **37**(37): p. 12892-8.
33. French, K.J., et al., *Discovery and evaluation of inhibitors of human sphingosine kinase.* Cancer Res, 2003. **63**(18): p. 5962-9.
34. Antoon, J.W., et al., *Dual inhibition of sphingosine kinase isoforms ablates TNF-induced drug resistance.* Oncol Rep, 2012. **27**(6): p. 1779-86.
35. Canals, D., et al., *Differential effects of ceramide and sphingosine 1-phosphate on ERM phosphorylation: probing sphingolipid signaling at the outer plasma membrane.* J Biol Chem, 2010. **285**(42): p. 32476-85.
36. Ohotski, J., et al., *Expression of sphingosine 1-phosphate receptor 4 and sphingosine kinase 1 is associated with outcome in oestrogen receptor-negative breast cancer.* Br J Cancer, 2012. **106**(8): p. 1453-9.
37. Ohtoyo, M., et al., *Sphingosine 1-phosphate lyase inhibition by 2-acetyl-4-(tetrahydroxybutyl)imidazole (THI) under conditions of vitamin B6 deficiency.* Mol Cell Biochem, 2015. **400**(1-2): p. 125-33.
38. Graf, C., et al., *Targeting Ceramide Metabolism with a Potent and Specific Ceramide Kinase Inhibitor.* Molecular Pharmacology, 2008. **74**(4): p. 925-932.
39. Graf, C., P. Rovina, and F. Bornancin, *A secondary assay for ceramide kinase inhibitors based on cell growth inhibition by short-chain ceramides.* Anal Biochem, 2009. **384**(1): p. 166-9.
40. Pastukhov, O., et al., *The ceramide kinase inhibitor NVP-231 inhibits breast and lung cancer cell proliferation by inducing M phase arrest and subsequent cell death.* Br J Pharmacol, 2014. **171**(24): p. 5829-44.
41. Vunnam, R.R. and N.S. Radin, *Analogs of ceramide that inhibit glucocerebroside synthetase in mouse brain.* Chem Phys Lipids, 1980. **26**(3): p. 265-78.
42. Inokuchi, J. and N.S. Radin, *Preparation of the active isomer of 1-phenyl-2-decanoylamino-3-morpholino-1-propanol, inhibitor of murine glucocerebroside synthetase.* J Lipid Res, 1987. **28**(5): p. 565-71.
43. Kolesnick, R. and Y.A. Hannun, *Ceramide and apoptosis.* Trends Biochem Sci, 1999. **24**(6): p. 224-5; author reply 227.
44. Tepper, A.D., et al., *Sphingomyelin Hydrolysis to Ceramide during the Execution Phase of Apoptosis Results from Phospholipid Scrambling and Alters Cell-Surface Morphology.* The Journal of Cell Biology, 2000. **150**(1): p. 155-164.
45. Megha, et al., *Effect of ceramide N-acyl chain and polar headgroup structure on the properties of ordered lipid domains (lipid rafts).* Biochimica et biophysica acta, 2007. **1768**(9): p. 2205-2212.
46. Blagoveshchenskaya, A., et al., *Integration of Golgi trafficking and growth factor signaling by the lipid phosphatase SAC1.* J Cell Biol, 2008. **180**(4): p. 803-12.
47. Breslow, D.K., et al., *Orm family proteins mediate sphingolipid homeostasis.* Nature, 2010. **463**(7284): p. 1048-53.

General discussion and outlook

In this thesis, we investigated the regulation of SPT and sphingolipid *de novo* synthesis in mammalian cells. We examined the mechanism of SPT inhibition by studying the effect of exogenously added sphingolipids, mostly C_6-ceramide, and its metabolism within the cell.

In the first part, we showed that expression levels of ORMDL proteins, which were identified in yeast to negatively regulate SPT [1], do not affect SPT activity and total sphingolipid levels (Chapter 1). We used several *in vitro* and *in vivo* models to study the role of ORMDL proteins, in particularly ORMDL3, as potential regulators of the mammalian SPT. Although total C18-sphingoid base levels were not altered, C18-sphinganine, which makes up about 10% of the sphingoid bases in the plasma [2] was significantly elevated in plasma, lung and liver tissues of Ormdl3 KO mice. Additionally, we found that SPT activity was not changed neither in MEFs from ORMDL3 KO mice nor in HEK293 cells overexpressing the individual ORMDL1-3 isoforms. In contrast, knockdown of all three but not of the individuals ORMDL isoforms resulted in increased SPT activity. This confirms earlier data reporting that ORMDL3 overexpression alone has no effect on *de novo* ceramide biosynthesis, probably as ORMDL3 is stoichiometrically-expressed in excess to the individual SPT subunits [3]. However, one needs to be cautious while interpreting these data, since the overexpression of ORMDL3 needs also to be confirmed for being correctly localized in the ER using immunofluorescence (IF) staining. To confirm a physical interaction of ORMDLs with SPT subunits, a proximity ligation assay (PLA) that combines traditional IF and co-localization methods could be used. PLA can distinguish even weak and dynamic protein interactions in living cells and could be an option for investigating the proposed interactions between the ORMDLs and SPT in a highly specific manner.

Moreover, using the SNP data from a clinical study (N=971 individuals) we showed that SNPs in ORMDL3 (including *rs7216389* that was strongly linked to childhood asthma) are not associated with significant changes in plasma sphingolipid levels. Despite the fact that we could not confirm a role of ORMDL3 in regulating SPT activity, the abovementioned SNP might still play a role in the pathogenesis of asthma. Therefore, it will be important to determine whether ORMDL3 KO and ORMDL3 TG mice have altered susceptibility for asthma e.g. by using an appropriate asthma model like house dust mite

(HDM) challenge. This will also allow to obtain asthma relevant data on inflammation or bronchial hyperactivity.

We further explored whether the metabolic feedback mechanism, which was shown in yeast, applies in the same way to mammalian cells. We found that treating HEK293 cells with exogenously added sphingolipids (SLs) including C_6-ceramide (C6Cer), sphingosine (SO) and sphinganine (SA), but not with sphingomyelin (SM), resulted in decreased SPT activity (Chapter 2). It seems that increasing intracellular SLs in mammalian cells activates a regulatory mechanism that leads to inhibition of SPT activity. This showed that mammalian SPT is also regulated by a metabolic feedback-loop, which is based on total cellular sphingolipid levels as it was shown for yeast [5, 6]. Notably, C6Cer-mediated regulation of SPT seems to be independent of whether the reaction is catalyzed by the SPTLC2 or SPTLC3. We showed that increasing amounts of C_{18}-based sphingolipids (C6Cer) decrease the *de novo* production of both C18SLs (mostly formed by SPTLC2) and atypical sphingolipids (C_{16}-/C_{17}-/C_{19}-based sphingoid bases), which are formed by SPTLC3 and 1-deoxySLs. It would be interesting to also treat cells with C16SO, C17SO or C19SO to check whether the addition of atypical sphingolipids has a similar effect on SPT activity as we saw it for C18SA and C18SO. Addition of 1-deoxySLs in HEK293 cells did not have an effect on SPT activity (data not shown). Moreover, C6-dihydroceramide (the inactive form of C6Cer) could be used to prove the specificity towards C6Cer.

Several mutations in SPT that are associated with HSAN1 showed increased canonical SPT activity [7]. We therefore investigated whether the regulatory mechanisms are altered in these mutants. Supplementing C6Cer to HEK293 cells expressing 'hyperactive' mutants still decreased SPT activity and SL *de novo* formation (Chapter 2).

Furthermore, we showed that raising intracellular SL levels with C6Cer resulted in significant SPT inhibition already 30 min post-treatment (Chapter 3). SPT activity was still blocked even 24h after C6Cer addition, although total intracellular SL levels were already back to baseline at that time. It would be therefore interesting to test the effect of C6Cer treatment in a pulse–chase approach and over more time points (e.g. 48-72h) to see when intracellular SLs are reaching baseline level again and whether this is associated with a recovery of SPT activity.

Interestingly, we found that the added C6Cer was almost exclusively converted to monohexosylceramide (MHCer), but not as rather expected to sphingomyelins (SM) (Chapter 3). However, the C6Cer-mediated inhibition of SPT was independent of this conversion. Therefore, we further investigated whether C6Cer by itself or the increase of a specific sphingolipid downstream metabolite is inducing SPT inhibition. We used a set of chemical inhibitors to specifically inhibit the enzymes along the SL pathway. We found that inhibition of SPT was reversed in the presence of the CerS inhibitor FB1 and the ceramidase inhibitor NOE - but not by inhibiting any of the other enzymes. Moreover, the combination of FB1 with SO resulted in an even greater rescue of SPT activity than seen for FB1+C6Cer. Earlier studies showed that C6Cer undergoes deacylation by ceramidase to sphingosine, which is later converted to long-chain ceramides by CerS via the salvage pathway [8]. Since FB1 blocks the reacylation of SO, which over time lowers Cer and releases inhibition of SPT. Therefore, we hypothesize that the reacylation of C6Cer is essential for the inhibition of SPT activity.

The identification of the responsible sphingolipid metabolite, which triggers the feedback inhibition is challenging. Due to several interconnections and crossroads in the sphingolipid metabolism, changes in one metabolite are expected to also alter the concentrations of the others. For example, an increase in ceramide can secondarily result in an increase in sphingomyelin, glucosylceramide, sphingosine-1-phosphate and sphingosine levels. Therefore, lipidomics approach is needed to identify the metabolite, which showed the closest correlation with changes in SPT activity. For that a C6Cer containing an isotope label on the long chain base would be helpful to track its metabolic conversion through the SL metabolic pathway over time. Unfortunately, such a standard is not commercially available.

In addition to their diversity, sphingolipids are also greatly compartmentalized in the cell. The total ceramide levels may differ depending on the organelles, since ceramides can be synthesized in the ER or produced as a result of degradation by SMases at the PM, lysosome and mitochondria. Therefore, it is not just the specific metabolite that has to be recognized, its localization within the specific organelles matters as well.

However, hydrophobicity of sphingolipids makes it challenging to study their functions [9]. The use of cell membrane-permeable short chain ceramides is therefore indispensable in research and translational medicine [10, 11]. However, the usage of

exogenous sphingolipids may also alter the biochemical properties of cells. Ceramide, due to its hydrophobicity has the tendency to stay in the compartment where it is synthesized. Changes in ceramide composition can alter the fluidity of the membranes [12-14]. Frequently C6-NBD-ceramide are used to study sphingolipid trafficking. It was demonstrated that C6-NBD-ceramide accumulates predominantly in the Golgi [15-17], and also gets further converted into C6-NBD-sphingomyelin and C6-NBD-glucosylceramide [18, 19]. However, the usage of fluorescent probes such as NBD may not reflect the native situation, as the hydrophilic NBD group may alter the biophysical properties of the lipid. Alternatively, the use of functional lipids bearing minor chemical modifications (e.g. "click"-lipids) could help in elucidating the localization and metabolism of the SLs within the cell.

One current hypothesis is that SPT is regulated based on the sphingolipid content in specific cellular compartments. As SPT is localized in the ER, where ceramide biosynthesis occurs, it would make sense that sensing of total Cer levels also happens in the ER. However, a precise measurement of the ceramide content in individual organelles of the cell is currently not possible. Estimates can be done based on specific Cer antibodies or subcellular fractionation methods. However, subcellular fractionation turned out to give unreliable results, probably as the organelles cannot be fully separated by each other (data not shown). Ideally scanning mass spectrometer could be used to measure the SL profile in various cellular compartments. However, the technology of these instruments is currently not sufficiently developed to enable subcellular resolution.

The sensor that regulates intracellular SL levels is currently not known. SMSr, an SMS like protein, which forms ceramide phosphoethanolamine (CPE) instead of SM, was suggested to be the ceramide sensor in the ER, since the suppression of SMSr activity was shown to increase ceramide levels in the ER [20]. Therefore, it would be interesting to knockdown SMSr and supplement the cells with C6Cer, which could reveal whether C6Cer inhibition of SPT is mediated through SMSr or not. However, Wattenberg and colleagues already showed that knockdown of SMSr in HeLa cells does not increase *de novo* synthesis of SLs [21].

The regulation of ceramide levels in the ER should also coordinate the actions of lipid transporters like ceramide transfer protein (CERT) in order to maintain the ceramide

homeostasis in the ER. CERT contains a PH domain that recognizes PI4P in the Golgi and transfers ceramide from the ER to the Golgi primarily for SM synthesis. LY-A cells with a mutation in the PH domain of CERT have disrupted transport of ceramides from the ER to the Golgi as the mutant CERT cannot bind to PI4P. To see if CERT activity is associated with SPT activity it would be interesting to measure SL *de novo* synthesis in LY-A cells.

Sac1 is a PI4P phosphatase, which is located in both, the ER and the Golgi [22-25]. It dephosphorylates PI4P to PI, which prevents CERT from binding to the Golgi. Therefore, it would be interesting to also test the role of cofactors that are involved in regulating CERT activity – such as Sac1, SMS1 (produces SM), PKD (inactivates CERT), PI4K (increases PI4P levels, activates CERT), OSBP (activates PI4K and CERT). In that respect the suppression of Sac1 would be expected to reverse the inhibition of SPT mediated by C6Cer. It would also be interesting to see whether the localization or expression levels of Sac1 change upon C6Cer treatment. Additionally, one could test whether specific transcription factors are up-/downregulated upon supplementation with C6Cer. In particular, diacylglycerol (DAG), which is released during SM synthesis, can activate PKD – a negative regulator of CERT. The DAG levels in the Golgi play an important role in fission and fusion in the organelle [26, 27]. DAG and PI4P, which are both bioactive lipids, might play a role connecting changes in SLs levels with other regulatory mechanisms in the cell.

In addition, cell culture models of sphingolipidoses (e.g. Gaucher disease), a class of diseases associated with impaired SL degradation [28, 29], might reveal additional information about the effect on SL metabolism when the ceramide recycling pathway is disrupted. It would be interesting to measure the SPT activity in cellular models of these diseases.

In summary, we showed that sphingolipid *de novo* synthesis is decreased upon increasing intracellular sphingolipid levels. This regulation is not mediated by ORMDL3 as suggested previously. However, we demonstrated that supplementation with C6Cer or the free LCBs (SO/SA) inhibits SPT activity, which proves the existence of a metabolic feedback regulation in mammalian cells.

References

1. Breslow, D.K., et al., *Orm family proteins mediate sphingolipid homeostasis.* Nature, 2010. **463**(7284): p. 1048-53.
2. Quehenberger, O., et al., *Lipidomics reveals a remarkable diversity of lipids in human plasma.* J Lipid Res, 2010. **51**(11): p. 3299-305.
3. Siow, D., et al., *ORMDL/serine palmitoyltransferase stoichiometry determines effects of ORMDL3 expression on sphingolipid biosynthesis.* J Lipid Res, 2015. **56**(4): p. 898-908.
4. Moffatt, M.F., et al., *Genetic variants regulating ORMDL3 expression contribute to the risk of childhood asthma.* Nature, 2007. **448**(7152): p. 470-3.
5. Tafesse, F.G. and J.C. Holthuis, *Cell biology: A brake on lipid synthesis.* Nature, 2010. **463**(7284): p. 1028-9.
6. Walther, T.C., *Keeping sphingolipid levels nORMal.* Proc Natl Acad Sci U S A, 2010. **107**(13): p. 5701-2.
7. Bode, H., et al., *HSAN1 mutations in serine palmitoyltransferase reveal a close structure-function-phenotype relationship.* Hum Mol Genet, 2015.
8. Ogretmen, B., et al., *Biochemical mechanisms of the generation of endogenous long chain ceramide in response to exogenous short chain ceramide in the A549 human lung adenocarcinoma cell line. Role for endogenous ceramide in mediating the action of exogenous ceramide.* J Biol Chem, 2002. **277**(15): p. 12960-9.
9. Hannun, Y.A. and L.M. Obeid, *Principles of bioactive lipid signalling: lessons from sphingolipids.* Nature Reviews Molecular Cell Biology, 2008. **9**(2): p. 139-150.
10. Selzner, M., et al., *Induction of apoptotic cell death and prevention of tumor growth by ceramide analogues in metastatic human colon cancer.* Cancer Res, 2001. **61**(3): p. 1233-40.
11. Charles, R., et al., *Ceramide-coated balloon catheters limit neointimal hyperplasia after stretch injury in carotid arteries.* Circ Res, 2000. **87**(4): p. 282-8.
12. Kolesnick, R. and Y.A. Hannun, *Ceramide and apoptosis.* Trends Biochem Sci, 1999. **24**(6): p. 224-5; author reply 227.
13. Tepper, A.D., et al., *Sphingomyelin Hydrolysis to Ceramide during the Execution Phase of Apoptosis Results from Phospholipid Scrambling and Alters Cell-Surface Morphology.* The Journal of Cell Biology, 2000. **150**(1): p. 155-164.
14. Megha, et al., *Effect of ceramide N-acyl chain and polar headgroup structure on the properties of ordered lipid domains (lipid rafts).* Biochimica et biophysica acta, 2007. **1768**(9): p. 2205-2212.
15. Lipsky, N.G. and R.E. Pagano, *Sphingolipid metabolism in cultured fibroblasts: microscopic and biochemical studies employing a fluorescent ceramide analogue.* Proc Natl Acad Sci U S A, 1983. **80**(9): p. 2608-12.
16. Pagano, R.E. and R.G. Sleight, *Defining lipid transport pathways in animal cells.* Science, 1985. **229**(4718): p. 1051-7.
17. de Melo, E.J. and W. de Souza, *Pathway of C6-NBD-Ceramide on the host cell infected with Toxoplasma gondii.* Cell Struct Funct, 1996. **21**(1): p. 47-52.
18. van Meer, G., et al., *Sorting of sphingolipids in epithelial (Madin-Darby canine kidney) cells.* J Cell Biol, 1987. **105**(4): p. 1623-35.
19. Lipsky, N.G. and R.E. Pagano, *Intracellular translocation of fluorescent sphingolipids in cultured fibroblasts: endogenously synthesized sphingomyelin and glucocerebroside analogues pass through the Golgi apparatus en route to the plasma membrane.* J Cell Biol, 1985. **100**(1): p. 27-34.
20. Vacaru, A.M., et al., *Sphingomyelin synthase-related protein SMSr controls ceramide homeostasis in the ER.* Journal of Cell Biology, 2009. **185**(6): p. 1013-1027.
21. Siow, D.L. and B.W. Wattenberg, *Mammalian ORMDL proteins mediate the feedback response in ceramide biosynthesis.* J Biol Chem, 2012. **287**(48): p. 40198-204.
22. Whitters, E.A., et al., *SAC1p is an integral membrane protein that influences the cellular requirement for phospholipid transfer protein function and inositol in yeast.* J Cell Biol, 1993. **122**(1): p. 79-94.
23. Cleves, A.E., P.J. Novick, and V.A. Bankaitis, *Mutations in the SAC1 gene suppress defects in yeast Golgi and yeast actin function.* J Cell Biol, 1989. **109**(6 Pt 1): p. 2939-50.
24. Nemoto, Y., et al., *Functional characterization of a mammalian Sac1 and mutants exhibiting substrate-specific defects in phosphoinositide phosphatase activity.* J Biol Chem, 2000. **275**(44): p. 34293-305.

25. Blagoveshchenskaya, A., et al., *Integration of Golgi trafficking and growth factor signaling by the lipid phosphatase SAC1.* J Cell Biol, 2008. **180**(4): p. 803-12.
26. Chernomordik, L., M.M. Kozlov, and J. Zimmerberg, *Lipids in biological membrane fusion.* J Membr Biol, 1995. **146**(1): p. 1-14.
27. Shemesh, T., et al., *Prefission constriction of Golgi tubular carriers driven by local lipid metabolism: a theoretical model.* Biophys J, 2003. **85**(6): p. 3813-27.
28. Park, J.H. and E.H. Schuchman, *Acid ceramidase and human disease.* Biochim Biophys Acta, 2006. **1758**(12): p. 2133-8.
29. Horinouchi, K., et al., *Acid sphingomyelinase deficient mice: a model of types A and B Niemann-Pick disease.* Nat Genet, 1995. **10**(3): p. 288-93.

Curriculum vitae

Personal information

Name: ZHAKUPOVA Assem
Birthdate: 05.11.1988
Birthplace/Nationality: Kazakhstan

Academic Education

2012-2016	**University of Zurich, Switzerland** **Integrative Molecular Medicine PhD program** Thesis title: "Regulation of the activity of mammalian serine palmitoyltransferase"
2011-2012	**Eurasian National University, Astana, Kazakhstan** **Master of Engineering and Technology** Thesis title: "Biologically active compounds of Cistanche deserticola in Kazakhstan's flora"
2006-2010	**Indiana University, Bloomington, IN, USA** **Bachelor of Science in Biotechnology** Major: Biotechnology
2003-2005	Specialized Boarding School for gifted children "Daryn", Karaganda, Kazakhstan

Publication list

Lou PH, Lucchinetti E, Zhang L, Affolter A, Gandhi M, **Zhakupova A**, Hersberger M, Hornemann T, Clanachan AS, Zaugg M (2015). Propofol (Diprivan) and Intralipid Exacerbate Insulin Resistance in Type-2 Diabetic Hearts by Impairing GLUT4 Trafficking. Anesth Analg, 120(2): 329-340.

Zhakupova A, Debeuf N, Krols M, Toussaint W, Vanhoutte L, Alecu I, Kutalik Z, Vollenweider P, Ernst D, von Eckardstein A, Lambrecht BN, Janssens S, Hornemann T. ORMDL3 expression levels have no influence on sphingolipid de novo synthesis (submitted)

Forny P, Schumann A, Mustedanagic M, Mathis D, Wulf MA, Naegele N, Langhans CD, **Zhakupova A**, Heeren J, Scheja L, Fingerhut R, Peters HL, Hornemann T, Thony B, Koelker S, Burda P, Froese DS, Devuyst O, Baumgartner MR. Novel mouse models of methylmalonic aciduria recapitulate phenotypic traits with a genetic dosage effect (submitted)

Bitter A, Klein K, **Zhakupova A**, Kandel B, Rieger J, Rümmele P, Nüssler AK, Zanger UM, Hornemann T, Trauner M, Schwab M, Burk O. Pregnane X receptor regulates de novo lipogenesis and sphingolipid synthesis in human non-alcoholic fatty liver disease (in preparation)

Oral presentations

- Radiz internal research seminar "Methods used for elucidating rare diseases" – Zurich, September 23, 2014
- Radiz internal research seminar "Pathomechanism behind the neurotoxicity of 1-deoxysphingolipids in rare disease HSAN1" – Zurich, March 9, 2015

Poster presentations

- 1st Radiz Summer School, Au, ZH – July 4-6, 2013 – best poster award
- 9th ZIHP Symposium, Zurich – August 23, 2013
- 7th International Ceramide Conference, Montauk, NY, USA – October 20-24, 2013
- Gordon Research Conference on Glycolipids and Sphingolipids, Ventura, CA, USA – January 12-17, 2014
- 2nd international congress on research of rare and orphan diseases, RE(ACT) CONGRESS, Basel – March 5-8, 2014
- 14th Day of Clinical Research, University Hospital Zurich – April 9, 2015
- 8th International Ceramide Conference, Cesme, Turkey – May 6-10, 2015
- 11th ZIHP Symposium, Zurich – August 21, 2015
- Gordon Research Conference on Glycolipids and Sphingolipids, Lucca, Italy – March 6-11, 2016

Acknowledgements

First of all I would like to thank Prof. Arnold von Eckardstein for allowing me to work in this lab at IKC. Thank you for your support, helpful feedback and advices throughout my PhD.

I am very grateful to my supervisor Thorsten for this interesting project and for believing in me from the beginning. Thank you for letting me to work independently, for your guidance and useful comments.

Furthermore, I would like to thank my committee members Prof. Stephan Neuhauss, Dr. Sabrina Sonda and Dr. Ludovic Gillet for the fruitful discussions and helpful suggestions during our meetings.

Big thanks to all the former and present members of our Hornemann lab for the great time we spent together both inside and outside the lab. This includes Daniela Ernst, Alaa Othman, Heiko Bode, Iryna Sutter, Irina Alecu, Yu Wei, Saranya Suriyanarayanan, Regula Steiner, Museer Lone and Gergely Karsai. Special thanks to Nina Steffen, Regula and Gergely for translating my Zusammenfassung.

Also, I would like to thank all the members of IKC and our Wagi 14 colleagues – Lucia Rohrer, Katrin Gebert, Silvija Radosavljevic, Vidya Velagapudi, Paolo Zanoni, Anton Potapenko, Mustafa Yalcinkaya, Reda Hasballa, Hans Reiser, Joanna Gawinecka, Tatiana Claro da Silva, Regina Krattinger, Gai Zhibo, Lisa Rigassi, Lisa Unterleutner and Yuliya Plutino. Thank you all for the fun times we had including eating fondue, raclette and birthday cakes together.

Special thanks to Aizhan Tastanova for suggesting Life Science Zurich program and your support throughout the application process.

I don't have enough words to describe how much I am grateful for my family for all their love, care and support. Thank you for letting me to pursue my dreams, to be independent and for everything that made me a person who I am today.